



PLACE IN RETURN BOX to remove this checkout from your record.
TO AVOID FINES return on or before date due.

DATE DUE	DATE DUE	DATE DUE
_____	_____	_____
_____	_____	_____
_____	_____	_____
_____	_____	_____
_____	_____	_____
_____	_____	_____
_____	_____	_____

MSU is An Affirmative Action/Equal Opportunity Institution

c:\cird\datedue.pm3-p.1

DISTRIBUT
PROJECTI
OF

in par

**DISTRIBUTION AND MORPHOLOGICAL FEATURES OF EFFERENT
PROJECTIONS FROM IDENTIFIED SUBDIVISIONAL AREAS
OF RAT TRIGEMINAL NUCLEUS INTERPOLARIS**

By

Mark Steven Cook

A DISSERTATION

**Submitted to
Michigan State University
in partial fulfillment of the requirements
for the degree of**

DOCTOR OF PHILOSOPHY

Department of Anatomy

1992

DISTRIBUT
PROJECT
OF

The rece
trigeminal nu
the developme
leucoagglutin
examination
PHA-L inject
including
ventrolatera
border region
the distribut
terminal axo
provided. T
subdivisiona
posteromedia
nuclear grou
nucleus (APT
nucleus (RPC
(VII), infer
cerebellum (
in dmVi wer

011-4344X

ABSTRACT

DISTRIBUTION AND MORPHOLOGICAL FEATURES OF EFFERENT PROJECTIONS FROM IDENTIFIED SUBDIVISIONAL AREAS OF RAT TRIGEMINAL NUCLEUS INTERPOLARIS

By

Mark Steven Cook

The recent delineation of six distinct subdivisions in trigeminal nucleus interpolaris (Vi) in the rat, along with the development of the anterograde tracer Phaseolus vulgaris-leucoagglutinin (PHA-L) have provided a basis for the re-examination of the efferent projections from Vi. Following PHA-L injections into four subdivisional regions of rat Vi, including the ventrolateral magnocellular (vlVimc), ventrolateral parvocellular (vlVipc), dorsomedial (dmVi) and border regions (brVi), detailed drawings and descriptions of the distribution and morphological characteristics of labeled terminal axonal arborizations in all target nuclei were provided. The results demonstrated that all four Vi subdivisional regions provide input to the ventral posteromedial thalamic nucleus (VPM), posterior thalamic nuclear group (Po), zona incerta (ZI), anterior pretectal nucleus (APT), superior colliculus (SC), parvocellular red nucleus (RPC), pontine nuclei (Pn), facial motor nucleus (VII), inferior olive (IO), sensory trigeminal complex (SVC), cerebellum (CB) and cervical spinal cord (CSC). Only neurons in dmVi were found to project to the medial accessory

oculomotor nu

all four Vi

projections t

were found w

four regions

and RPC, w

topographica

SC. In the

projected p

dorsal acce

differences

the CB, al

mainly to

regions, in

lobule and

to the deep

greatest i

projected

dorsal hor

contralate

oculomotor nuclei (MA3) in the midbrain. In the diencephalon, all four Vi subdivisional regions gave rise to similar projections to Po and ZI, however, topographical differences were found with the projections to VPM. In the midbrain, all four regions of Vi gave rise to similar projections to APT and RPC, while only dmVi provided input to (MA3) and topographical differences were found with the projections to SC. In the pons and medulla, the four regions of Vi all projected predominantly to medial Pn, dorsal VII, and the dorsal accessory olivary nucleus, however, topographical differences were found with the projections to the SVC. In the CB, all four Vi subdivisional regions provided input mainly to the granule cell layer of the orofacial tactile regions, including Crura I and II, paramedian lobule, simple lobule and the uvula, as well as collateralized projections to the deep cerebellar nuclei. Neurons in dmVi provided the greatest input to CB. In the CSC, all four Vi regions projected to laminae III and IV of the ipsilateral cervical dorsal horn, while only dmVi and vlVimc projected to the contralateral dorsal and ventral horns.

I would
advisor, Dr.
and encourag
to thank th
Grofova, J.
their guidan

I also
support of m
my wife, Lin

ACKNOWLEDGMENTS

I would like to express my appreciation and thanks to my advisor, Dr. William M. Falls, for his leadership, support and encouragement during my graduate training. I also wish to thank the members of my graduate committee, Drs. Irena Grofova, J.I. Johnson, Kathryn Lovell, and Duke Tanaka for their guidance.

I also wish to express my deep appreciation for the support of my family and friends. Finally, I want to thank my wife, Linda, for her unrelenting support and patience.

List of Figures

Abbreviations

Introduction

Chapter I

Chapter II

Chapter III

TABLE OF CONTENTS

List of Figures	vi
Abbreviations	viii
Introduction	1
Chapter I Efferent projections of neurons in four sub- divisional regions of rat trigeminal nucleus interpolaris to the diencephalon and midbrain: APHA-L study.....	3
Introduction.....	3
Materials and Methods.....	5
Results.....	8
Discussion.....	20
Figures.....	47
Bibliography.....	71
Chapter II Efferent projections of neurons in four sub- divisional regions of rat trigeminal nucleus interpolaris to pontomedullary regions: A PHA-L study.....	82
Introduction.....	82
Materials and Methods.....	84
Results.....	84
Discussion.....	90
Figures.....	104
Bibliography.....	118
Chapter III Efferent projections of neurons in four sub- divisional regions of rat trigeminal nucleus interpolaris to the cerebellum and spinal cord: APHA-L study.....	125
Introduction.....	125
Materials and Methods.....	127
Results.....	128
Discussion.....	138
Figures.....	160
Bibliography.....	186

CHAPTER I

Figure 1:

Figure 2:

Figure 3:

Figure 4:

Figure 5:

Figure 6:

Figure 7:

Figure 8:

Figure 9:

Figure 10:

Figure 11:

Figure 12:

CHAPTER II

Figure 1:

Figure 2:

LIST OF FIGURES

CHAPTER I

Figure 1:	PHA-L Injection Sites	48
Figure 2:	Diencephalic Projections from vlVimc and vlVipc	50
Figure 3:	Diencephalic Projections from dmVi and brVi	52
Figure 4:	Midbrain Projections from vlVimc and vlVipc	54
Figure 5:	Midbrain Projections from dmVi and brVi ...	56
Figure 6:	Drawings of Terminal Axonal Arborizations in VPM	58
Figure 7:	Drawings of Terminal Axonal Arborizations in Po and ZI	60
Figure 8:	Drawings of Terminal Axonal Arborizations in APT and SC	62
Figure 9:	Drawings of Terminal Axonal Arborizations in RPC and MA3	64
Figure 10:	Photomicrographs of Terminal Axonal Arborizations in VPM, Po and ZI	66
Figure 11:	Photomicrographs of Terminal Axonal Arborizations in ZI, APT and SC	68
Figure 12:	Photomicrographs of Terminal Axonal Arborizations in SC, RPC and MA3	70

CHAPTER II

Figure 1:	PHA-L Injection Sites	105
Figure 2:	Projections from Vi Subdivisional Regions to Pn	107

Figure 3: P
a

Figure 4: P
b

Figure 5: D
i

Figure 6: D
i

Figure 7: P
A

CHAPTER III

Figure 1: I

Figure 2: C

Figure 3:

Figure 4:

Figure 5:

Figure 6:

Figure 7:

Figure 8:

Figure 9:

Figure 10:

Figure 11:

Figure 12:

Figure 13:

Figure 3:	Pontomedullary Projections from vlVimc and vlVipc	109
Figure 4:	Pontomedullary Projections from dmVi and brVi	111
Figure 5:	Drawings of Terminal Axonal Arborizations in Pn and VII	113
Figure 6:	Drawings of Terminal Axonal Arborizations in IO and SVC	115
Figure 7:	Photomicrographs of Terminal Axonal Arborizations in Pn, VII, IO and SVC	117
CHAPTER III		
Figure 1:	PHA-L Injection Sites	161
Figure 2:	Cerebellar Projections from dmVi	163
Figure 3:	Cerebellar Projections from dmVi	165
Figure 4:	Cerebellar Projections from vlVimc	167
Figure 5:	Cerebellar Projections from vlVipc	169
Figure 6:	Cerebellar Projections from brVi	171
Figure 7:	Drawings of Mossy Fibers in CB Granule Cell Layer	173
Figure 8:	Drawing of Terminal Axonal Arborizations in DCN	175
Figure 9:	Spinal Cord Projections from vlVipc and vlVimc	177
Figure 10:	Spinal Cord Projections from brVi and dmVi	179
Figure 11:	Drawings of Terminal Axonal Arborizations in CSC	181
Figure 12:	Photomicrographs of Mossy Fibers in CB	183
Figure 13:	Photomicrographs of Terminal Axonal Arborizations in DCN and CSC	185

APT	ante
brVi	borc
CB	cer
CE	cer
CSC	cer
DAB	dee
DCN	dee
dcVi	do
dlVi	do
dmVi	do
GCL	gr
HRP	h
InG	i
INT	i
InWh	i
IO	
IOD	
IOPr	
irVi	
IS	
LAT	
MA3	

ABBREVIATIONS

APT	anterior pretectal nucleus
brVi	border region of Vi
CB	cerebellum
CE	cervical enlargement
CSC	cervical spinal cord
DAB	deep axonal bundle
DCN	deep cerebellar nuclei
dcVi	dorsal cap of Vi
dlVi	dorsolateral Vi
dmVi	dorsomedial Vi
GCL	granule cell layer of CB
HRP	horseradish peroxidase
InG	intermediate gray layer superior colliculus
INT	intermediate cerebellar nucleus
InWh	intermediate white layer superior colliculus
IO	inferior olive
IOD	inferior olive dorsal nucleus
IOPr	inferior olive principal nucleus
irVi	intermediate region Vi
IS	injection site
LAT	lateral cerebellar nucleus
MA3	medial accessory oculomotor nucleus

MDH	med
MED	med
MF	mos
ML	me
PCRT	pa
PHA-L	Ph
PML	pa
Pn	po
Po	po
RCC	r
RF	r
RMC	m
RN	r
RPC	P
SC	s
SIM	s
SVC	s
Vi	
VII	
vlVimc	
vlVipc	
Vms	
Vo	
VPM	
WGA	
ZI	

MDH	medullary dorsal horn
MED	medial cerebellar nucleus
MF	mossy fiber
ML	medial lemniscus
PCRT	parvocellular reticular nucleus
PHA-L	Phaseolus vulgaris leucoagglutinin
PML	paramedian lobule
Pn	pontine nuclei
Po	posterior thalamic nucleus
RCC	rostral cervical cord
RF	receptive field
RMC	magnocellular red nucleus
RN	red nucleus
RPC	parvocellular red nucleus
SC	superior colliculus
SIM	simple lobule
SVC	sensory trigeminal complex
Vi	trigeminal nucleus interpolaris
VII	facial motor nucleus
vlVimc	ventrolateral magnocellular Vi
vlVipc	ventrolateral parvocellular Vi
Vms	trigeminal main sensory nucleus
Vo	trigeminal nucleus oralis
VPM	ventral posteromedial thalamic nucleus
WGA	wheat germ agglutinin
ZI	zona incerta

Trigem
of the s
information
relaying it
midbrain, p
researchers
Vi of the
regarding s
specific
arborizati
characteri
informatio
projection
difference
provided i
of projec
subdivisio
the reexa
anterograde
L).

The p
in four s

INTRODUCTION

Trigeminal nucleus interpolaris (Vi), one of the nuclei of the sensory trigeminal complex, receives tactile information from orofacial regions and modifies it before relaying it to several target nuclei in the diencephalon, midbrain, pons, medulla, cerebellum and spinal cord. Many researchers have investigated the projections from neurons in Vi of the rat, however, few have provided information regarding subdivisional differences with these projections, specific distribution patterns of terminal axonal arborizations in target nuclei, or the morphological characteristics of the terminal arbors. The lack of information pertaining to these aspects of Vi efferent projections was due to insufficient data on Vi subdivisional differences and the utilization of neuronal tracers which provided inadequate labeling of terminal axonal arborizations of projection neurons. The recent delineation of six Vi subdivisions has served as a basis, in the present study, for the reexamination of projections from Vi utilizing the anterograde tracer *Phaseolus vulgaris* leucoagglutinin (PHA-L).

The present study describes the projections from neurons in four subdivisional regions of Vi in the rat, including

ventrolateral

parvocellular

(brVi) area

distribution

axonal arbor

nucleus (VPM

incerta (ZI

colliculus

accessory o

facial moto

trigeminal c

cord (CSC).

ventrolateral magnocellular (vlVimc), ventrolateral parvocellular (vlVipc), dorsomedial (dmVi) and border region (brVi) areas. This study also describes the specific distribution and morphological characteristics of terminal axonal arborizations in the ventral posteromedial thalamic nucleus (VPM), posterior thalamic nuclear complex (Po), zona incerta (ZI), anterior pretectal nucleus (APT), superior colliculus (SC), parvocellular red nucleus (RPC), medial accessory oculomotor nucleus (MA3), pontine nuclei (Pn), facial motor nucleus (VII), inferior olive (IO), sensory trigeminal complex (SVC), cerebellum (CB) and cervical spinal cord (CSC).

Efferent Pro

of Ra

Di

Trigemi

information

orofacial r

sensory inf

before being

nuclei alo

anatomical a

recordings,

which term

midbrain. Th

nucleus (

incerta (29

superior co

Effere

midbrain ar

for their s

to be expect

distinct su

CHAPTER I

Efferent Projections of Neurons in Four Subdivisional Regions of Rat Trigeminal Nucleus Interpolaris to the Diencephalon and Midbrain: A PHA-L Study

INTRODUCTION

Trigeminal nucleus interpolaris (Vi) receives sensory information from primary trigeminal neurons innervating orofacial receptive fields. Within Vi, this orofacial sensory information undergoes processing and modification before being relayed by projection neurons to several target nuclei along the neuraxis (39,40,49,51). Utilizing anatomical axonal tracing techniques and electrophysiological recordings, neurons in rat Vi have been shown to emit axons which terminate in various nuclei of the thalamus and midbrain. These nuclei include ventral posteromedial thalamic nucleus (17,21,22,28,29,35,49,67,81,84,87,118,102), zona incerta (29,84,96), posterior thalamic nuclei (21,22,84) and superior colliculus (1,17,34,45,61,91,92,99,102,106).

Efferent Vi projections to well-known thalamic and midbrain areas have been described without much consideration for their subdivisional origin within the nucleus. This is to be expected, since only recently have six separate and distinct subdivisions of rat Vi been delineated based on

differences in their overall cyto- and myeloarchitecture, as well as connectional criteria (85). The six Vi subdivisions include ventrolateral magnocellular (vlVimc), ventrolateral parvocellular (vlVipc), border region (brVi), dorsolateral (dlVi), dorsal cap (dcVi) and intermediate region (irVi). In addition, previous studies have provided relatively little information regarding the morphological characteristics of the terminal axonal arborizations of Vi projection neurons. The present study was conducted to determine the distribution of efferent axons from neurons in four distinct Vi subdivisional regions to target nuclei along the neuraxis, as well as to describe the morphological characteristics of the terminal axonal arborizations of these neurons. The four subdivisional regions of Vi from which these projections are described include vlVimc, vlVipc, brVi and dorsomedial Vi (dmVi). The subdivisional region, dmVi, includes dlVi, dcVi and irVi. Iontophoretic injections of the anterograde tracer, Phaseolus vulgaris leucoagglutinin (PHA-L), permit one to make injections into Vi subdivisional regions and visualize the distribution and morphological characteristics of the axons and terminal arborizations of Vi neurons in the various target nuclei. The morphological details of Vi axons and their terminal arborizations are necessary if one is to begin to understand the effects of Vi inputs on the activity of neurons in target nuclei in the thalamus and midbrain.

All an.
for postop
guidelines.
grams) used
pentobarbit
apparatus.
opened and
(tip diame
PHA-L (reco
at 25mg/m
according
atlas of P
Phelan and
injected a
for approx
the microp
and the o
10-12 day
under he
fixative
a 0.1 M
another
paraforma

MATERIALS AND METHODS

All animals were housed, prepared for surgery and cared for postoperatively according to federally prescribed guidelines. The eight adult male Sprague-Dawley rats (250-300 grams) used in this study were anesthetized with sodium pentobarbital (35-40 mg/kg) and placed in a stereotaxic apparatus. The cranium overlying the cerebellar cortex was opened and the dura mater reflected. A glass micropipette (tip diameter approximately 20 μ m), filled with 1.0 μ l of PHA-L (reconstituted in 10 mM phosphate buffer at a pH of 8.0 at 25mg/ml), was lowered into a Vi subdivision region according to precalculated stereotaxic coordinates from the atlas of Paxinos and Watson (83) and the previous studies of Phelan and Falls (85,87). The PHA-L was iontophoretically injected at 5.0 microamperes of alternating positive current for approximately 25-35 minutes. Following the removal of the micropipette, Gelfoam was placed over the cranial opening and the overlying skin was closed with wound clips. After 10-12 days of survival, each rat was transcardially perfused under heavy anesthesia (sodium pentobarbital), with a fixative solution (500 ml) containing 4% paraformaldehyde in a 0.1 M acetate buffer (pH 6.5) followed immediately by another fixative solution (500 ml) containing 4% paraformaldehyde and 0.5% glutaraldehyde in 0.1 M borate

buffer (pH
stored in a
Twenty-four
sectioned at
transverse
collected i
adjusted to
processed f
Gerfen and
conducted a
three rins
sections we
normal Rabb
by a 5 m.
incubation
Antibody t
agitation,
antibody, s
each) and
antibody,
Labs. Inc.)
at 5 min.
incubation
horseradish
sections w
TX100. The

buffer (pH 9.5). The brain was immediately removed and stored in a fresh solution of the latter fixative at 4⁰C. Twenty-four hours later, the thalamus and midbrain were sectioned at 30-50 μ m on an Oxford Vibratome in either the transverse or horizontal plane. Tissue sections were collected in a 0.05 M Tris-buffered 0.15 M saline (TBS), adjusted to a pH of 7.6 at room temperature , and immediately processed for PHA-L reaction product by a modification of the Gerfen and Sawchenko method (37). All subsequent steps were conducted at room temperature unless otherwise noted. After three rinses in TBS with 0.2% Triton X100 (TBS-TX100), sections were incubated for 30 minutes in TBS-TX100 with normal Rabbit Serum (Vector Labs. Inc.). This was followed by a 5 minute rinse in TBS-TX100 and then a 48 hour incubation in primary antibody, consisting of a 1:2,000 Goat Antibody to PHA-L (Vector Labs. Inc.) in TBS-TX100, with agitation, at 5⁰C. After the incubation in the primary antibody, sections were rinsed 3 times in TBS-TX100 (5 min. each) and then incubated for 90 minutes in secondary antibody, which consisted of Rabbit antibody Goat (Vector Labs. Inc.) in TBS-TX100. Sections were then rinsed (3 times at 5 min. each) with TBS-TX100 followed by a 1-2 hour incubation in a solution of Avidin and Biotinylated horseradish peroxidase (Vector Labs. Inc.) in TBS-TX100. The sections were then rinsed 4 times (5 min. each) with TBS-TX100. The final step consisted of exposing the sections to

a solution of diaminobenzidine (DAB) and glucose oxidase at a ratio of 10:1. The reaction was terminated with 4 rinses of TBS-TX100. Sections were then placed on gelatin-coated glass slides, stained with cresyl violet and coverslipped for light microscopic analysis. All sections were viewed with a Leitz Laborlux 12 microscope fitted with a drawing tube. Low-power drawings of the location and distribution of Vi efferent axons to thalamic and midbrain regions were made by using a 2.5X objective lens at a magnification of 31X. Morphologically distinct types of Vi terminal axonal arborizations in each of the described target nuclei were visually assessed by observing each area at high power light microscopy, using a 100X oil immersion lens, and several terminal arborizations, representative of each type identified, were drawn using a drawing tube at a magnification of 1,250X. Although most of the representative terminal arborizations drawn were from single tissue sections, some terminal arbors were reconstructed from adjacent sections. The distinction of the various types of Vi terminal arborizations in this study were based on axonal diameter, degree of branching, as well as frequency and size of boutons.



PHA-L Inje

The

successful
two for ea
two separa
subdivision
for each
representat
centered in
region of c
labeled ce
labeling was
was devoid
reaction pro
the adjacent
rostrally in
oralis (Vo)
portion of th
vlVipc (Fig
subdivision,
the middle a
into brvi a
injection si

RESULTS

PHA-L Injection Sites

The data provided for this study were based on successful injections of PHA-L in a total of eight animals, two for each of the four Vi subdivisional regions. Although two separate injections were made into each of the four Vi subdivisional regions, only one representative injection site for each will be used for illustrative purposes. The representative injection site in vlVimc (Fig. 1A) was centered in the middle of this subdivision with a dark brown region of dense PHA-L reaction product, defined by solidly labeled cell bodies. Surrounding this dense "core" of labeling was a lighter brown spread of reaction product which was devoid of labeled cell bodies. A slight spread of the reaction product extended laterally into brvi, medially into the adjacent parvocellular reticular formation (PCrt) and rostrally into the caudalmost extent of trigeminal nucleus oralis (Vo), where it was located in the ventrolateral portion of the nucleus. The representative injection site in vlVipc (Fig. 1B) was centered in the middle of this subdivision, with a dark brown region of reaction product in the middle and a lighter brown periphery extending laterally into brvi and medially into PCrt. The representative injection site in dmVi (Fig. 1C) showed dark brown reaction

product in dlvi, dcvi and irvi and a lighter brown spread of the reaction product extending ventrally into the dorsal portion of brvi and dorsal vlVimc. The representative injection site in brVi (Fig. 1D) showed a dark brown reaction product in the caudal two-thirds of the subdivision and a lighter brown spread of reaction product in the lateral-most portion of vlVipc. Only a few retrogradely labeled cells were located in the medullary dorsal horn (MDH: trigeminal nucleus caudalis), and no retrogradely labeled axons were found in the sensory root of the trigeminal nerve.

Projections to the Thalamus

Injections of PHA-L into any of the four Vi subdivisional regions, vlVimc, vlVipc, dmVi and brVi, labeled projection neurons whose axons exited Vi ventromedially and coursed through the parvocellular reticular formation toward the midline. The converging axons then coursed immediately dorsal to the ipsilateral inferior olive, decussated, and collected into a loose bundle located dorsal to the medial portion of the pyramidal tract. As they ascended, the fibers shifted dorsally in the rostral pons, coursed rostrally through the midbrain and entered the diencephalon interspersed with fibers of the medial lemniscus (ML). Labeled axons from all Vi subdivisional regions exited ML and coursed either dorsally or ventrally and gave rise to terminal arborizations in the contralateral ventral

posteromedial nucleus of the thalamus (VPM), the medial portion of the posterior nuclei (Po) and the zona incerta (ZI) (Figs. 2,3). With each injection, the density of terminal axonal arborizations was greatest in ZI, less in VPM and least in Po. No labeled terminal axonal arborizations were found ipsilaterally in these target nuclei.

Projections to the Ventral Posteromedial Thalamic Nucleus

In the caudal diencephalon, Vi-VPM parent axons (approximately 1.5 μ m in diameter) exited the contralateral ML and traveled dorsally and rostrally in VPM where they gave rise to terminal arbors in various portions of the nucleus depending on the Vi subdivisional region of origin. Axons from neurons in vlVimc, vlVipc, dmVi and brVi gave rise to terminal arborizations throughout the rostrocaudal extent of contralateral VPM, with the majority of arbors located in the middle one-third of the nucleus. Aside from these consistencies, topographical differences were found with the distribution of terminal arbors from the various Vi subdivisional regions.

Axons from vlVimc neurons gave rise to terminal arborizations located dorsomedially in VPM (Fig. 2A-D). Terminal arbors from axons of vlVipc neurons were found dorsomedially in rostral VPM (Fig. 2E,F) and dorsolaterally in caudal VPM (Fig. 2G,H). The terminal arbors from axons of dmVi neurons were primarily located ventrolaterally in VPM

(Fig. 3B-D), and those from axons of brVi neurons were primarily found in the dorsal-most portion of VPM (Fig. 3E-H). A small number of terminal arborizations from axons of neurons in each Vi subdivisional region were located dorsomedially in the rostral-most portion of VPM (Figs. 2A,E; 3A,E). In all cases, the number of terminals at the rostral- and caudal-most extent of VPM were sparse.

All of the PHA-L injections into Vi subdivisional regions produced two morphologically distinct types of terminal axonal arborizations in VPM, a thin-VPM type and a thick-VPM type. Both types of terminal arbors were usually found intermingled throughout the receptive regions of VPM and were formed either by collaterals of the parent fiber or at the terminal end of the parent axon. The terminal arbors were often intermingled and formed patches (6A). The thin-VPM type (Figs. 6B 3,4; 10B) was characterized by a relatively thin, branched terminal strand (approximately 0.5 μm in diameter), with oval to irregularly shaped boutons (approximately from 1.0 to 2.5 μm in diameter). The thick-VPM type (Figs. 6B 1,2; 10A) was characterized by a thicker, branched terminal strand (approximately 1.0 μm in diameter). It gave rise to irregularly shaped boutons (approximately from 1.0 to 4.0 μm in diameter).

Projections to the Posterior Thalamic Nuclear Group

Parent axons (approximately 1.0 to 1.5 μm in diameter) which gave rise to terminal arbors in medial Po coursed dorsally from contralateral ML, traversed VPM, and traveled medially before giving rise to terminal arbors in Po. The arbors in Po were widely scattered throughout the rostrocaudal extent of the nucleus, just medial to VPM (Figs. 2,3).

Although Vi-Po axons traversed VPM receptive zones on their way to Po, it could not be determined whether or not they provided collateralized input to VPM. Only one morphologically distinct type of terminal axonal arborization was located in medial Po following injections in each of the Vi subdivisional regions (Figs. 7A, 10C). The Po-type of terminal arbor was characterized by a thin, sparsely branched terminal strand (approximately 0.5 μm in diameter) with relatively few, widely spaced boutons en passant measuring approximately from 1.0 to 1.5 μm in diameter. The Po-type of arbor was unique from the other terminal arbors described in this study. It had a long filamentous terminal strand, which either came off as a side branch of the parent fiber, or as the termination, and invariably produced a relatively large bouton (approximately 2.0 μm in diameter) at the end of the terminal strand.

Projections to Zona Incerta

Neurons in vlVimc, vlVipc, dmVi and brVi gave rise to axons (approximately 1.0 to 1.5 μm in diameter) which exited ML ventrally in the contralateral diencephalon, and coursed to the subjacent ZI. The labeled axons passed ventrally, through the dorsal portion of ZI, before producing relatively large, dense patches of terminal arborizations in the ventral zone. Axons of vlVimc neurons gave rise to terminal arbors in the caudal two-thirds of the ventral zone of ZI (Fig. 2A-D), with the greatest density in the caudal one-third. Terminal arbors from axons of vlVipc neurons were distributed similarly (Fig. 2E-H). Axons from neurons in dmVi gave rise to terminal arbors located throughout the rostrocaudal extent of the ventral zone, with the greatest density in the caudal one-third (Fig. 3A-D). Axons of brVi neurons gave rise to terminal arbors throughout the caudal one-half of the ventral zone of ZI, with the greatest density in the caudal one-fourth (Fig. 3E-H). Although the majority of the terminal arbors were located in the ventral portion of ZI, labeled arbors were also found sparsely scattered in the dorsal region. The majority of terminal arbors in ZI from all of the Vi subdivisional regions were in the caudal one-fourth of the ventral zone, however, the terminal zone that resulted from vlVimc and brVi injections were located more laterally than those that resulted from vlVipc and dmVi injections.

Axons (approximately 1.0 to 1.5 μm in diameter) from

neurons in
morphological
arborizations
the parent fi
types of term
orientation i
7B 1,2; 10D)
strand (appr
closely spac
diameter).
characterize
(approximate
boutons (app
types of te
the recepti

Axons
which gave
exited Vi m
contralate
All four v
terminal a
superior c
Only dmVi
located in

neurons in all Vi subdivisional regions provided two morphologically distinct types of terminal axonal arborizations, a complex-ZI type and a simple-ZI type. As the parent fibers coursed from dorsal to ventral in ZI, both types of terminal strands generally assumed a medio-lateral orientation in the ventral zone. The complex-ZI type (Figs. 7B 1,2; 10D) was characterized by a thin, branched terminal strand (approximately 0.5 μm in diameter) with multiple, closely spaced boutons (approximately from 1.0 to 2.0 μm in diameter). The simple-ZI type (Figs. 7B 3,4; 11A) was characterized by a thin, sparsely branched terminal strand (approximately 0.5 μm in diameter) with fewer, widely spaced boutons (approximately from 1.0 to 2.0 μm in diameter). Both types of terminal arbors were found interspersed throughout the receptive zone of ZI.

Projections to the Midbrain

Axons from neurons in vlVimc, vlVipc, dmVi and brVi, which gave rise to terminal arborizations in the midbrain exited Vi medially, decussated in the midline and ascended in contralateral ML with the Vi axons traveling to the thalamus. All four Vi subdivisional areas had axons which gave rise to terminal arbors in the anterior pretectal nucleus (APT), superior colliculus (SC) and parvocellular red nucleus (RPC). Only dmVi injections produced labeling of terminal arbors located in the medial accessory oculomotor nucleus (MA3).

The midbrain areas that received the most dense projections from Vi subdivisional regions were APT and SC. These were followed, in order of descending densities, by RPC and MA3.

Projections to the Anterior Pretectal Nucleus

In the rostral midbrain, labeled axons (approximately 1.0 to 1.5 μm in diameter) from neurons in vlVimc, vlVipc, dmVi and brVi coursed dorsally from ML, through the midbrain reticular formation before giving rise to terminal arbors in contralateral APT. Regardless of the Vi subdivision, injections of PHA-L resulted in a large dense patch of terminal arbors in the caudal one-half of APT (Figs. 4A,E; 5A,E). With each injection, the region of APT labeling was situated midway between the dorsal and ventral portions of the nucleus, and included portions of both. A slight medio-lateral difference in the location of terminal labeling was observed depending on the subdivisional region of Vi injected. The large terminal patch shifted from a centrally located position in APT following dmVi and vlVipc injections to a medial position following vlVimc and brVi injections. No terminal arbors were found in ipsilateral APT.

The labeled axons from Vi gave rise to two types of terminal arborizations in APT, a complex-APT type and a simple-APT type. The orientation of the terminal strands was difficult to ascertain due to the density of the terminal arborizations in the receptive zone. The complex-APT type

(Figs. 8A 1,
branched ter
with multipl
to 2.5 μ m in
11C) was cha
strand (app
few, widely
in diameter
found inter

Projections

Labelle
from neuron
from contra
caudal midk
SC (Figs.
mainly cont
dmVi gave
decussating
terminal a
The majori
the interm
sparsely s
arbors we
neurons in
arbors tha

(Figs. 8A 1,2; 11B) was characterized by a thin, moderately branched terminal strand (approximately 0.5 μm in diameter) with multiple, closely spaced boutons (approximately from 1.0 to 2.5 μm in diameter). The simple-APT type (Figs. 8A 3,4; 11C) was characterized by a thin, sparsely branched terminal strand (approximately 0.5 μm in diameter) with relatively few, widely spaced boutons (approximately from 1.0 to 2.0 μm in diameter). Both types of terminal arborizations were found intermingled throughout the receptive zone.

Projections to the Superior Colliculus

Labeled axons (approximately 1.0 to 1.5 μm in diameter) from neurons in all Vi subdivisional regions coursed dorsally from contralateral ML, through the reticular formation in the caudal midbrain, and gave rise to terminal arborizations in SC (Figs. 4,5). Although projections from Vi to SC were mainly contralateral, a small number of axons from neurons in dmVi gave rise to terminal arbors ipsilaterally by decussating from contralateral SC to ipsilateral SC. Labeled terminal arborizations in SC were in the form of patches. The majority of these labeled terminal patches were found in the intermediate gray (InG) and white (InWh) layers with only sparsely scattered fibers in the deep layers. No labeled arbors were found in the superficial layers. Although neurons in all Vi subdivisional regions gave rise to terminal arbors that were predominantly located in InG and InWh, there

were to
the e
subdivi
were si
rise to
the gre
(Figs.
aspect
the la
termina
dense
contral
limits
the la
medial-
in dm
ipsilat
arbors
as tho
of InG
could
to ter
of con
thirds
predom
their

were topographical differences in terminal labeling between the efferent projections arising from some of the subdivisional regions. Projections from vlVimc and vlVipc were similar. Neurons from both subdivisional regions gave rise to terminal arbors in the rostral two-thirds of SC, with the greatest density in the rostral one-half of the nucleus (Figs. 4B-D, F-H). These arbors extended to the medial-most aspect of contralateral SC, although they were most dense in the lateral one-third to one-half of the nucleus. The terminal arbors of axons originating in dmVi were relatively dense throughout most of the rostrocaudal extent of contralateral SC, except at the rostral- and caudal-most limits where they were sparse. The arbors were confined to the lateral one-third of SC, and no arbors extended to the medial-most portion of SC (Figs. 5B-D). In addition, neurons in dmVi were the only Vi neurons which projected to ipsilateral SC. Although much more sparse, the terminal arbors in ipsilateral SC were found in the same region of SC, as those located contralaterally, in the lateral-most portion of InG and InWh. The course of dmVi axons to ipsilateral SC could not be determined. Axons from brVi neurons gave rise to terminal arborizations throughout the rostrocaudal extent of contralateral SC, but were most dense in the rostral two-thirds of the nucleus. These terminal arbors were predominantly found in InG and InWh (Figs. 5F-H), throughout their mediolateral extent.



The lab
lateral to me
terminal stra
the parent fi
Two morphol
arborization
simple-SC ty
characteriz
(approximat
spaced ova
diameter).
a thin, sp
 μ m in d
(approxima
of termin
receptive

Projection

In
1.0 to
subdivis
contrala
gave ris
portion
injected
similar.

The labeled axons traversed contralateral SC in a lateral to medial direction, and gave rise to bouton-bearing terminal strands either as collaterals along the course of the parent fiber, or at the terminal end of the parent fiber. Two morphologically distinct types of terminal axonal arborizations were found in SC, a complex-SC type and a simple-SC type. The complex-SC type (Figs. 8B 1,2; 11D) was characterized by a thin, branched terminal strand (approximately 0.5 μm in diameter), with multiple, closely spaced oval boutons (approximately from 1.5 to 2.5 μm in diameter). The simple-SC type (Figs. 8B 3,4; 12A) displayed a thin, sparsely branched terminal strand (approximately 0.5 μm in diameter) with fewer, widely spaced boutons (approximately from 1.0 to 2.0 μm in diameter). Both types of terminal arborizations were found throughout the SC receptive zones.

Projections to the Parvocellular Red Nucleus

In the rostral midbrain, labeled axons (approximately 1.0 to 1.5 μm in diameter) from neurons in all Vi subdivisional regions traveled dorsomedially from contralateral ML to the adjacent red nucleus (RN) where they gave rise to terminal arborizations in the parvocellular portion (RPC). Regardless of the Vi subdivisional region injected with PHA-L, the labeling produced in RPC was similar. Terminal arborizations were located dorsally

throughout the rostrocaudal extent of RPC (Figs. 4,5), primarily in the dorsal region. No labeling was found in the magnocellular portion of the contralateral red nucleus, or in any portion of the ipsilateral red nucleus. One type of terminal arborization was located in RPC. The RPC-type (Figs. 9A; 12B) was characterized by a thin, branched terminal strand (approximately 0.5 μm in diameter) with multiple closely spaced boutons (approximately from 1.0 to 3.0 μm in diameter). The terminal strands in RPC were observed coursing in various directions.

Projections to the Medial Accessory Oculomotor Nucleus

Only one of the Vi subdivisional regions, dmVi, projected to the medial accessory oculomotor nucleus (MA3) of the midbrain. Although MA3 receives the most sparse labeling of all nuclei studied, it was nonetheless substantial. Labeled axons (approximately 1.0 μm in diameter) coursed dorsomedially from contralateral ML, either through or dorsal to RN, before giving rise to terminal arbors in MA3. The terminal arbors were located bilaterally throughout the rostrocaudal extent of MA3, with contralateral predominance (Fig. 5A).

One type of terminal axonal arborization was found in MA3, which were generally oriented dorsoventrally. The MA3-type (Figs. 9B; 12C,D) was depicted by a long, thin, sparsely branched terminal strand (approximately 0.5 μm in diameter)

with a mod

2.0 μ m in

This

morpholo

arboriz

diencep

method.

nuclei

descri

subdiv

charac

These

apply

delin

vi su

the

not

but

reve

info

with a moderate number of boutons (approximately from 1.0 to 2.0 μm in diameter).

DISCUSSION

This study shows for the first time the distribution and morphological characteristics of terminal axonal arborizations of neurons in four Vi subdivisional regions, to diencephalic and midbrain target nuclei utilizing the PHA-L method. Although projections from Vi to some of the target nuclei described in this study have been previously described, information regarding the specific Vi subdivisional region of origin, as well as the morphological characteristics of the terminal arborizations, is limited. These aspects of Vi projection neurons were evaluated by applying the anterograde PHA-L method (37) to the recently delineated Vi subdivisions (85).

Vi Subdivisional Regions

In this present study, it was important to re-evaluate the projections from neurons in the different regions of Vi, not only based on evidence of subdivisional differences (85), but also based on the results of previous studies which have revealed that different portions of Vi process sensory information from different orofacial receptive fields.

The m
fields in
trigeminal
maxillary
In addition
from spi
nerves V.
the red
(36,79,1
medullar
primary
and ind

In
fibers
so tha
invert
ophtha
to con
hairs
record
that t
vibris
innocu
throug
same t
vibris

The majority of primary afferent input from receptive fields in the orofacial region is conveyed to the sensory trigeminal nuclear complex (SVC) via the ophthalmic, maxillary and mandibular divisions of the trigeminal nerve. In addition, SVC also receives primary afferent information from spinal cord dorsal roots (57,86,98,109), and cranial nerves VII, IX and X (57), as well as non-primary inputs from the red nucleus (27,32,71), serotonergic raphe nuclei (36,79,105), locus coeruleus and lateral tegmental and dorsal medullary noradrenergic neuron groups (72). Other non-primary inputs arise from the cerebral cortex (15,55,63,116) and individual trigeminal sensory nuclei (38,43,46,47,74,80).

In rodents, the central processes of primary afferent fibers terminate in Vi from ventral to dorsal, respectively, so that the orofacial representation within the nucleus is inverted and medially facing (3,5,6,20,29,51). Maxillary-ophthalmic divisions of the trigeminal nerve have been shown to convey sensory information from mystacial vibrissae, guard hairs and hairy skin to ventrolateral Vi (3,8). Intra-axonal recording followed by HRP labeling in the rat have revealed that the vibrissa primary afferent map of a subpopulation of vibrissa afferents (which conduct rapidly and respond to innocuous stimulation) was inverted and medially oriented throughout the rostrocaudal extent of Vi (51). However, the same techniques utilized in the hamster reveal a tendency for vibrissa primary afferents to avoid the rostralmost portion

of Vi (20). Supportive of the latter findings, transganglionic transport of HRP in the rat showed that although the representation of the vibrissa rows appeared as virtually uninterrupted columns through the sensory trigeminal nuclei, there were regional variations in the density of terminal labeling such that there were more collaterals in caudal Vi from vibrissae afferents (as well as from nociceptive and lingual mucosa afferents) than in rostral Vi (3,5,50). These findings may suggest that there may be a segregation of primary afferent modalities such that more vibrissa-sensitive fibers terminate more in the caudal portion of Vi and more non-vibrissa sensitive fibers terminate more in the rostral portion of the nucleus; i.e., that vlVimc is more involved with processing information from non-vibrissa primary afferents from the guard hairs and hairy skin of the snout, while vlVipc may be more involved with processing information from mystacial vibrissa primary afferents. Another previous study (4) demonstrated that HRP-labeled central processes of the inferior alveolar nerve of the cat, which relays pain information from tooth pulp, project to all of the nuclei of the ipsilateral sensory trigeminal complex as a column located in the dorsal to middle portion of Vms, Vo, Vi and MDH. Although this study was in the cat, this may indicate that the dorsal portion of Vi (dmVi) is more involved with the relay of pain information from tooth pulp.

Utilization of the PHA-L Method

Previous anatomical studies have relied on methodology such as degeneration techniques, tritiated amino acids, anterograde and retrograde transport of HRP, anterograde transport of WGA-HRP and fluorescent dyes, to obtain information regarding the major efferent projections of Vi neurons. For the purpose of this study, these methods would have been limiting due to factors such as take-up by, or damage to, fibers of passage (WGA-HRP and degeneration techniques) and failure to reveal morphological details of axons and terminal arborizations due to the reaction product properties (tritiated amino acids) or to retrograde transport of the tracer (HRP, fluorescent dyes). The anterograde tracer PHA-L was utilized because, once taken up by cell bodies and dendrites of Vi neurons at the injection site, it completely fills the axons and their terminal arborizations, thereby permitting visualization of not only the distribution of the efferent axons to target nuclei, but also the exact location and morphological characteristics of their terminal arbors within these nuclei. In this study, data were obtained only from those injections which labeled cell bodies in the respective Vi subdivisional regions. Although it has been shown that PHA-L can be transported retrogradely (91) and anterogradely by fibers of passage (25), these modes of transportation did not appear to affect the results of this study. No labeled cell bodies were seen in regions outside

of the
in rost
passage
traject
midbra
ventro
ascend
axons
nuclei
fibers

Proje

anato

inclu

cat

arbor

known

somat

(21, 2

degen

spec

The 1

in v

resu

repr

of the injection site, except for a few labeled cell bodies in rostral MDH. The potential uptake of PHA-L by fibers of passage did not influence the results of this study. The trajectory of the axons which travel to the diencephalon and midbrain, emerge from the medial aspect of Vi, course ventromedially toward the midline and decussate before ascending to the target nuclei. However, the intratrigeminal axons which ascend and descend within the sensory trigeminal nuclei, may be considered vulnerable to PHA-L uptake as fibers of passage.

Projections to the Ventral Posteromedial Thalamic Nucleus

Thalamic projections from Vi have been studied anatomically and electrophysiologically in several mammals including the rat (17,21,22,28,29,35,49,67,81,84,102,118) and cat (18,69,119). The greatest number of terminal arborizations from Vi axons were observed in VPM, which is known to be the principal part of the thalamus which receives somatosensory information from orofacial regions (21,29,49,67,82,87). Previous studies using anterograde degeneration and HRP techniques (6,29) have described a specific somatotopic organization in the Vi-VPM projection. The facial representation in Vi is rotated approximately 225° in VPM. This rotation in the Vi-VPM axons essentially results in an upright and medially oriented facial representation in VPM. This organization would imply that

neurons

and the

ventral

the pr

subdiv

arbori

inject

termin

result

are d

this

subdi

proje

of in

(20)

affer

term

sugg

moda

the

from

port

of

thic

sugg

neurons in the ventral portion of Vi terminate in dorsal VPM, and those in the dorsal portion of Vi would project to ventral VPM. This is generally supported by the results of the present study, in which injections made in ventral Vi subdivisional regions resulted in labeled terminal arborizations primarily in the dorsal portion of VPM, and injections in dorsal Vi subdivisional regions labeled terminal arbors located primarily in ventral VPM. These results indicate that the various Vi subdivisional regions are different based on their projections to VPM. Although this somatotopic difference is apparent between the Vi subdivisional regions, differences in vlVimc and vlVipc projections suggest that they may also relay separate types of information. It has been suggested that in the hamster (20) and rat (3), there is a tendency for vibrissa primary afferents to avoid the rostralmost portion of Vi (vlVimc) and terminate more densely at caudal levels (vlVipc). These data suggest that there may be a segregation of primary afferent modalities such that vibrissa-sensitive fibers terminate in the caudal portion of Vi (vlVipc) and non-vibrissa fibers from guard hairs and hairy skin terminate in the rostral portion (vlVimc).

In the present study, two morphologically distinct types of vlVimc terminal arborizations were located in VPM, a thick-VPM type and a thin-VPM type. These findings may suggest that two types of Vi neurons convey orofacial sensory

information to VPM. In addition, terminal arbors from the thick-VPM type arbors often formed distinct patches among the more diffusely distributed thin-VPM type arbors. Although there is little support in the literature for two distinct types of Vi terminal axonal arborizations in VPM, a previous study in which WGA-HRP was injected into rat Vi described the distribution and some of the morphological characteristics of Vi axons terminating in VPM (84). Terminals from neurons in ventral Vi were located primarily in the dorsal portion of VPM, in what appeared to be a "patch-like" distribution. These "patches", referred to as "bushy arbors", gave rise to numerous irregular swellings up to 5 μm in diameter. Although this study did not identify two types of Vi terminal arbors in VPM, the type that was described is similar to the thick-VPM type described in the present study. It may be suggested that the "patches" formed by the thick-VPM type terminal arbors may be conveying specific somatosensory information to specific neuronal aggregates in VPM, while the thin-VPM type arbors may be sending information to VPM in a more diffuse and nonspecific manner. This suggestion is only speculative, and should be investigated more thoroughly through the use of electrophysiological and/or intracellular labeling techniques.

The functional importance of the Vi-VPM projection lies in the well-documented relationship between the mystacial vibrissae, VPM and the somatosensory cortices. When the

cytoarchitectonic organization of rodent Vi and VPM were investigated, through the use of the succinic dehydrogenase (SDH) method (8,65), an organization between the two nuclei was revealed in which rows of cellular clusters mainly in the ventrolateral portion of Vi, reminiscent of the rows of vibrissae on the rat's snout, was also apparent in the dorsomedial portion of the ventrobasal complex, i.e., dorsal VPM. Furthermore, the dorsomedial area of the ventrobasal complex corresponds to that which has been shown electrophysiologically to contain a somatotopic map of the rat vibrissae (8). These subcortical patterns of discrete clusters, referred to as barreloids, are also remarkably reminiscent of the pattern of barrels and SDH segmentation seen in layer IV of somatosensory cortex, and all of these patterns replicate the pattern of mystacial vibrissae on the rodent face (8,60,65,110,117). VPM has been shown to be reciprocally connected in a topographically organized manner with the first (SI) and second (SII) somatosensory cortices (26,59,100,114). Anatomical and electrophysiological studies on the organization of SI and SII have shown that their connections are somatotopically organized with the thalamus. It is likely that the functional significance of the Vi-VPM-SI/SII projection is to alert the cerebral cortex of well-localized orofacial stimulation so that it may be consciously perceived.

Projection

Pro

anatomic

(21,22,8

of the

medial

more di

topogra

there w

project

produce

adjacen

of Vi

distin

that s

projec

anatom

concur

Vi neu

that 7

VPM, 1

sugges

projec

both n

T

medial

Projections to the Posterior Thalamic Nuclear Group

Projections from Vi to medial Po have been studied anatomically and electrophysiologically in the rat (21,22,84). The present study is consistent with the findings of the previous studies in that the projection from Vi to medial Po was not as dense as was observed in VPM, and was more diffuse and widespread. There was also no obvious topographical organization with the projections to Po like there was in VPM. Although each Vi subdivisional region of Vi projects to a different region of VPM, all subdivisions produced scattered terminals in the medial portion of Po, adjacent to VPM. This study also revealed that the one type of Vi terminal arborization in medial Po as morphologically distinct, and different than those in VPM. This may infer that separate groups of Vi neurons give rise to Po and VPM projections. This is generally supported by previous anatomical studies in which fluorescent dyes, that were concurrently deposited into Po and VPM, retrogradely labeled Vi neurons (21). The results of this experiment revealed that 75% of the retrogradely labeled cells in Vi projected to VPM, 17.4% to medial Po and 7.4% were double-labeled. This suggests that at least two major populations of Vi neurons project to VPM and Po, and possibly a third which projects to both nuclei.

The functional significance of the projection from Vi to medial Po is still unclear. Previous studies have shown that

the media

with SI

the con

topograp

that in

which a

(30).

orofac

which

Althou

descr

invol

nucle

noxio

in

reco

inje

util

resp

disp

noxi

elec

fiel

larg

rest

for

the medial part of Po has reciprocal ipsilateral connections with SI (30,52,62,78). With the use of fluorescent tracers, the connections between medial Po and SI has revealed a topographically organized pattern of connections exists such that in medial Po, a map of the rat face is a mirror image which abuts the upright and medially oriented image in VPM (30). The areas of medial Po which receive input from orofacial regions of SI appear to overlap with the areas which receive Vi input as described in the present study. Although reciprocal connections between Po and SI have been described, it is not clear what type of information is involved. It has been suggested that the posterior thalamic nucleus is concerned with the perception of painful and noxious stimuli (11,12,58,88). However, a more recent study in which extracellular recording and intracellular recordings, as well as intracellular horseradish peroxidase injections, and receptive field mapping techniques were utilized (22), determined that 40% of the neurons in Po responded to vibrissae deflection, 18% by guard hair displacement, and the remainder by other stimuli including noxious stimuli. It has also been shown, through the use of electrophysiological techniques (22) that the receptive fields of vibrissa-sensitive cells in medial Po were much larger than those of cells in VPM which were quite restricted, and that the difference in receptive field size for neurons in the two nuclei is likely to reflect basic

different

neuronal

it has

electrical

Po and

tactile

precise

correction

has shown

with

space

terminal

for

somatosensory

response

tactile

Project

are

afferent

input

location

Utilization

technical

definition

differences in the processing operations carried out by the neurons of these two portions of the thalamus. Specifically, it has been suggested, as a result of combined anatomical and electrophysiological studies (21,22), that neurons in medial Po are specialized for processing more global aspects of tactile stimulation rather than stimulus magnitude and precise somatotopic locale. These findings and suggestions correspond well with the results in the present study which has shown that Vi projects to medial Po in a diffuse manner, with thin, sparsely branched terminal arbors with few, widely spaced boutons, while projections to VPM form discrete terminal patches. Thus, VPM does appear to be responsible for relaying specific tactile information from Vi to the somatosensory cortex, while medial Po appears to be responsible for relaying to the cortex more non-discrete tactile information from Vi.

Projections to Zona Incerta

Rat ZI has been shown to consist of six subregions which are different based on cytoarchitecture (56) as well as afferent (96) and efferent (94,97,111) connectivity. Vi input to ZI, one of the densest of the Vi projections, was located throughout the ventral subregion contralaterally. Utilizing anterograde degeneration (29) and WGA-HRP (84,96) techniques, previous studies have also described a well-defined contralateral projection from rat Vi to the ventral

ZI subregion. This ZI subregion also receives overlapping input from other somatosensory areas, including the somatosensory cortex, the dorsal column nuclei, and deep layers of SC (96,97). Taken together, these data appear to indicate that the ventral ZI subregion receives specific tactile afferents from the dorsal column nuclei and Vi, as well as somatosensory information from SC and the cerebral cortex. ZI neurons have been shown to project to several areas along the neuraxis, some of which also receive direct projections from Vi. These areas include SC, APT, RPC, inferior olive and cervical spinal cord (94,111). Using the method of retrograde transport of HRP, ZI neurons projecting to SC and APT are located in the ventral subregion. The precise location of ZI neurons projecting to RPC, IO and cervical spinal cord, however, is unclear. Although all Vi subdivisional regions projected to the ventral subregion of ZI, there were medio-lateral differences in the specific termination zone. The majority of terminal arbors from vlVipc and dmVi were located most medially in ventral ZI, while those from vlVimc and brVi were located more laterally. Although the facial representation in ZI is unclear, it is possible that the shift in termination zones of Vi terminal arbors is either due to different areas of facial representation in ZI, or to differences in the type of orofacial sensory input relayed by Vi to ZI. The former explanation seems less likely, based on the evidence that

vlVimc and vlVipc receive information from the same facial region.

At this point, the projection from Vi to ZI is still unclear. However, based on the findings that ZI neurons have been shown to project to several areas which receive direct projections from Vi, including SC, APT, RPC, inferior olive and cervical spinal cord (94,111), it appears that ZI may be used as an alternative route to areas that receive direct Vi projections. Two morphologically distinct types of PHA-L labeled terminal arbors were found in contralateral ZI after Vi injections, a complex-ZI type and a simple-ZI type. These findings suggest that perhaps at least two different types of Vi neurons convey information to this nucleus. The labeling of terminal arbors in ventral ZI following the various Vi injections was consistently dense, with the majority of them bearing multiple boutons.

Projections to the Anterior Pretectal Nucleus

The pretectal area has been studied anatomically in several species including rat (41,101,103) and cat (9,10,53). Although it is well known that part of the pretectum receives direct input from the retina (10,53) and projects to diencephalic structures related to the visual system (10,48), less is known about pretectal regions which do not appear to be connected to the visual system. Some regions of the pretectum have been shown to receive information from non-

visu

the

Foll

a de

in t

term

medi

part

be d

to :

dege

info

cort

inpu

that

conn

visu

subc

for

from

and

nucl

pulv

as

soma

visual somatosensory regions such as somatosensory areas of the cerebral cortex and the dorsal column nuclei (9,64,115). Following injections of PHA-L into Vi subdivisional regions, a dense patch of labeled terminal arborizations was located in the caudal one half of contralateral APT. Here the terminal patch is either centrally (vlVipc and dmVi) or medially (vlVimc and brVi) located, depending on the particular Vi subdivisional region injected. This may either be due to the specific somatotopical organization in APT, or to functional differences in APT. Autoradiographic and degeneration studies in the cat (9) have shown that afferent information from the dorsal column nuclei and somatosensory cortex terminate in a similar region of APT which receives Vi input in the rat. The present study supports the suggestion that the pretectum appears to be part of a circuit which connects peripheral and cortical somatosensory input with visually related structures (9).

APT has been shown to be involved with cortical and subcortical visual function, particularly the reflex pathway for the pupillary response, by receiving direct projections from the retina, SC, visual cortex and frontal eye fields, and projecting to visually related structures such as SC, nucleus of the optic tract, lateral geniculate nucleus, the pulvinar, and the nucleus of Edinger-Westphal (10), as well as some non-visual somatosensory regions such as somatosensory areas of the cerebral cortex and the dorsal

colum

could

rat i

input

visua

inhib

the r

compl

invol

docum

with

ventr

retic

(7,10

antir

which

the t

of w

Two t

APT 1

regio

that

proje

column nuclei (9,64,115). The circuit between Vi and APT could possibly play a role in the visual orientation of the rat in response to somatosensory input from orofacial sensory input. It has also been suggested that in addition to visually-related functions, APT may also be involved in inhibiting the jaw-opening reflex in rats and in inhibiting the responses of some neurons in the trigeminal nuclear complex, possibly as an antinociceptive effect (23,24). The involvement of APT in pain modulation is not unlikely, due to documented projections from APT to areas known to be involved with pain reception such as the intralaminar nuclei and ventrolateral nuclei of the thalamus, thalamic and midbrain reticular formation, zona incerta and the periaqueductal gray (7,10,66,112). The suggestion that APT plays a role in antinociception is supported by other studies in the rat which have provided evidence that APT stimulation inhibits the tail flick reflex and depresses the nociceptive responses of wide dynamic range neurons in the spinal cord (89,95). Two types of terminal axonal arborizations were located in APT following injections into each of the Vi subdivisional regions, a complex-APT type and a simple-APT type, suggesting that perhaps two types of Vi neurons contribute to this projection.

Projections to Superior Colliculus

The projection from Vi to SC is well-documented in several anatomical (17,45,61,91,102,106) and electrophysiological (1,34,92,99) studies in rodents, and cat (44,70,113). The Vi-SC projection in many of these studies is consistent with the findings of the present study, which reveals a predominantly contralateral projection to lateral portions of InG and InWh of rostral SC, as well as less dense labeling in the deep layers (53). Many of the anterograde studies on trigeminotectal projections from Vi describe the pattern of termination of the terminal arbors in SC as "discontinuous" or "patch-like" (44,45,61,91). This "patch-like" termination was also apparent in the present study. The distribution pattern of the patches of labeled terminal axonal arborizations from axons of neurons in some of the Vi subdivisional regions varied. Axons of vlVimc and vlVipc neurons gave rise to terminal axonal arborizations that were concentrated in the lateral one-third to one-half of contralateral SC, with some arbors located in the medial-most extent. Axons of neurons in dmVi gave rise to terminal arbors confined to the lateral-most portion of contralateral SC, and no arbors from axons of dmVi neurons were located in the medial part of SC. In addition, dmVi was the only region to produce labeled terminal arbors in ipsilateral SC. The projection from brVi was also different than the others, by giving rise to terminal arbors that were equally dense

throughout the mediolateral extent of contralateral SC. This difference in projections from the Vi subdivisional regions corresponds with the position of the rat face in contralateral SC (54). The somatotopic organization of tactile areas in SC is such that the face is upright and laterally oriented. The intermediate gray layer receives tactile projections from contralateral receptors of the orofacial region in a manner so that most of the tactile area is devoted to projections from the mystacial vibrissae. With this distorted facial representation in SC, the mystacial vibrissae occupies approximately the lateral two-thirds of SC, with the lateral-most portion used for input from the upper and lower lips. This supports the findings of the present study in which afferents from the snout (including mystacial vibrissae) are relayed by vlVimc and vlVipc to the lateral two-thirds of SC, and those from the upper and lower lips are relayed by dmVi to the lateral-most portion of SC.

Two morphologically distinct types of Vi terminal axonal arborizations were located in the receptive areas of SC in the present study. A complex-SC type and a simple-SC type were observed and this may suggest that two different populations of Vi neurons project to SC. Although several studies describe projections from individual nuclei of SVC to SC, relatively little is known about the morphological characteristics of their terminal arborizations. Single fiber recording and injection experiments in the hamster

descr

intra

that

respo

defle

and g

bouto

fashi

and g

bouto

arbor

camer

types

study

morph

but a

the i

likel

anima

evide

alter

infer

cord

may

infor

described the morphological characteristics of seven intracellularly HRP filled axons and terminal arbors in SC that responded to stimuli delivered to Vi (91). One type responded in an irregular but slowly adapting fashion to deflection of any one of eleven different mystacial vibrissae and gave rise to several branches which exhibited multiple boutons. The second type responded in a rapidly adapting fashion to deflection of any one of seven mystacial vibrissae and gave rise to significantly fewer branches with fewer boutons. These two functionally distinct types of terminal arbors also appear to be morphologically distinct, based on camera lucida drawings, and appear to be similar to the two types of Vi terminal arborizations described in the present study. This not only supports the suggestion that two morphologically distinct types of Vi axons terminate in SC, but also suggests that they are functionally distinct.

The functional significance of a projection from Vi to the intermediate and deep layers of SC, like in APT, most likely provides for visual and nonvisual orientation of the animal to orofacial stimulation. However, there is also evidence which suggests that SC may serve as part of alternative pathways to other Vi projection targets such as inferior olive (1,42), cerebellum (54) and cervical spinal cord (73,93). The two types of terminal axonal arborizations may indicate a separation of two different kinds of information relayed to SC from Vi, or may be utilized to

conve

Proje

devel

nucle

rostr

small

mixtu

disti

being

most

betwe

recei

cereb

porti

the c

Altho

the r

(82),

proba

termi

trige

subst

regio

recip

convey the same kind of information in different ways.

Projections to Parvocellular Red Nucleus

The rat red nucleus (RN), as in other mammals, is well developed and generally separated into a caudal magnocellular nucleus (RMC) which contains numerous large neurons, a rostral parvocellular nucleus (RPC) which contains numerous small cells, and an intermediate area which contains a mixture of large and small neurons (82,90). The ease of distinction of RPC and RMC varies from species to species being relatively difficult to distinguish in the cat (14) and most distinct in primates (33). The rat falls somewhere between these two extremes (90). The magnocellular portion receives most of its afferent input from the interpositus cerebellar nucleus (31,77,82), while the parvocellular portion receives input primarily from nucleus lateralis of the cerebellum and the sensorimotor cortex (19,75,76,77,82). Although the main efferent projection from the red nucleus is the rubrospinal tract, arising primarily from neurons in RMC (82), it also provides a crossed rubrobulbar projection, probably via collaterals of the rubrospinal tract, which terminate in a number of brain stem centers including the trigeminal nuclei (68,82). The present study shows a substantial projection from each of the Vi subdivisional regions to contralateral RPC, suggesting a possible reciprocal connection between Vi and RN. However, one

previ
vi to
SVC,
but n

somew
proje
proje
Thus,
an a
possi
throu
Altho
rubre
contr
corr
circ
info
spin
the
Only
loca
in v
arbo
cell
RPC

previous study does not support a significant projection from Vi to RN (113). Following injections of WGA-HRP into cat SVC, labeling was observed in several mesencephalic nuclei, but not RN.

The function of the projections from Vi to RPC is still somewhat unclear, due to a lack of clarity in the efferent projections of RPC. Some studies support a rubro-olivary projection in the rat (107,108) while others do not (2). Thus, it is difficult to conclude whether or not RN provides an alternative pathway to inferior olive from Vi. It is possible, however, that RPC serves as an alternative nucleus through which Vi communicates with the cervical spinal cord. Although it has long been known that RMC gives rise to rubrospinal axons, some studies have provided evidence for a contribution from RPC (16,32,82). If these latter data are correct, this sets up a potential trigemino-rubro-spinal circuit in the rat that could potentially relay somatosensory information from orofacial primary afferents to the cervical spinal cord. The purpose of such a pathway may provide for the orientation of the head and neck to orofacial stimuli. Only one type of Vi efferent terminal axonal arborization was located in RPC, possibly suggesting that one type of neuron in Vi projects to RPC. The boutons of the RPC-type terminal arborizations were often closely approximated to neuronal cell bodies, suggesting a potentially influential input on to RPC neurons.

Projections to the Medial Accessory Oculomotor Nucleus

The projection to the area labeled by Paxinos and Watson (83) as MA3 occurred only as a result of injections into dmVi. None of the other Vi subdivisional regions gave rise to terminal arbors in this nucleus. There is very little information regarding the afferent and efferent connectivity of MA3 in the rat, which is located medial to the fibers of the medial longitudinal fasciculus in the rostral midbrain (83). Because of a lack of information on MA3, the functional significance of the projection to this area is unclear. However, the oculomotor complex as a whole appears to serve to integrate vestibular input with input from the cerebral cortex and SC, while input from the retina may also contribute (13). In electrophysiological experiments in which portions of the complex were stimulated, rotation of the head, ocular torsion, and deviation of the eyes have been observed. Thus, it can only be assumed at this time, that MA3 in the rat has related functions to those described above, and that the projection from dmVi to this area helps to coordinate head and eye movement in response to orofacial tactile stimuli. However, this is only speculative, and should be further substantiated.

Differences in Projections from Vi Subdivisional Regions

The main differences in the projections from the four Vi subdivisional regions to diencephalic and midbrain target

nucle

regio

form

vlVip

proje

dorse

diff

repr

neuro

simil

proje

subdi

from

scatt

The c

was

arbor

conce

in th

shift

compa

dmVi

under

affer

A si

subdi

nuclei were primarily topographical differences. All four regions projected to contralateral VPM and terminated in the form of discrete patches. The projection from vlVimc and vlVipc were confined to the dorsal portion of VPM, while projections from dmVi and brVi terminated in ventral and dorsolateral portions, respectively. These topographical differences seem to correspond well with the orofacial representations in Vi and VPM. In addition, axons from neurons in each of the four Vi subdivisions gave rise to similar types of terminal arborizations in VPM. The projections to the medial Po was similar from all Vi subdivisional regions. The terminal axonal arborizations from all Vi-Po axons were similar in morphology and widely scattered throughout contralateral Po, just medial to VPM. The distribution of labeled terminal arbors from Vi-ZI axons was similar from the four Vi subdivisional regions. The arbors were similar from all regions of Vi and were concentrated in the ventral zone of contralateral ZI, mainly in the caudal portion. There was, however, a slight lateral shift in the terminal zones of axons from vlVimc and brVi as compared to the areas of termination following vlVipc and dmVi injections. The significance of this shift is not understood due to the lack of information regarding specific afferent and efferent connectivity in the ventral zone of ZI. A similar set of circumstances exists in APT. All Vi subdivisional regions projected to the caudal one-half of

cont

resu

cent

resu

loca

soma

deta

orga

dedu

proj

vent

from

arbo

half

term

in d

in t

prec

dmV

Thes

corr

dema

repr

No c

red

sim

contralateral APT, however, the large terminal patch that resulted from vlVipc and dmVi injections were located more centrally in the nucleus, while the terminal zones that resulted from vlVimc and brVi injections were more medially located. It has been shown that this area of APT receives somatosensory input from other nuclei, however, lack of more detailed descriptions of the connectivity and/or somatotopic organization in this portion of APT makes it difficult to deduce the significance of the Vi projections. The projections to SC were topographically different from the ventrolateral, dorsomedial and border regions of Vi. Axons from neurons in vlVimc and vlVipc gave rise to terminal arborizations mainly located in the lateral one-third to one-half of contralateral SC, while those from neurons in brVi terminated throughout the mediolateral extent of SC. Neurons in dmVi were different from those in the other regions of Vi in that they projected bilaterally to SC, with contralateral predominance. In addition, the terminal arborizations from dmVi neurons were confined to the lateralmost portion of SC. These differences in the four groups of Vi-SC projections correspond with the somatotopical organization that has been demonstrated in SC (54), which reveals a facial representation that is upright and laterally facing in SC. No obvious differences were found in the projections to the red nucleus from the Vi subdivisions. They all projected to similar portions of RPC. Only injections into dmVi produced

label

termin

predo

funct

ascen

acces

speci

input

diffe

three

repr

inje

of

diffe

are

stud

Coll

furt

extr

char

arbo

Thro

Vi

cour

labeled terminal arbors in MA3. Although sparse, the labeled terminal arbors were located bilaterally with contralateral predominance. There is little information on rat MA3, so the functional significance of this projection is difficult to ascertain. However, based on what is known about the accessory oculomotor nuclei, in general, dmVi may play a special role in visual orientation to orofacial sensory input. Finally, it is possible that some subdivisional differences in Vi may have been masked by consolidating the three dorsal Vi subdivisions (irVi, dcVi and dlVi) as represented by dmVi. Attempts to make precise, well-contained injections in the three dorsal subdivisions led to spreading of the PHA-L tracer into adjacent subdivisions. Thus, differences in the projections from the six Vi subdivisions are possibly greater than those revealed by the present study.

Collateral Projections

Without the use of intracellular labeling techniques and further anterograde and retrograde transport studies, it is extremely difficult to visualize the morphological characteristics of somata, dendrites, axons and terminal arborizations of Vi projection neurons simultaneously. Throughout this study it has been assumed that the axons of Vi projection neurons do not collateralize during their course to their target nuclei, and that morphologically

distinct terminal axonal arborizations may be indicative of different types of Vi neurons. If this were the case, however, these data would suggest that at least five types of Vi neurons project to the various target nuclei described above. Two distinct types would project only to VPM, a third type to Po, a fourth type to ZI, APT, SC and RPC, and a fifth type to ZI, APT, SC and MA3. It is suggested here that, regardless of whether morphologically distinct Vi efferent terminal axonal arborizations are monosynaptic connections from distinct neuron groups, or if they are collaterals from the same neuron groups, the "complex" type of terminal arbors are more influential in the various target nuclei than are the "simple" types. This suggestion is based on the higher degree of branching of the "complex" type as well as the greater frequency of synaptic boutons. Without the application of immunohistochemical and/or electron microscopic techniques, it can not be absolutely determined if the connections described in this study are excitatory or inhibitory, however, the "complex" type terminal arbors would probably have a stronger excitatory or inhibitory effect on the target nuclei than would the "simple-type".

Previous studies have indicated that collateralization of the axons of some of the projection neurons in Vi to more than one target nucleus does occur. Double retrograde fluorescent labeling techniques in the rat have shown a significant number of neurons in Vi which project to both the

thalamic ventrobasal complex and the cerebellum (81,102). This has been refuted by antidromic collision techniques, combined electrophysiological recording and antidromic stimulation techniques, and double retrograde transport of Fast Blue and HRP, which have revealed that very few, if any, Vi neurons project to both the ventrobasal thalamus and the cerebellum (49,67,118). Although the collateralization of trigeminothalamic axons to the cerebellum is debatable, it appears less doubtful that trigeminothalamic axons from Vi do send collaterals to SC. Double retrograde transport of fluorescent dyes, and combined electrophysiological recordings and antidromic stimulation techniques in rodents reveal substantial collateralization of trigeminothalamic axons to SC (17,49,102,106). Also demonstrated by these techniques is collateralization of trigeminothalamic axons to main sensory trigeminal nucleus (49,102). Anterograde and retrograde transport studies suggest that dorsal accessory and principal nuclei of the inferior olive receive input from Vi neurons which also innervate SC and receive the same kind of tactile input (45). A more recent study revealed that at least some of the axons of Vi cells are collateralized (87). When HRP was injected into the thalamus, 80% of the large multipolar neurons were labeled, 50% of these neurons were labeled after cerebellar injections, and 60% were labeled following spinal cord injections. These data indicate that there must be collateralization of at least 30% of the large

multipolar neurons in this region. It has been suggested by Phelan and Falls ('90) that since the collateralization of trigeminothalamic and trigeminospinal cells has not previously been reported, the collateralization must exist between trigeminothalamic and trigeminocerebellar neurons. In addition, it has been previously suggested that main sensory trigeminal efferents terminating in ZI are collaterals of those destined for the thalamus (104).

Several of the above studies provide convincing evidence that some collateralization of Vi neurons does occur, especially the collateralization of some trigeminothalamic axons. Given these data, and the fact that Vi terminal axonal arborizations in VPM are morphologically distinct from Vi terminal axonal arborizations in the other target areas, it is suggested that some Vi-thalamic neurons give rise to collaterals which innervate different target nuclei, and that the terminal axonal arborizations of these collateralized axons are probably morphologically different. Thus, the number of different types of Vi neurons which give rise to projections described in this study may be less than five. However, without additional retrograde studies from the described target nuclei, numbers of distinct neuronal types projecting to these targets cannot be determined absolutely.

Figure 1: PHA-L Injection Sites.

Schematic drawings (E-H) of representative transverse sections (A-D) through PHA-L injection sites (IS) in four subdivisional regions of rat trigeminal nucleus interpolaris (Vi), which include: ventrolateral magnocellular (vlVimc; A, E), ventrolateral parvocellular (vlVipc; B, F), dorsomedial (dmVi; C, G) and border region (brVi; D, H). The injection sites were, for the most part, confined to the respective subdivisional area of rat Vi. Amb, ambiguous nucleus; IO, inferior olive; svt, spinal trigeminal tract.

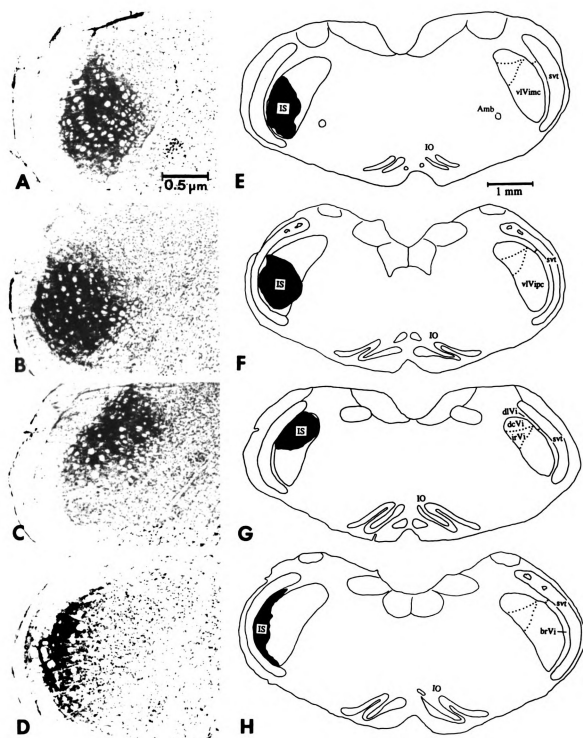


Figure 1

Figure 2: Diencephalic Projections from vlVimc and vlVipc.

A-D. Schematic drawings of representative transverse sections through the diencephalon from rostral to caudal, at the approximate interaural levels of 6.20 mm, 5.86 mm, 5.40 mm and 4.84 mm, respectively, which show the distribution of vlVimc efferent terminal axonal arborizations in dorsal ventral posteromedial thalamic nucleus (VPM), medial posterior thalamic nucleus (Po) and ventral zone of zona incerta (ZI). E-H. Distribution of vlVipc efferent terminal axonal arborizations in the dorsal portion of VPM, medial Po and ventral zone of ZI. fr, fasciculus retroflexus; ic, internal capsule; ml, medial lemniscus; PF, parafascicular thalamic nucleus; Re, reuniens thalamic nucleus; STh, subthalamic nucleus; VPL, ventral posterolateral thalamic nucleus.

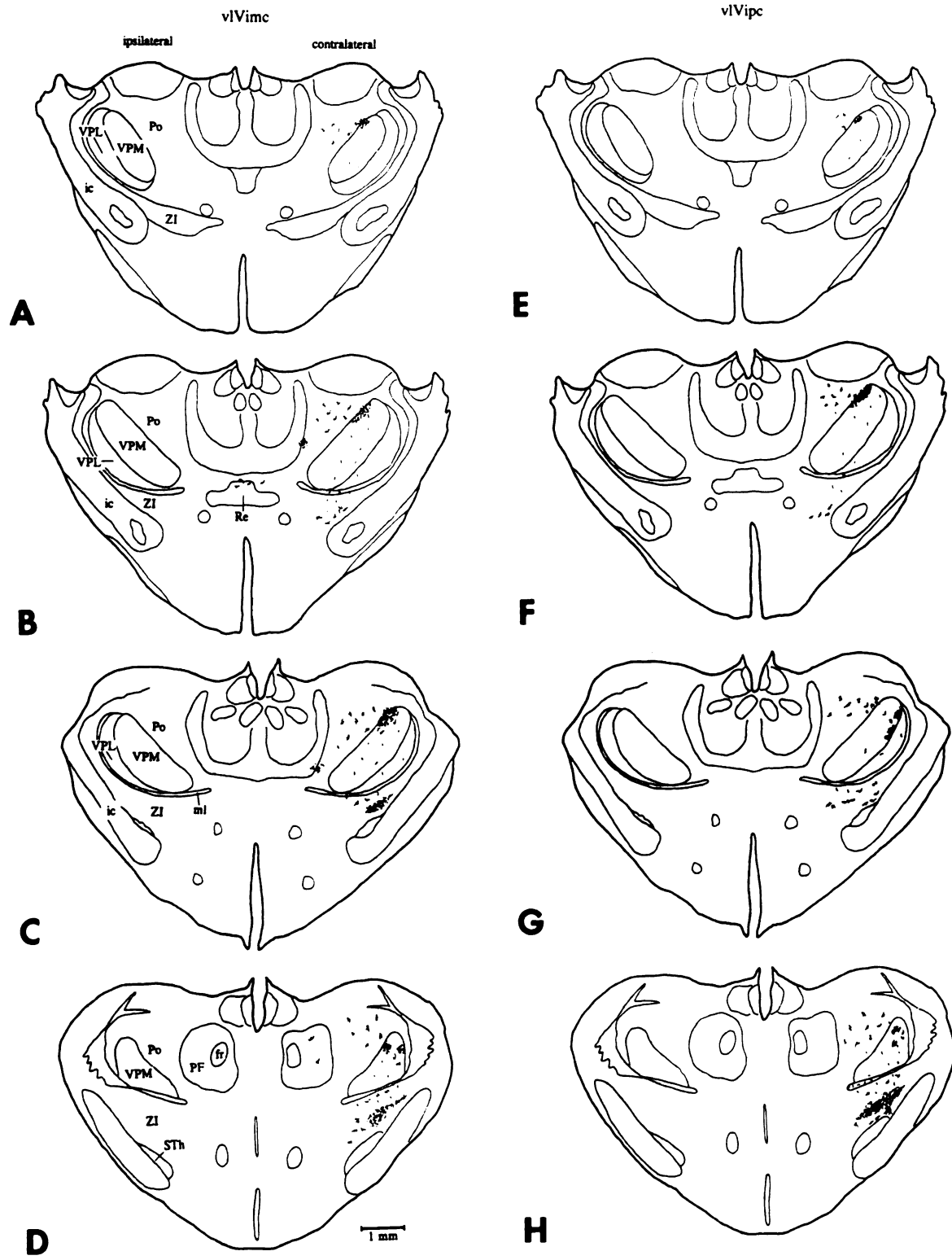


Figure 2

Figure 3: Diencephalic Projections from dmVi and brVi.

A-D. Schematic drawings of representative transverse sections through the diencephalon from rostral to caudal, respectively, showing the distribution of dmVi efferent terminal axonal arborizations in the ventral portion of VPM, medial Po and ventral zone of ZI. E-H. Distribution of brVi efferent terminal axonal arborizations in the lateralmost portion of VPM, medial Po and ventral zone of ZI.

Figure 4: Midbrain Projections from vlVimc and vlVipc.

A-D. Schematic drawings of representative transverse sections through the midbrain from rostral to caudal, at the approximate interaural levels of 3.70 mm, 3.20 mm, 2.20 mm and 1.70 mm, respectively, showing the distribution of vlVimc efferent terminal axonal arborizations in the medial portion of anterior pretectal nucleus (APT), dorsal parvocellular red nucleus (RPC), and the lateral two-thirds of intermediate gray (InG) and intermediate white (InWh) layers of superior colliculus (SC). E-H. Distribution of vlVipc efferent terminal axonal arborizations in central APT, dorsal RPC, and lateral two-thirds of InG and InWh of SC. CG, central gray; DK, nucleus Darkschewitsch; III, oculomotor nucleus; MA3, medial accessory oculomotor nucleus; MGN, medial geniculate nucleus; ml, medial lemniscus; Op, optic nerve layer superior colliculus; Pn, pontine nuclei; SuG, superficial gray layer superior colliculus.

A

B

C

D

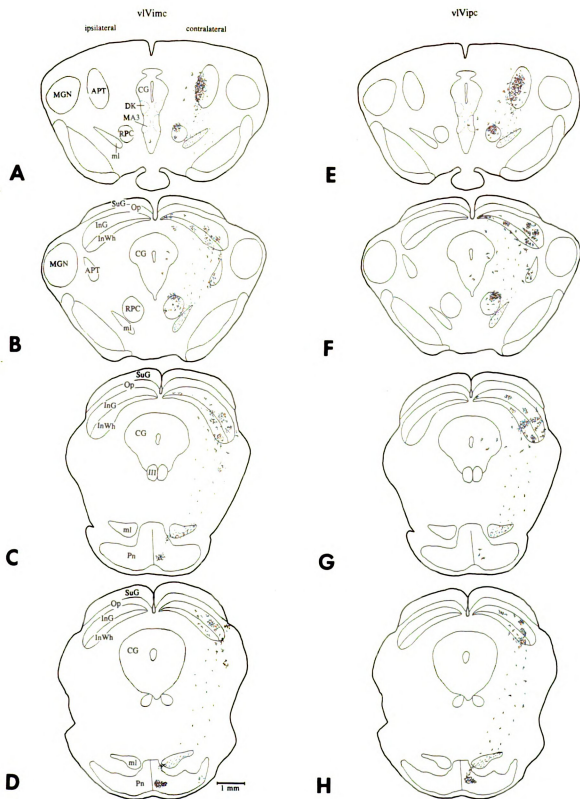


Figure 4

Figure 5: Midbrain Projections from dmVi and brVi.

A-D. Schematic drawings of transverse sections through the midbrain from rostral to caudal, respectively, showing the distribution of dmVi efferent terminal axonal arborizations in the central portion of APT, dorsal RPC, contralateral and ipsilateral MA3, and lateralmost portion of contralateral and ipsilateral InG and InWh of SC. E-H. Distribution of brVi efferent terminal axonal arborizations in medial APT, dorsal RPC, and throughout the mediolateral extent of InG and InWh of SC.

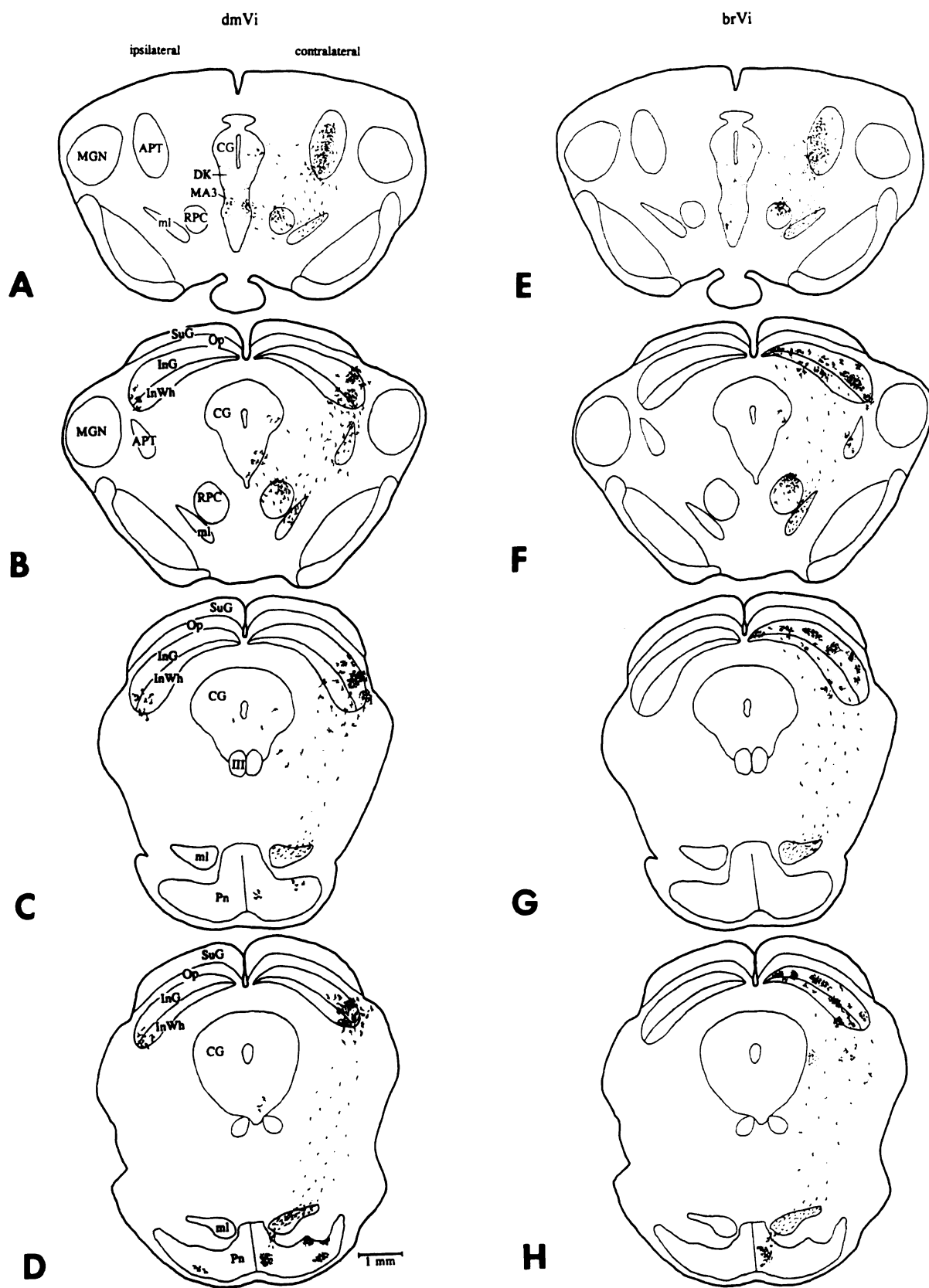


Figure 5

Figure 6: Drawings of Terminal Axonal Arborizations in VPM.

A. Drawing of a typical Vi terminal "patch" in VPM, comprised of thick-VPM and thin-VPM type terminal axonal arborizations. B. Representative drawings of thick-VPM type terminal arbor (1,2), characterized by relatively thick terminal strands (ts) and large, irregularly shaped boutons (b), and thin-VPM type terminal arbor (3,4), characterized by thinner terminal strands and large, irregularly shaped boutons. pf, parent fiber.

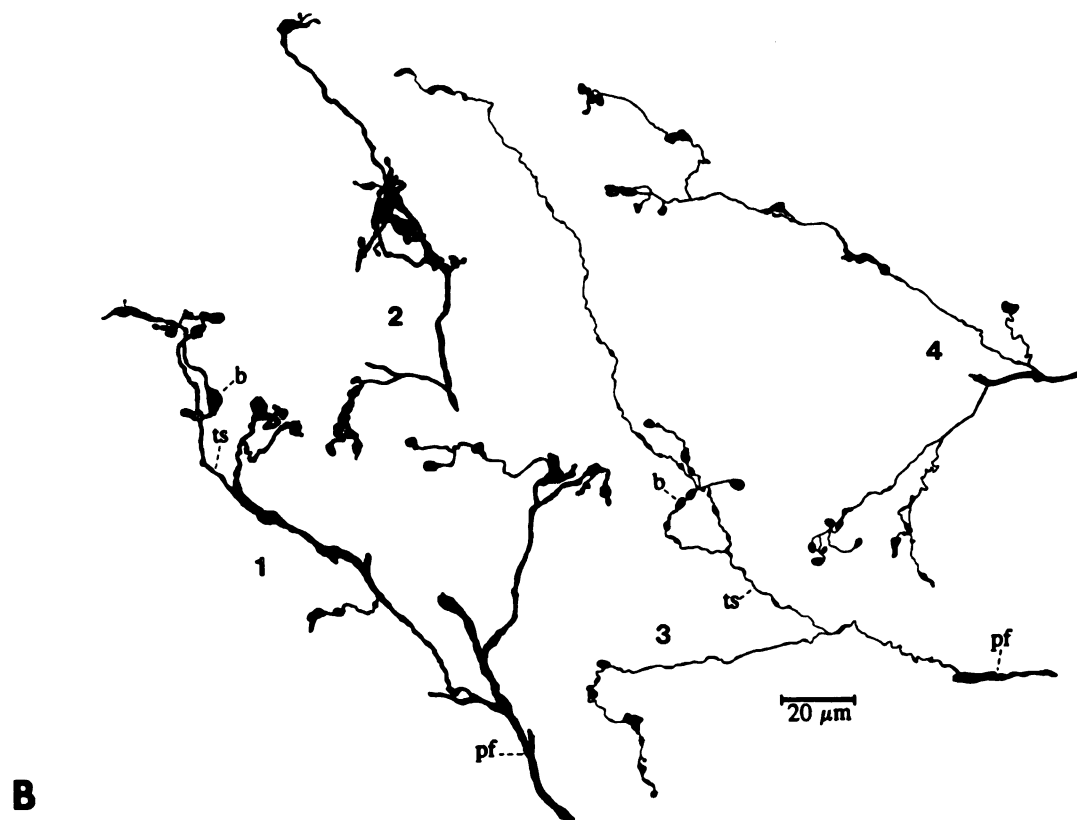
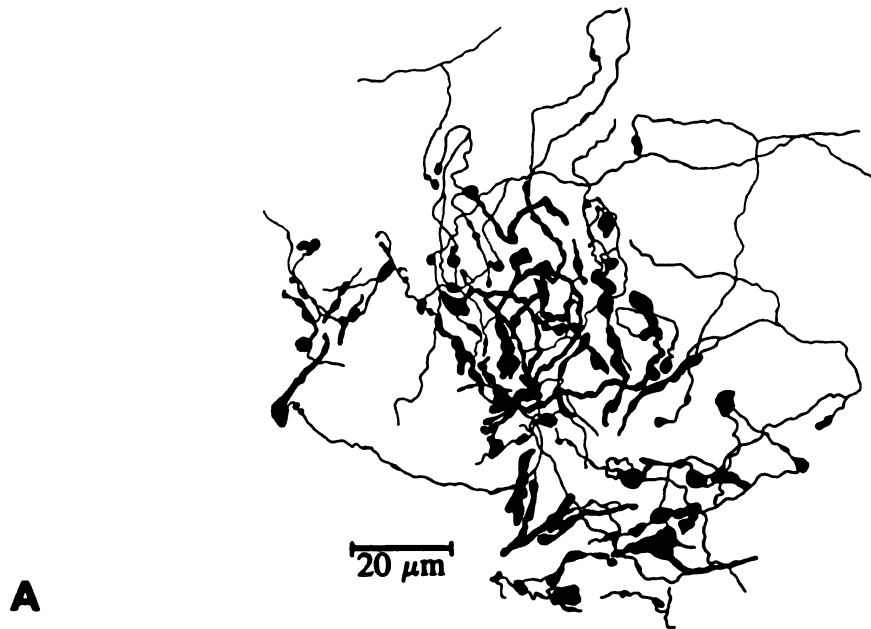


Figure 6

Figure 7: Drawings of Terminal Axonal Arborizations in Po and ZI.

A. Representative drawings of Po-type terminal axonal arborization in Po, characterized by long, thin filamentous terminal strands and a relatively large terminal bouton. B. Representative drawings of complex-ZI type terminal arbor (1,2), characterized by branched terminal strands with multiple boutons, and simple-ZI type terminal axonal arbor (3,4), characterized by more sparsely branched terminal strands with fewer, widely spaced boutons.

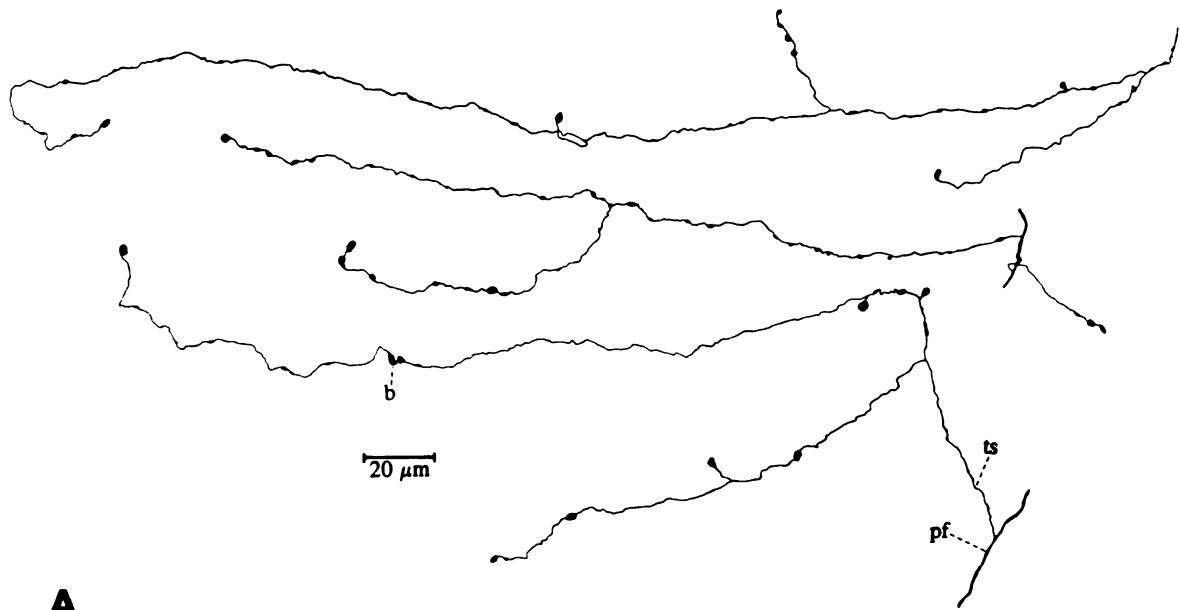
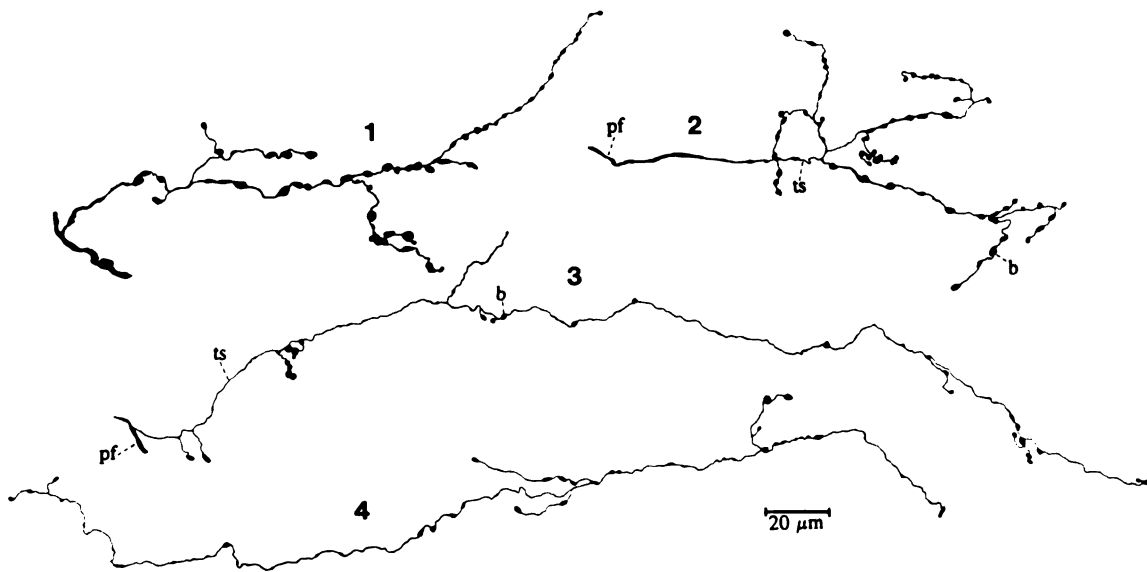
**A****B**

Figure 7

**Figure 8: Drawings of Terminal Axonal Arborizations in
APT and SC.**

A. Representative drawings of complex-APT type terminal arbors (1,2), characterized by branched terminal strands with multiple boutons, and simple-APT type terminal arbors (3,4), characterized by more sparsely branched terminal strands with fewer, widely spaced boutons. B. Representative drawings of complex-SC type terminal arbors (1,2), characterized by branched terminal strands with multiple boutons, and simple-SC type terminal arbors (3,4), characterized by more sparsely branched terminal strands with fewer, widely spaced boutons.

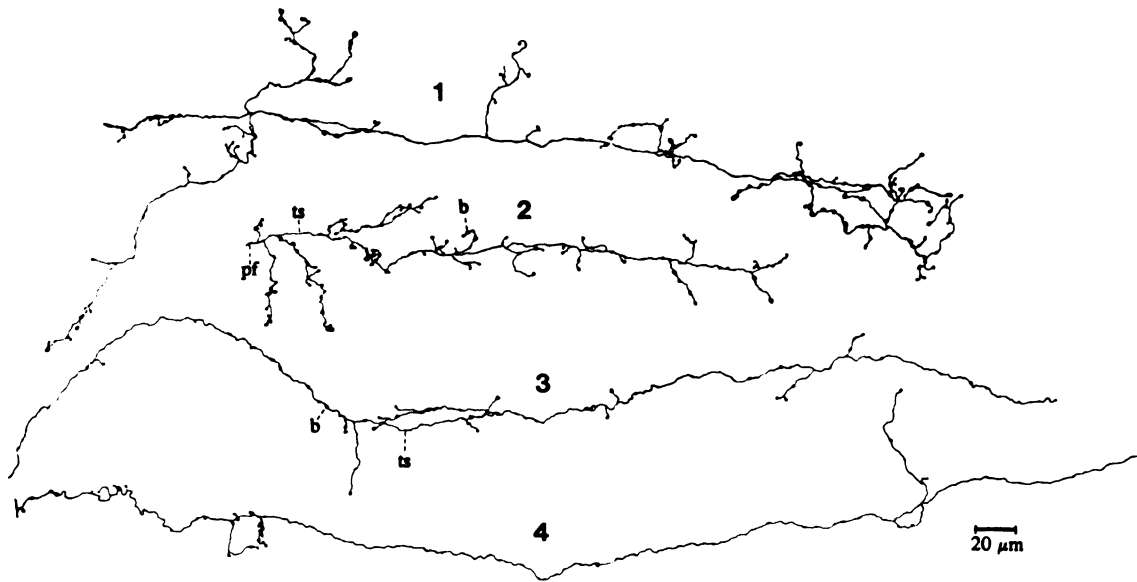
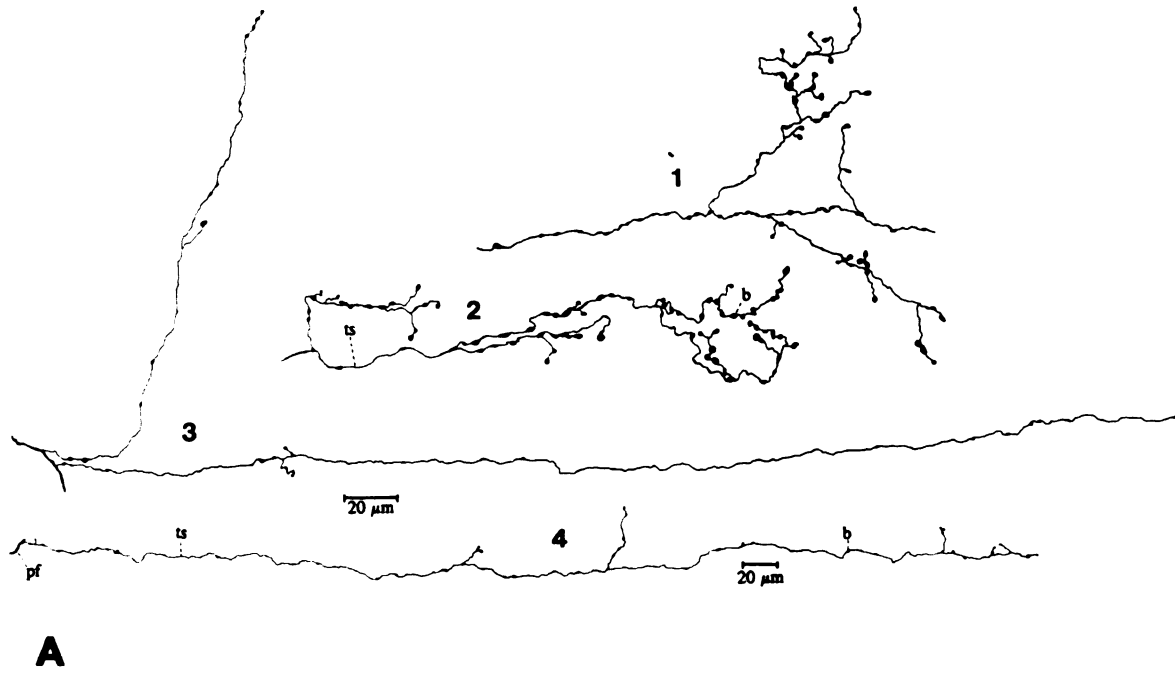



Figure 8



**Figure 9: Drawings of Terminal Axonal Arborizations in
RPC and MA3.**

A. Representative drawings of RPC-type terminal axonal arbors, characterized by branched terminal strands with multiple, closely spaced boutons. B. Representative drawings of MA3-type terminal arbors, characterized by sparsely branched terminal strands with fewer boutons.

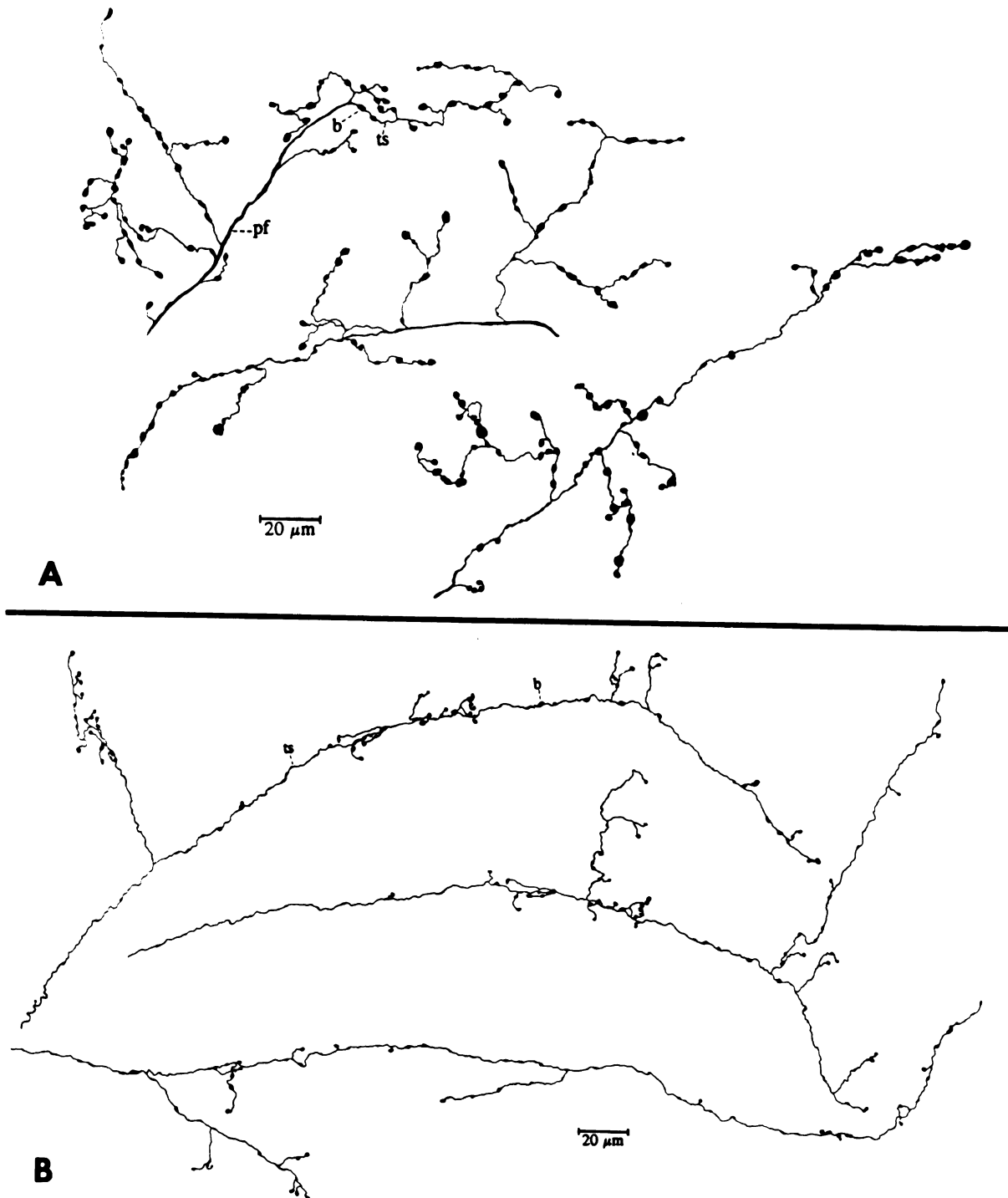


Figure 9

**Figure 10: Photomicrographs of Terminal Axonal Arborizations
in VPM, Po and ZI.**

Photomicrographs that document the morphological characteristics of the thick-VPM type (A), thin-VPM type (B), Po-type (C) and complex-ZI type (D) efferent terminal axonal arborizations from neurons in Vi.

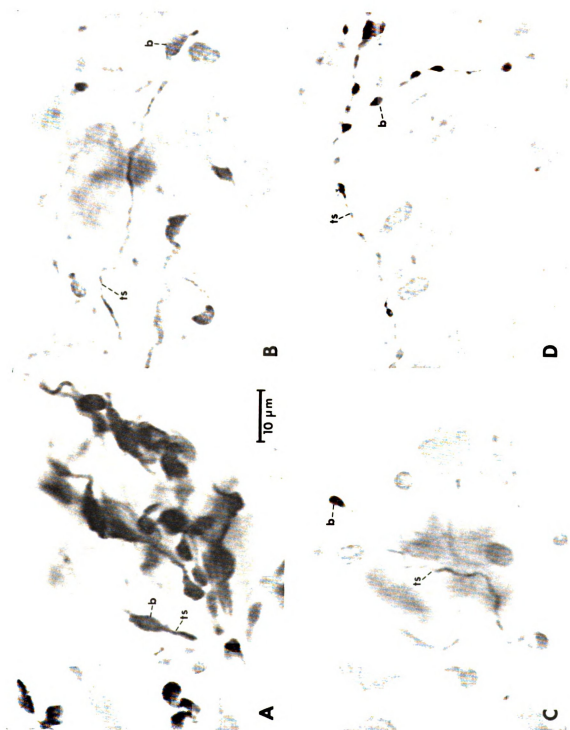



Figure 10



**Figure 11: Photomicrographs of Terminal Axonal Arborizations
in ZI, APT and SC.**

Photomicrographs that document the morphological characteristics of the simple-ZI type (A), complex-APT type (B), simple-APT type (C) and complex-SC type (D) efferent terminal axonal arborizations from neurons in Vi.

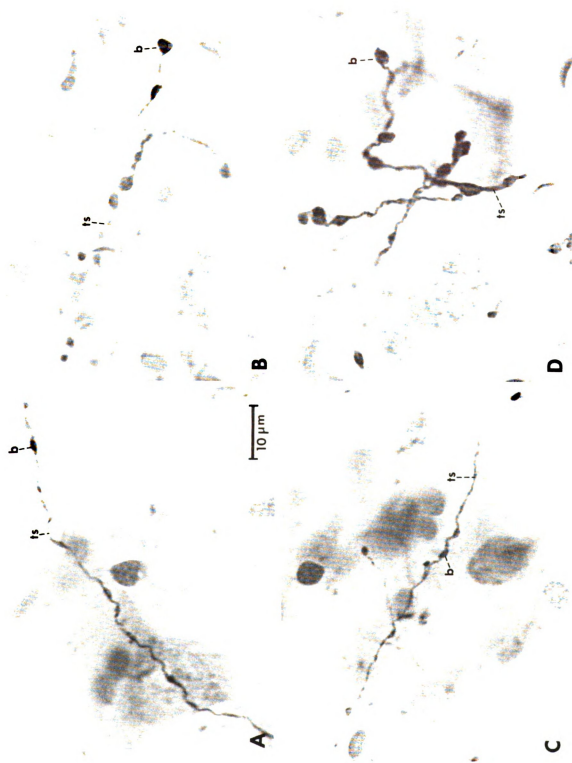
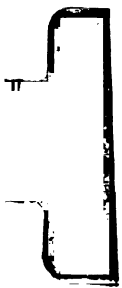


Figure 11



**Figure 12: Photomicrographs of Terminal Axonal Arborizations
in SC, RPC and MA3.**

Photomicrographs that document the morphological characteristics of the simple-SC type (A), RPC-type (B) and MA3-type (C,D) efferent terminal axonal arborizations from neurons in Vi.

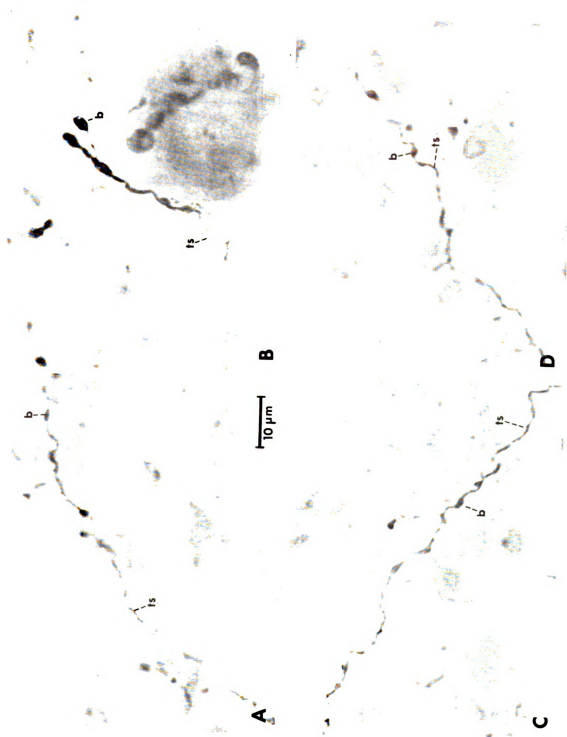


Figure 12

BIBLIOGRAPHY

1. Akaike, T. (1988) Electrophysiological analysis of the trigemino-tecto-olivo-cerebellar (crus II) projection in the rat. *Brain Res.* 442:373-378.
2. Anderson, W.A., J.G. Rutherford, and D.C. Gwyn. (1983) Midbrain and diencephalic projections to the inferior olive in rat. *Proc. Fed. Biol. Soc.* 26:132.
3. Arvidsson, J. (1982) Somatotopic organization of vibrissae afferents in the trigeminal sensory nuclei of the rat studied by transganglionic transport of HRP. *J. Comp. Neurol.* 211:84-92.
4. Arvidsson, J. and S. Gobel (1980) An HRP study of the central projections of primary trigeminal neurons which innervate tooth pulps in the cat. *Brain Res.* 210:1-16.
5. Arvidsson, J. and F.L. Rice (1991) Central projections of primary sensory neurons innervating different parts of the vibrissae follicles and intervibrissal skin on the mystacial pad of the rat. *J. Comp. Neurol.* 309:1-16.
6. Bates, C.A., and H.P. Killackey. (1985) The organization of the neonatal rat's brainstem trigeminal complex and its role in the formation of central trigeminal patterns. *J. Comp. Neurol.* 240:265-287.
7. Beitz, A.J. (1982) The organization of afferent projections to the midbrain periaqueductal gray of the rat. *Neurosci.* 7:133-159.
8. Belford, G.R., and H.P. Killackey. (1979) Vibrissae representation in subcortical trigeminal centers of the neonatal rat. *J. Comp. Neurol.* 183:305-322.
9. Berkley, K.J., and D.C. Mash. (1978) Somatic sensory projections to the pretectum in the cat. *Brain Res.* 158:445-449.
10. Berman, N. (1977) Connections of the pretectum in the cat. *J. Comp. Neurol.* 174:227-254.
11. Boivie, J. (1979) An anatomical reinvestigation of the termination of the spinothalamic tract in the monkey. *J. Comp. Neurol.* 186:343-370.

12. Bowsher, D. (1957) Termination of the central pain pathway: The conscious appreciation of pain. *Brain*. 80:606-622.
13. Brodal, A. (1981) Neurological Anatomy in Relation to Clinical Medicine. Third Ed. Oxford Univ. Press, N.Y.
14. Brodal, A., and A.C. Gogstad. (1954) Rubrocerebellar connections. An experimental study in the cat. *Anat. Rec.* 118:455-485.
15. Brodal, A., T. Szabo, and A. Torvik. (1956) Corticofugal fibers to sensory trigeminal nuclei and nucleus of the solitary tract. An experimental study in the cat. *J. Comp. Neurol.* 106:527-556.
16. Brown, L.T. (1974) Rubrospinal projections in the rat. *J. Comp. Neurol.* 154:169-187.
17. Bruce, L.L., J.G. McHaffie, and B.E. Stein. (1987) The organization of trigeminothalamic and trigeminothalamic neurons in rodents: A double-labeling study with fluorescent dyes. *J. Comp. Neurol.* 262:315-330.
18. Burton, H., and A.D. Craig Jr. (1979) Distribution of trigeminothalamic projection cells in the cat and monkey. *Brain Res.* 161:515-521.
19. Caughell, K.A., and B.A. Flumerfelt. (1977) The organization of the cerebellorubral projection: An experimental study in the rat. *J. Comp. Neurol.* 176:295-306.
20. Chiaia, N.L., P.R. Hess, M. Hosoi, and R.W. Rhoades. (1987) Morphological characteristics of low-threshold primary afferents in the trigeminal subnuclei interpolaris and caudalis (the medullary dorsal horn) of the golden hamster. *J. Comp. Neurol.* 264:527-546.
21. Chiaia, N.L., R.W. Rhoades, C.A. Bennett-Clarke, S.E. Fish, and H.P. Killackey. (1991) Thalamic Processing of Vibrissal Information in the Rat. I. Afferent Input to the Medial Ventral Posterior and Posterior Nuclei. *J. Comp. Neurol.* 314:201-216.
22. Chiaia, N.L., R.W. Rhoades, S.E. Fish, and H.P. Killackey. (1991) Thalamic Processing of Vibrissal Information in the Rat: II. Morphological and Functional Properties of Medial Ventral Posterior Nucleus and Posterior Nucleus Neurons. *J. Comp. Neurol.* 314:217-236.

23. Chiang, C.Y., I.C. Chen, J.O. Dostrovsky and B.J. Sessle. (1989) Inhibitory effect of stimulation of the anterior pretectal nucleus on the jaw-opening reflex. *Brain Res.* 497:325-333.
24. Chiang, C.Y., J.O. Dostrovsky and B.J. Sessle. (1990) Role of anterior pretectal nucleus in somatosensory cortical descending modulation of jaw-opening reflex in rats. *Brain Res.* 515:219-226.
25. Cliffer, K.D., and G.J. Giesler Jr. (1988) PHA-L can be transported anterogradely through fibers of passage. *Brain Res.* 458:185-191.
26. Donaldson, L., P.J. Hand and A.R. Morrison. (1975) Cortical-thalamic relationships in the rat. *Exp. Neurol.* 47:448-458.
27. Edwards, S.B. (1972) The ascending and descending projections of the red nucleus in the cat: An experimental study using an autoradiographic tracing method. *Brain Res.* 48:45-63.
28. Erzurumlu, R.S., C.A. Bates, and H.P. Killackey. (1980) Differential organization of thalamic projection cells in the brainstem trigeminal complex of the rat. *Brain Res.* 198:427-433.
29. Erzurumlu, R.S., and H.P. Killackey. (1980) Diencephalic projections of the subnucleus interpolaris of the brainstem trigeminal complex in the rat. *Neurosci.* 5:1891-1901.
30. Fabri, M., and H. Burton. (1991) Topography of connections between primary somatosensory cortex and posterior complex in rat: a multiple fluorescent tracer study. *Brain Res.* 538:351-357.
31. Flumerfelt, B.A. (1980) An ultrastructural investigation of afferent connections of the red nucleus in the rat. *J. Anat.* 131:621-633.
32. Flumerfelt, B.A. and D.G. Gwyn. (1974) The red nucleus of the rat: Its organization and interconnections. *J. Anat.* 118:374.
33. Flumerfelt, B.A., S. Otabe, and J. Courville. (1973) Distinct projections to the red nucleus from the dentate and interposed nuclei in the monkey. *Brain Res.* 50:408-414.

34. Fujikado, T., Y. Fukuda, and K. Iwama. (1981) Two pathways from the facial skin to the superior colliculus in the rat. *Brain Res.* 212: 131-135.
35. Fukushima, T., and F.W.L. Kerr. (1979) Organization of trigeminothalamic tracts and other thalamic afferent systems of the brainstem in the rat: Presence of gelatinosa neurons with thalamic connections. *J. Comp. Neurol.* 183:169-184.
36. Fuxe, K. (1965) Evidence for the existence of monoamine neurons in the central nervous system. IV. Distribution of monoamine terminals in the central nervous system. *Acta Physiol. Scand.* 64 (Suppl. 247):37-85.
37. Gerfen, C.R., and P.E. Sawchenko. (1984) An anterograde neuroanatomical tracing method that shows the detailed morphology of neurons, their axons and terminals: Immunohistochemical localization of an axonally transported plant lectin, *Phaseolus vulgaris* leucoagglutinin (PHA-L). *Brain Res.* 290:219-238.
38. Gobel, S., and M.B. Purvis. (1972) Anatomical studies of the organization of the spinal V nucleus: The deep bundles and the spinal V tract. *Brain Res.* 48:27-44.
39. Hayashi, H. (1985) Morphology of central termination of intra-axonally stained, large myelinated primary afferent fibers from facial skin in the rat. *J. Comp. Neurol.* 237:195-215.
40. Hayashi, H., R. Sumino and B.J. Sessle. (1984) Functional organization of trigeminal subnucleus interpolaris: Nociceptive and innocuous afferent inputs, projections to thalamus, cerebellum, and spinal cord and descending modulation from periaqueductal gray. *J. Neurophysiol.* 51:890-905.
41. Hayhow, W.R., A. Sefton, and C. Webb. (1962) Primary optic centers of the rat in relation to the terminal distribution of the crossed and uncrossed optic nerve fibers. *J. Comp. Neurol.* 118:295-322.
42. Hess, D.T. (1982) The tecto-olivo-cerebellar pathway. *Brain Res.* 250:143-148.
43. Hockfield, S., and S. Gobel. (1982) Anatomical demonstration of projections to the medullary dorsal horn (trigeminal nucleus caudalis) from rostral trigeminal nuclei and the contralateral caudal medulla. *Brain Res.* 252:203-211.

44. Huerta, M.F., A.J. Frankfurter, and J.K. Harting. (1981) The trigeminocollicular projection in the cat. Patch-like endings within the intermediate gray. Brain Res. 211:1-3.
45. Huerta, M.F., A.J. Frankfurter, and J.K. Harting. (1983) Studies of the principal sensory and spinal trigeminal nuclei of the rat: Projections to the superior colliculus, inferior olive, and cerebellum. J. Comp. Neurol. 220:147-167.
46. Ikeda, M., M. Matsushita and T. Tanami. (1982) Termination and cells of origin of the ascending intranuclear fibers in the spinal trigeminal nucleus of the cat. A study with the horseradish peroxidase technique. Neurosci. Lett. 31:215-220.
47. Ikeda, M., T. Tanami, and M. Matsushita. (1984) Ascending and descending internuclear connections of the trigeminal sensory nuclei in the cat. A study with the retrograde and anterograde horseradish peroxidase technique. Neurosci. 12:1243-1260.
48. Itoh, K. (1977) Efferent projections of the pretectum in the cat. Exp. Brain Res. 30:89-106.
49. Jacquin, M.F., R.D. Mooney, and R.W. Rhoades. (1986) Morphology, response properties, and collateral projections of trigeminothalamic neurons in the brainstem subnucleus interpolaris of rat. Exp. Brain Res. 61:457-468.
50. Jacquin, M.F., R.A. Stennett, W.E. Renehan and R.W. Rhoades (1988) Structure-function relationships in the rat brainstem subnucleus interpolaris: II. Low and high threshold trigeminal primary afferents. J. Comp. Neurol. 267:107-130
51. Jacquin, M.F., D. Woerner, A.M. Szczepanik, V. Riecker, R.D. Mooney, and R.W. Rhoades. (1986) Structure-function relationships in rat brainstem subnucleus interpolaris. I. Vibrissa primary afferents. J. Comp. Neurol. 243:266-279.
52. Jones, E.G. (1985) The Thalamus. Plenum, New York.
53. Kanaseki, T., and J.M. Sprague. (1974) Anatomical organization of pretectal nuclei and tectal laminae in the cat. J. Comp. Neurol. 158:319-337.

54. Kassel, J. (1980) Superior colliculus projections to tactile areas of rat cerebellar hemispheres. *Brain Res.* 202:291-305.
55. Kawana, E. (1969) Projections of the anterior ectosylvian gyrus to the thalamus, the dorsal column nuclei, the trigeminal nuclei and the spinal cord in cats. *Brain Res.* 14:117-136.
56. Kawana, E., and K. Watanabe. (1981) A cytoarchitectonic study of zona incerta in the rat. *J. Hirnforsch.* 22:535-541.
57. Kerr, F.W.L. (1963) The divisional organization of afferent fibers of the trigeminal nerve. *Brain.* 86:721-732.
58. Kerr, F.W.L. (1975) Neuroanatomical substrates of nociception in the spinal cord. *Pain.* 1:325-356.
59. Killackey, H.P. (1973) Anatomical evidence for cortical subdivisions based on vertically discrete thalamic projections from the ventral posterior nucleus to cortical barrels in the rat. *Brain Res.* 51:326-331.
60. Killackey, H.P. and G.R. Belford. (1979) The formation of afferent patterns in the somatosensory cortex of the neonatal rat. *J. Comp. Neurol.* 183:285-304.
61. Killackey, H.P. and R.S. Erzurumlu. (1981) Trigeminal projections to the superior colliculus of the rat. *J. Comp. Neurol.* 201:221-242.
62. Koralek, K.A., K.F. Jensen, and H.P. Killackey. (1988) Evidence for two complementary patterns of thalamic input to the rat somatosensory cortex. *Brain Res.* 463:346-351.
63. Kuypers, H.G.J.M. (1960) Central cortical projections to motor and somatosensory cell groups. *Brain* 83:161-184.
64. Lund, R.D., and K.E. Webster. (1967) Thalamic afferents from the dorsal column nuclei: An experimental study in the rat. *J. Comp. Neurol.* 130:301-312.
65. Ma, P.M. and T.A. Woolsey. (1984) Cytoarchitectonic correlates of the vibrissae in the medullary trigeminal complex of the mouse. *Brain Res.* 306:374-379.
66. Mackel, R. and T. Noda. (1989) The pretectum as a site for relaying dorsal column input to thalamic VL neurons. *Brain Res.* 476:135-139.

67. Mantle-St.John, L.A., and D.J. Tracey. (1987) Somatosensory nuclei in the brainstem of the rat: Independent projections to the thalamus and cerebellum. *J. Comp. Neurol.* 255:259-271.
68. Martin, G.F., R. Dom, S. Katz, and J.S. King. (1974) The organization of projection neurons in the opossum red nucleus. *Brain Res.* 78:17-34.
69. Matsushita, M., M. Ikeda, and N. Okado. (1982) The cells of origin of the trigeminothalamic, trigeminospinal and trigeminocerebellar projections in the cat. *Neurosci.* 7:1439-1454.
70. McHaffie, J.G., K. Ogasawara, and B.E. Stein. (1986) Trigeminothalamic and other trigeminofugal projections in neonatal kittens: An anatomical demonstration with horseradish peroxidase and tritiated leucine. *J. Comp. Neurol.* 249:411-427.
71. Miller, R.A., and N.L. Strominger. (1973) Efferent connections of the red nucleus in the brainstem and spinal cord of the rhesus monkey. *J. Comp. Neurol.* 152:327-346.
72. Moore, R.Y., and F.E. Bloom. (1979) Central catecholamine neuron systems: Anatomy and physiology of the norepinephrine and epinephrine systems. *Annu. Rev. Neurosci.* 2:113-168.
73. Murray, E.A., and J.D. Coulter. (1981) Organization of tectospinal neurons in the cat and rat superior colliculus. *Brain Res.* 243:201-214.
74. Nasution, I.D., and Y. Shigenaga. (1987) Ascending and descending internuclear projections within the trigeminal sensory nuclear complex. *Brain Res.* 425:234-247.
75. Naus, C.G., B.A. Flumerfelt, and A.W. Hryciyshyn. (1984a) Topographic specificity of aberrant cerebellorubral projections following neonatal hemicerebellectomy in the rat. *Brain Res.* 309:1-15.
76. Naus, C.G., B.A. Flumerfelt, and A.W. Hryciyshyn. (1984b) Topographic specificity of aberrant corticorubral projections following neonatal cortical lesions in the rat. *Soc. Neurosci. Abstr.* 10:1035.
77. Naus, C.G., B.A. Flumerfelt, and A.W. Hryciyshyn. (1985) An HRP-TMB ultrastructural study of rubral afferents in the rat. *J. Comp. Neurol.* 239:453-465.

78. Nothias, F., M. Peschanski, and J.M. Besson. (1988) Somatotopic reciprocal connections between the somatosensory cortex and the thalamic Po nucleus in the rat. *Brain Res.* 447:169-174.
79. Palkovits, M., M. Brownstein, J.M. Saavedra, and J. Axelrod. (1974) Norepinephrine and dopamine content of hypothalamic nuclei of the rat. *Brain Res.* 77:137-149.
80. Panneton, W.M., and H. Burton. (1982) Origin of ascending intratrigeminal pathways in the cat. *Brain Res.* 236:463-470.
81. Patrick, G.W., and M.A. Robinson. (1987) Collateral projections from trigeminal sensory nuclei to ventrobasal thalamus and cerebellar cortex in rats. *J. Morphol.* 192:229-236.
82. Paxinos, G. (1985) The Rat Nervous System. Vol. 2.: Hindbrain and Spinal Cord. Academic Press Australia.
83. Paxinos, G., and C. Watson. (1986) The Rat Brain in Stereotaxic Coordinates. Academic Press, New York.
84. Peschanski, M. (1984) Trigeminal afferents to the diencephalon in the rat. *Neurosci.* 12:465-487.
85. Phelan, K.D. and W.M. Falls. (1989) An analysis of the cyto- and myeloarchitectonic organization of trigeminal nucleus interpolaris in the rat. *Somatosensory Res.* Vol. 6, 4:333-366.
86. Phelan, K.D., and W.M. Falls. (1991) The spino-trigeminal pathway and its spatial relationship to the origin of trigeminospinal projections in the rat. *Neurosci.* 40:477-496.
87. Phelan, K.D., and W.M. Falls. (1991) A comparison of the distribution and morphology of thalamic, cerebellar and spinal projection neurons in rat trigeminal nucleus interpolaris. *Neurosci.* 40:497-511.
88. Poggio, G.F., and V.B. Mountcastle. (1960) A study of the functional contributions of the lemniscal and spinothalamic systems to somatic sensibility: central nervous mechanisms in pain. *Bull. Johns Hopkins Hosp.* 106:266-316.
89. Rees, H. and M.H.T. Roberts. (1987) Anterior pretectal stimulation alters the response of spinal dorsal horn neurons to cutaneous stimulation in the rat. *J. Physiol. (Lond.)* 385:415-436.

90. Reid, J.M., D.G. Gwym, and B.A. Flumerfelt. (1975) A cytoarchitectonic and Golgi study of the red nucleus in the rat. *J. Comp. Neurol.* 162:337-362.
91. Rhoades, R.W., S.E. Fish, N.L. Chiaia, C. Bennett-Clarke, and R.D. Mooney. (1989) Organization of the projections from the trigeminal brainstem complex to the superior colliculus in the rat and hamster: Anterograde tracing with phaseolus vulgaris leukoagglutinin and intra-axonal injection. *J. Comp. Neurol.* 289:641-656.
92. Rhoades, R.W., R.D. Mooney, and M. F. Jacquin. (1983) Complex somatosensory receptive fields of cells in the deep laminae of the hamster's superior colliculus. *J. Neurosci.* 3:1342-1354.
93. Rhoades, R.W., R.D. Mooney, B.G. Klein, M.F. Jacquin, A.M. Szczepanik, and N.L. Chiaia. (1987) The structural and functional characteristics of tectospinal neurons in the golden hamster. *J. Comp. Neurol.* 255:451-465.
94. Ricardo, J.A. (1981) Efferent connections of the subthalamic region in the rat. II. The zona incerta. *Brain Res.* 214:43-60.
95. Roberts, M.H.T. and H. Rees. (1986) The antinociceptive effects of stimulating the pretectal nucleus of the rat. *Pain.* 25:83-93.
96. Roger, M., and J. Cadusseau. (1985) Afferents to the zona incerta in the rat: A combined retrograde and anterograde study. *J. Comp. Neurol.* 241:480-492.
97. Romanowski, C.A.J., I.J. Mitchell, and A.R. Crossman. (1985) The organisation of the efferent projections of the zona incerta. *J. Anat.* 143:75-95.
98. Rossi, G.F., and A. Brodal. (1956) Spinal afferents to the trigeminal sensory nuclei and the nucleus of the solitary tract. *Confin. Neurol. (Basel)* 16:321-332.
99. Sahibzada, N., P. Dean, and P. Redgrave. (1986) Movements resembling orientation or avoidance elicited by electrical stimulation of the superior colliculus in rats. *J. Neurosci.* 6:723-733.
100. Saporta, S. and L. Kruger. (1977) The organization of thalamocortical relay neurons in the rat ventrobasal complex studied by the retrograde transport of horseradish peroxidase. *J. Comp. Neurol.* 174:187-208.

101. Scalia, F. (1972) The termination of retinal axons in the pretectal region of mammals. *J. Comp. Neurol.* 145:223-258.
102. Silverman, J.D., and L. Kruger. (1985) Projections of the rat trigeminal sensory nuclear complex demonstrated by multiple fluorescent dye retrograde transport. *Brain Res. Short Comm.* 383-388.
103. Siminoff, R., H.O. Schwassmann, and L. Kruger. (1967) Unit analysis of the pretectal nuclear group in the rat. *J. Comp. Neurol.* 130:329-342.
104. Smith, R.L. (1973) The ascending fiber projections from the principal sensory trigeminal nucleus in the rat. *J. Comp. Neurol.* 148:423-441.
105. Steinbusch, H.W.M. (1981) Distribution of serotonin-immunoreactivity in the central nervous system of the rat cell bodies and terminals. *Neurosci.* 6:557-618.
106. Steindler, D.A. (1985) Trigemino-cerebellar, trigemino-tectal, and trigemino-thalamic projections: A double retrograde axonal tracing study in the mouse. *J. Comp. Neurol.* 237:155-175.
107. Swenson, R.S., and A.J. Castro. (1983a) The afferent connections of the inferior olivary complex in rat: A study using the retrograde transport of horseradish peroxidase. *Am. J. Anat.* 166:329-341.
108. Swenson, R.S., and A.J. Castro. (1983b) The afferent connections of the inferior olivary complex in rats. An anterograde study using autoradiographic and axonal degeneration techniques. *Neurosci.* 8:259-275.
109. Torvik, A. (1956) Afferent connections to the sensory trigeminal nuclei, the nucleus of the solitary tract and adjacent structures. An experimental study in the rat. *J. Comp. Neurol.* 106:51-142.
110. Vander Loos, H. (1976) Barreloids in the mouse somatosensory thalamus. *Neurosci. Lett.* 2:1-6.
111. Watanabe, K., and E. Kawana. (1982) The cells of origin of the incertofugal projections to the tectum, thalamus, tegmentum and spinal cord in the rat. A study using the autoradiographic and horseradish peroxidase methods. *Neurosci.* 7:2389-2406.

112. Weber, J.T. and J.K. Harting. (1980) The efferent projections of the pretectal complex: an autoradiographic and horseradish peroxidase analysis. Brain Res. 194:1-28.
113. Wiberg, M., J. Westman, and A. Blomquist. (1986) The projection to the mesencephalon from the sensory trigeminal nuclei. An anatomical study in the cat. Brain Res. 399:51-68.
114. Wise, S.D. (1975) The laminar organization of certain afferent and efferent fiber systems in the rat somatosensory cortex. Brain Res. 90:139-142.
115. Wise, S.P., and E.G. Jones. (1977) Cells of origin and terminal distribution of descending projections of the rat somatic sensory cortex. J. Comp. Neurol. 175:129-158.
116. Wise, S.P., E.A. Murray, and J.D. Coulter. (1979) Somatotopic organization of corticospinal and corticotrigeminal neurons in the rat. Neurosci. 4:65-78.
117. Woolsey, T.A. and H. Vander Loos (1970) The structural organization of layer IV in the somatosensory region (SI) of mouse cerebral cortex. Brain Res. 17:205-242.
118. Woolston, D.C., J.R. LaLonde, and J.M. Gibson. (1982) Comparison of response properties of cerebellar- and thalamic-projecting interpo-laris neurons. J. Neurophys. 48:160-173.
119. Yasui, Y., K. Itoh, N. Mizuno, S. Nomura, M. Takada, A. Konishi, and M. Kudo. (1983) The posteromedial ventral nucleus of the thalamus (VPM) of the cat: Direct ascending projections to the cytoarchitectonic subdivisions. J. Comp. Neurol. 220:219-228.

CHAPTER II

Efferent Projections of Neurons in Four Subdivisional Regions of Rat Nucleus Interpolaris to Pontomedullary Regions:

A PHA-L Study

INTRODUCTION

Trigeminal nucleus interpolaris (Vi) receives sensory information from primary trigeminal neurons innervating orofacial receptive fields. Within Vi, this orofacial sensory information undergoes processing and modification before being relayed by projection neurons to several well-established pontomedullary target nuclei, including the inferior olive (1,8,10,15,18,31,65, 69) and other nuclei of the sensory trigeminal complex (23,24,29,30,33,34,35,49,52). The projection from Vi to the facial motor nucleus has received less attention (21).

Efferent Vi projections to these pontomedullary regions have been described without much consideration for their subdivisional origin within the nucleus. This is to be expected, since only recently have six separate and distinct subdivisions of rat Vi been delineated based on differences in their overall cyto- and myeloarchitecture, as well as connectional criteria (55). The six Vi subdivisions include

ventrolateral magnocellular (vlVimc), ventrolateral parvocellular (vlVipc), border region (brVi), dorsolateral (dlVi), dorsal cap (dcVi) and intermediate region (irVi). In addition, previous studies have provided relatively little information regarding the morphological characteristics of the terminal axonal arborizations of Vi projection neurons, mainly due to the utilization of neuroanatomical tracers which do not provide this information as does PHA-L.

The present study was conducted to re-evaluate the distribution of Vi efferent axons to pontomedullary target nuclei based on subdivisional differences recently delineated in Vi, and provide detailed descriptions of the morphological characteristics of the terminal arborizations of these axons. The distribution of Vi axons and morphological details of their terminal arborizations are necessary if one is to begin to understand the effects of Vi inputs on the activity of neurons in target nuclei in pontomedullary regions. Research has been conducted regarding the distribution and morphology of efferent axons and terminal arborizations from these four Vi subdivisional areas to the diencephalon and midbrain (16) as well as cerebellum and spinal cord (17).

MATERIALS AND METHODS

The descriptions of experimental procedures and methods of data collection outlined in Chapter 1 of this thesis should be referred to for this study as well. The injection sites and identification of pontomedullary target nuclei were also based on descriptions by Paxinos and Watson (54) and the previous studies of Phelan and Falls (55,56).

RESULTS

The data provided for this study were based on successful injections of PHA-L in a total of eight animals, two for each of the four Vi subdivisional regions. Although two separate injections were made into each of the four Vi subdivisional regions, only one representative injection site for each will be used for illustrative purposes (Fig. 1). For a description of the individual PHA-L injection sites, see the Results section of Chapter I.

Projections to the Pontine Nuclei

Labeled axons from neurons in all four Vi subdivisional regions coursed in a ventromedial direction from the injection site, decussated in the midline and ascended to the rostral pons in the contralateral medial lemniscus (ML).

From ML, Vi-Pn axons coursed ventromedially a short distance to Pn. Axons which gave rise to terminal arbors in ipsilateral Pn crossed the midline within Pn. The major projection from all four Vi subdivisional regions was to the medial portion of contralateral Pn (Fig. 2B,D,F,H), however, some differences in terminal arbor distribution were observed. Labeled axons from neurons in vlVimc gave rise to terminal arbors in the caudal two-thirds of Pn. Although the majority of terminal arbors from vlVimc-Pn axons were located in the medial portion of Pn, a few were also found in the lateral portion of the caudal one-third of the nucleus (Figs. 2A,B). Labeled axons from vlVipic neurons produced terminal arborizations in the medial portion of contralateral Pn, throughout the rostral two-thirds (Figs. 2C,D). Neurons in dmVi were the only ones to project bilaterally in Pn (Figs. 2E,F). Contralaterally, dmVi-Pn axons gave rise to terminal arbors in the caudal one-half of Pn which were predominantly located in the medial portion, however, a substantial number of arbors were also found in portions of Pn just ventral to the cerebral peduncle (Fig. 2F). Ipsilaterally, a smaller number of terminal arbors were observed ventrally in the middle of Pn. Labeled axons from brVi neurons emitted terminal arbors in the medial portion of contralateral Pn, throughout the caudal one-half of the nucleus (Figs. 2G,H).

Axons in Pn (approximately 1.0 to 1.5 μm in diameter) gave rise to only one type of terminal arborization. The Pn-

type (Figs. 5A, 7A) was characterized by a thin, multiple branched terminal strand (approximately 0.5 μm in diameter) with multiple, closely spaced boutons en passant and end boutons (approximately from 1.0 to 2.0 μm in diameter). Due to the dense intermingling of terminal arbors in the Vi-receptive zones in Pn, no particular orientation of the terminal arbors could be determined.

Projections to the Facial Motor Nucleus

Labeled axons from neurons in all Vi subdivisional regions traveled ventromedially from the injection sites to the ipsilateral facial motor nucleus, and gave rise to terminal arborizations throughout the rostrocaudal extent of the nucleus. Only axons from dmVi neurons crossed the midline and produced terminal arbors in contralateral VII. Those from neurons in vlVimc were most dense in the middle one-third of VII. More specifically, these terminal arbors were found in the dorsal intermediate and dorsolateral subnuclei of ipsilateral VII (Fig. 3B). Axons from neurons in vlVipic also gave rise to terminal arbors that were located in the dorsolateral subnucleus of the caudal one-half of VII (Fig. 3G). PHA-L injections in dmVi produced labeled terminal arbors bilaterally in VII, with ipsilateral predominance (Fig. 4B). Ipsilaterally, the terminal arbors were located in the dorsal intermediate and dorsomedial subnuclei. Contra- laterally, they were much more sparse and

found in the dorsomedial subnucleus of the rostral two-thirds of VII. Axons from neurons in brVi gave rise to terminal arbors located in the dorsal intermediate subnucleus of the rostral one-half of VII, and in the dorsolateral subnucleus of the caudal one-half of VII.

Axons in VII (approximately 1.0 to 1.5 μm in diameter) gave rise to one type of terminal arborization. The VII-type arbor (Figs. 5B, 7B) was characterized by a thin, branched terminal strand (approximately 0.5 μm in diameter) with multiple boutons en passant and end boutons (approximately 1.0 to 2.0 μm in diameter). The labeled fibers entered ipsilateral VII from a dorsolateral direction and gave rise to bouton bearing terminal strands either as collaterals along the length of the parent fiber, or at its terminal end. The axons from dmVi neurons, after giving rise to collaterals in ipsilateral VII, entered contralateral VII from a medial direction before terminating in the nucleus.

Projections to the Inferior Olive

Labeled axons from neurons in vlVimc, vlVipc, dmVi and brVi emerged from the medial aspect of the injection sites and coursed ventromedially through the adjacent reticular formation toward the midline. Many axons passed through, and dorsal to, the ipsilateral inferior olive (IO) before decussating in the midline and giving rise to terminal arbors in contralateral IO. Some axons issued collaterals which

arborized in ipsilateral IO before decussating. Axons from neurons in all Vi subdivisional regions gave rise to terminal arbors bilaterally in the rostral one-third of IO, with contralateral predominance. The distribution of terminal arbors following vlVimc and vlVipic injections was similar (Figs. 3C,D,H,I), with a dense patch of terminal arbors in the medial portion of the contralateral dorsal nucleus of the inferior olive (IOD). A few terminal arbors were found in the medial portions of ipsilateral IOD and the principal nucleus of the inferior olive (IOPr). The projections from dmVi (Figs. 4C,D) and brVi (Figs. 4H,I) were different. Axons from neurons in dmVi gave rise to terminal arbors mainly in medial IOD contralaterally with a smaller number located in the medial portion of IOPr contralaterally and medial IOD ipsilaterally. Terminal arbors in IO following brVi injections were found in the middle of IOPr and IOD contralaterally, with those in IOD at more rostral levels. In addition, axons from brVi neurons produced fewer arbors in the medial and lateral portions of IOD, ipsilaterally.

Axons (approximately 1.0 μm in diameter) from all four Vi subdivisional regions gave rise to one type of terminal arborization in IO (Figs. 6A, 7C). The IO-type terminal arbor was characterized by sparsely branched terminal strands (approximately 1.0 μm in diameter) with multiple, closely spaced boutons en passant and end boutons (approximately 1.5 to 2.0 μm in diameter). These terminal strands emanated

either as collaterals or from the terminal end of the axon.

Projections to the Sensory Trigeminal Complex

Labeled axons from neurons in all Vi subdivisional regions gave rise to terminal arborizations that were distributed ipsilaterally to the other nuclei of the sensory trigeminal nuclear complex (SVC), as well as contralaterally to Vi. The other nuclei of the SVC include Vms, Vo and MDH. Axons from neurons in vlVimc and vlVipc gave rise to terminal arbors in the ventrolateral portion of the other nuclei of the SVC (Figs. 3A-J), while those from neurons in dmVi and brVi gave rise to terminals in the dorsal (Figs. 4A-E) and border regions (Figs. 4F-J) of the SVC, respectively. In caudal MDH, however, the terminal arbors from all Vi subdivisional regions shifted to a medial position. In addition, axons from neurons in vlVimc, vlVipc, dmVi and brVi gave rise to a relatively small number of terminal arbors in the same respective subdivisional regions of contralateral Vi. The ipsilateral course taken by Vi parent axons to the other nuclei of the SVC appeared to occur by means of three pathways. One route was intranuclear, through the deep axonal bundles (DABs) running rostrocaudally through SVC. The other two routes were internuclear, through the spinal V tract (svt) laterally and the adjacent reticular formation medially. Vi axons which gave rise to terminal arbors in contralateral Vi took a direct route through the ipsilateral

and contralateral PCrt. Many of the terminal arbors in the ventrolateral and dorsal portions of SVC were oriented rostrocaudally, while the exact orientation of those confined to the border zone was not as apparent.

Axons (approximately 1.0 μm in diameter) in SVC gave rise to one type of terminal arborization (Figs. 6B, 7D). The SVC-type arbor was characterized by thin, multiple branched terminal strands (approximately 0.5 μm in diameter) with many en passant and end boutons (approximately 1.0 to 2.0 μm in diameter). The terminal strands emanated as axon collaterals or as thin terminal continuations of the fibers. Although one basic type of terminal arbor was found in SVC, the terminal arbors in ventrolateral and dorsomedial portions of SVC (Fig. 6B 3,4) were more expansive, and oriented rostrocaudally, while those in border regions (Fig. 6B 1,2) were more compact and had variable orientations.

DISCUSSION

This study shows for the first time the distribution and morphological characteristics of terminal axonal arborizations of neurons in four Vi subdivisional regions, to pontomedullary target nuclei utilizing the PHA-L method. Although projections from Vi to some of these target nuclei have been previously described, information regarding their specific Vi subdivisional region of origin, as well as the

morphological characteristics of the terminal arbors is limited. These aspects of Vi projection neurons were determined by applying the anterograde PHA-L method to the recently delineated Vi subdivisions (55). For a discussion of differences between the various Vi subdivisions and the benefits of utilizing the anterograde PHA-L method in this study, see the Discussion section of Chapter I. However, it is important to mention here that although it has been shown that PHA-L can be transported retrogradely (60) and anterogradely by fibers of passage (14), these modes of transportation did not appear to affect the results of this study regarding the Vi projections to Pn, VII and IO. As far as retrograde transport of the tracer is concerned, no labeled cell bodies were seen in regions outside of the injection site, except for a few labeled cell bodies in rostral MDH. Regarding the labeling of fibers of passage, the course of trigeminal axons to Pn, VII and IO makes it improbable for this method of transport to be a factor. Since the axons of trigeminal projection neurons to these targets emerge from the medial aspect of the SVC without traveling rostrally or caudally within the nuclei, the injections into Vi would not be taken up by these fibers. However, the axons of intratrigeminal projection neurons do course rostrally and caudally through the nuclei of SVC and may have been subject to labeling by PHA-L through the various Vi injections.

Projections to the Pontine Nuclei

The pontine nuclei (Pn) are the most extensive of precerebellar nuclei, which serve as an important relay for pathways from the cerebral cortex to the cerebellum (CB) (53). They are located in the basilar pons surrounding the descending fibers of the cerebral peduncle. The rat basilar pons can be divided into four major subdivisions including medial, ventral, lateral and peduncular nuclei, according to their position with respect to the cerebral peduncle (45). The pontine nuclei of the rat receive input from several sources including various regions of the cerebral cortex, superior and inferior colliculi, lateral geniculate nuclei, deep CB nuclei, as well as others (53,71). The most important input appears to be that from the sensorimotor cortex. Autoradiographic techniques have revealed that the motor, somatosensory and visual cortices terminate in Pn in a medial to lateral succession, respectively (53,72). There also appears to be some topographic segregation of input to Pn such that the forelimb sensorimotor and visual cortices project to rostral portions of ipsilateral Pn, while hindlimb sensorimotor cortex projects to more caudal levels (44,71,72). Electrophysiological data in rat show that the facial areas of sensorimotor cortex provide an unproportionately large projection to Pn (58). Electrophysiological methods do not reveal a point-to-point projection pattern. Many neurons in the pontine nuclei

receive convergent inputs from functionally different cortical areas (58,53), which may be due to overlapping zones of corticopontine projections or due to interconnections in Pn from interneurons. However, local convergence may be due to the tendency of the dendritic trees of Pn neurons to extend into neighboring areas, as shown by Golgi preparations (45). Projections from Vi to Pn have received little attention in the literature, which is surprising, due to the density of this projection. Vi projections have been shown to terminate in medial (vlVimc, vlVipc, dmVi and brVi), ventral (dmVi) and lateral portions of Pn (vlVipc). Although each Vi subdivisional region differed slightly in their projections to Pn, a consistent feature of these projections was the presence of a relatively dense area of terminal arbor distribution contralaterally in the medial portion of the nucleus. Axons from dmVi neurons were the only ones to give rise to terminal arbors in ipsilateral Pn. In terms of efferent connectivity, Pn provides a major source of mossy fibers to most regions of the cerebellar cortex and deep cerebellar nuclei, and it is generally accepted that all cells in Pn project predominantly to the contralateral CB (53). The areas of Pn shown by this study to receive Vi input, have been shown to project to orofacial portions of CB including simple lobule, paramedian lobule and crura I and II (12,43). These regions of CB also receive direct Vi projections (17).

Thus, the functional significance of the projection from Vi to Pn, may be at least two-fold. First, it appears that through the extensive direct and indirect (Vi to Pn) projections to CB, that Vi plays an important role related to the execution of orofacial movements performed by CB. Secondly, based on the knowledge that the Pn constitute the most important relay in the conduction of impulses from the cerebral cortex to CB, it is also possible that Vi plays a role in the modulation of cortical input from facial regions of the sensorimotor cortex to Pn.

Projections to the Facial Motor Nucleus

The projection from Vi to VII has been previously described in the rat utilizing axonal degeneration (21). This study described an ipsilateral projection to VII from Vi that was more sparse and widely distributed than were the projections from Vms and MDH. It also showed that the termination of axons from neurons in Vi extended into the lateral, dorsal and intermediate regions of ipsilateral VII. In addition, Vo was shown to be the only nucleus of SVC to project bilaterally to VII, but still with ipsilateral predominance (21). The present study partially supports these findings, by showing that Vi does project to dorsal (dorsal intermediate), lateral (dorsolateral) and intermediate regions of ipsilateral VII, however, it also shows a small contralateral projection to VII from dmVi.

Failure to report the contralateral projection is surprising when considering the position of the illustrated lesion site, which was centered in the dorsal portion of Vi.

The neurons of VII, which innervate the superficial muscles of the head and neck, are separated into several subdivisions. The distinction of subdivisions varies in nomenclature (53), however, the terminology used to describe them in the present study are consistent with those from the atlas of Paxinos and Watson (54). The organization of rat VII has been mapped for both nerve representation within the nucleus (42,66) and muscle representation (62,70). In general, dorsal muscles are represented dorsally, ventral muscles ventrally and the anterior-posterior axis lateromedially (53,59). Thus, those Vi subdivisional regions which project to neurons in the dorsolateral subdivision of VII (vlVimc, vlVipc, brVi) probably innervate superior labial and naris dilator muscles, those which project to the dorsal intermediate subdivision (vlVimc, dmVi, brVi) probably innervate frontalis and zygomatic muscles, and those to the dorsomedial subdivision (dmVi) probably innervate anterior auricular muscles (53,70).

Thus, the functional significance of the projection from Vi to VII most likely lies in the innervation of facial musculature. The results provided by this study may imply that in the rat, the orofacial tactile input relayed from Vi to VII activates motor neurons in VII responsible for

innervating muscles of the face and auricles utilized in whisking and orienting when engaged in exploratory behavior. The input from Vi to VII, however, does not appear to be as dense and widespread as described from Vo (63). This may suggest that the type of orofacial sensory information relayed by Vi does not require as important a response from VII as does the information relayed by Vo. It may also suggest that the motor response elicited as a result of Vi input to VII is more crude or general, while the input from Vo produces more specific motor responses.

Projections to the Inferior Olive

The present study demonstrates a predominantly contralateral projection to rostral IO from the four Vi subdivisional regions. The densest region of termination in IO from Vi subdivisional regions was in the rostromedial portion of IOD. This finding is supported by anatomical and electrophysiological studies in rat (10,15,31,65) as well as cat (8,18,32,46,69). Only a few studies describe an ipsilateral component (41,65,69). Although differences were seen in the projections to IO from the four Vi subdivisional regions, they all had a common input to the rostromedial portion of contralateral IOD. The trigeminorecipient zone in rostromedial IOD is sometimes referred to by others as the junction between IOD and IOPr (15,31,32). Some studies also include the medial nucleus of the inferior olive as a

trigeminoceptive region, however, this area was not shown to be a target for Vi fibers. The high density of Vi axonal termination in IO is not surprising, since Vi has been shown to be the primary source of trigemino-olivary axons (31,32,65,69). Stimulation of the maxillary nerve, which conveys information from the mystacial vibrissae and whose primary afferents most likely terminate in vlVimc and vlVipc, has been shown to be most effective in evoking responses of olivary neurons in medial IOD and IOPr (15). The Vi projection to rostromedial IOD coincides with the precise somatotopy of somatosensory inputs into IO, as revealed by autoradiographic and axonal degeneration techniques in rats (65), which indicate that afferents from the spinal trigeminal nuclei, dorsal column nuclei, and spinal cord terminate from medial to lateral in IO, respectively. Electrophysiological and autoradiographic studies in cat (27,32) reveal two somatosensory maps in IOD. One is located in its rostral one-half and responds mostly to cutaneous stimulation, while the other is located caudally and responds primarily to deep stimulation. The cells in rostral IOD have been shown not only to respond to cutaneous stimulation, but also exhibit a high degree of somatotopy, relative to the other portions of IO (27,32). In rostral IOD, the face is represented medially. Therefore, the relay of sensory information from orofacial regions by Vi to rostromedial IOD, corresponds well with this cutaneous map of the face.

The IO is thought to be the sole source of cerebellar climbing fibers in the rat (2,19). It is generally accepted that all neurons within IO send their axons to CB. The trigeminoreceptive regions of IO have been shown to provide climbing fiber input to the same areas that receive direct mossy fiber input from Vi. Anatomical and electrophysiological studies in the rat (1,11,31) reveal that neurons in rostral IO project to the orofacial tactile regions of the CB cortex which include crura I and II, paramedian lobule and simple lobule. As a result of the combined mossy fiber input from direct Vi-CB projections (and indirect Vi-Pn-CB projections), as well as indirect climbing fiber input from Vi-IO-CB projections, Vi has the potential to strongly influence the activity of a large region of CB including the vermis (which receives input from Vi and IO) and the hemispheres (which receives input from Vi and Pn). The response of CB to this input may be for the purpose of coordinating orienting movements of the rat head and neck.

Projections to the Sensory Trigeminal Complex

Projections which interconnect SVC have been described in the rat (23,24,29,35) and cat (29,30,33,34,49). Depending on where the axons course, those which interconnect the various portions of SVC are either referred to as intranuclear or internuclear connections (34,35). Axons connecting SVC by traveling within the intranuclear bundles

or DABs, form intranuclear connections, while those coursing through SVT or the adjacent reticular formation form internuclear connections with ipsilateral Vms, Vo, MDH, and contralateral Vi and suggests that SVC nuclei communicate by means of both intra- and internuclear projections. More specifically, the various Vi subdivisional regions of Vi project ipsilaterally to similar regions in the other nuclei of SVC, and contralaterally with the same Vi subdivisions. The axons which gave rise to terminal arborizations in contralateral Vi took a direct route through the ipsilateral and contralateral reticular formation. Some previous studies, using HRP in the cat, have shown that cells in the caudal portion of Vi provide ascending and descending axons to SVC (34,49). A more recent study, using PHA-L in the rat, demonstrated that injections into either Vms, Vi or MDH produced dense anterograde labeling in each of the other nuclei of SVC, with Vms projecting cells located at each rostrocaudal level of Vi (35). It also showed the existence of ascending and descending internuclear projections from all four Vi subdivisional regions in the rat, including rostral injections in vlVimc and caudal injections in vlVipc. The projection pattern described in the present study which shows connections between Vi subdivisional regions and similar areas of the other nuclei of SVC, is generally supported by an HRP study in the cat (52) which shows that neurons located in the dorsomedial portion of Vi were labeled after dorsal

injections in Vms, and neurons located ventrolaterally were labeled after more ventral Vms injections.

The parent axons from neurons in all Vi subdivisional regions gave rise to a single type of arbor, characterized by branched, bouton-bearing terminal strands. However, the axons from brVi neurons gave rise to terminal arbors that were more compact and less expansive than those from the other Vi subdivisional regions. This difference may be due to the fact that the border region of Vi and similar regions in the other nuclei of SVC are narrow regions which may result in the compactness of the terminal arbors. Although Gobel and Purvis ('72) previously described the morphology of Golgi stained collaterals of ascending DAB axons as "simple", "branch infrequently" and "bear relatively few endings", more recent findings obtained through the utilization of PHA-L (35) are consistent with those of the present study. They describe their intertrigeminal collaterals as "highly branched" arbors with a "large number" of en passant and end boutons or swellings.

Light and electron microscopic studies of HRP labeled ascending intranuclear axons from MDH to Vo in the rat (24) have revealed two populations of MDH axons. One type gives rise to a collateral which enters Vo on its way to Vms, while the other type terminates directly in Vo. Electron microscopic analysis of these two types shows that the first type has boutons filled with small round synaptic vesicles

and forms asymmetrical synaptic contacts with large (proximal) dendritic shafts, while the second type has axonal endings filled with pleomorphic shaped synaptic vesicles and forms symmetrical synaptic junctions with small diameter (distal) dendrites. These data suggest that inter- and intranuclear connections can serve both excitatory and inhibitory functions.

Although the specific functions of inter- and intranuclear projections cannot be determined without further anatomical and electrophysiological studies, it appears that the projections from Vi to the other regions of SVC allows for intercommunication within the complex, which may serve to modulate orofacial sensory input to these regions for the possible transmission to the various projection sites such as the ventral posteromedial thalamic nucleus, superior colliculus, CB and cervical spinal cord. Projections to contralateral Vi suggests coordination in the central processing of incoming orofacial sensory input also takes place between right and left nuclei.

Similarities and differences in the projections from the four Vi subdivisional regions

The differences in the projections from the four Vi subdivisional regions to pontomedullary nuclei were primarily topographical differences. All four regions issued projections to Pn, VII, IO and SVC. In the rostral pons, all

subdivisions provided input to the medial portion of contralateral Pn. However, dmVi provided additional input to regions of contralateral Pn, just ventral to the cerebral peduncle, as well as to the ventral portion of ipsilateral Pn. Similarly, all four Vi subdivisional regions projected to ipsilateral VII, mainly to dorsal and medial portions, while dmVi provided additional input to the dorsal portion of contralateral VII. The projections to IO were similar from all regions of Vi. They were bilateral with contralateral predominance, and with the greater density in IOD. In the nuclei of the SVC, each Vi subdivisional region projected primarily to a corresponding area of ipsilateral Vms, Vo and MDH, as well as contralateral Vi. In addition, the morphological characteristics of the terminal arborizations in each of the target nuclei were similar from all regions of Vi. Thus, the projections from vlVimc, vlVipc, dmVi and brVi to pontomedullary target nuclei were similar except for some topographical differences and the bilaterality of projections from dmVi to Pn and VII.

It is possible, however, that some differences in the projections from Vi subdivisions may have been masked by consolidating the three dorsal Vi subdivisions (irVi, dcVi and dlVi) as represented by dmVi. These three dorsal subdivisions, which have been shown to be cyto- and myeloarchitecturally distinct (55), have also been shown to differ based on afferent input from primary trigeminal

neurons innervating orofacial regions (36,67). Attempts to make precise, well-contained injections in the three dorsal Vi subdivisions were unsuccessful due to their relatively small size. Thus, differences in the projections from the six Vi subdivisions are possibly greater than those revealed by the present study.

Comparison of Vi terminal axonal arborizations in Pontomedullary Nuclei

The morphological characteristics of the terminal axonal arborizations in Pn, VII, IO and SVC are similar types based on the criteria utilized in this study. They were depicted by thin, branched terminal strands with boutons en passant and end boutons. These features also characterized terminal arbors located in other nuclei which receive Vi input, including zona incerta, the anterior pretectal nucleus, superior colliculus and red nucleus (16), as well as the spinal cord and deep CB nuclei (17). It is possible that the axons of neurons in Vi collateralize to various combinations of these target nuclei, however, this could not be determined in this study, based on labeling technique and process of tissue sectioning. In order to determine which Vi projections are separate and which are collateralized, double-labeling retrograde techniques would have to be conducted in future studies.

Figure 1: PHA-L Injection Sites.

Schematic drawings (E-H) and photomicrographs (A-D) of representative transverse sections through PHA-L injection sites (IS) in four subdivisional regions of rat trigeminal nucleus interpolaris (Vi), which include: ventrolateral magnocellular (vlVimc;A,E), ventrolateral parvocellular (vlVipc;B,F), dorsomedial (dmVi;C,G) and border region (brVi;D,H). The injection sites were, for the most part, confined to the respective subdivisional area of rat Vi. Amb, ambiguous nucleus; IO, inferior olive; svt, spinal trigeminal tract.

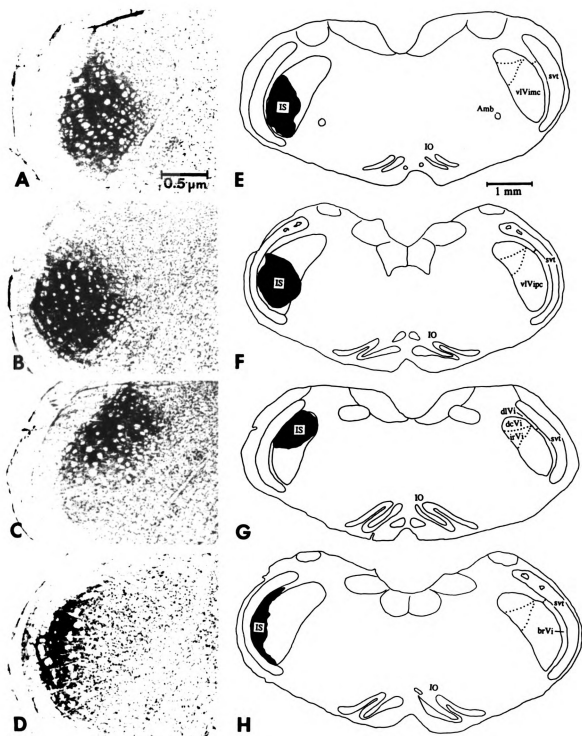


Figure 1

**Figure 2: Projections from Vi Subdivisional Regions to
Pn.**

A,B. Schematic drawings of representative transverse sections through rostral and caudal levels of the pontine nuclei at the approximate interaural levels of 2.20 mm and 1.70 mm, respectively, showing the distribution of vlVimc efferent terminal axonal arborizations in contralateral pontine nuclei (Pn). C,D. Shows distribution of vlVipc efferent terminal arbors contralaterally in Pn. E,F. Shows the distribution of dmVi efferent terminal arbors bilaterally in Pn, with contralateral predominance. G-H. Shows distribution of brVi terminal arbors in contralateral Pn. ml, medial lemniscus.

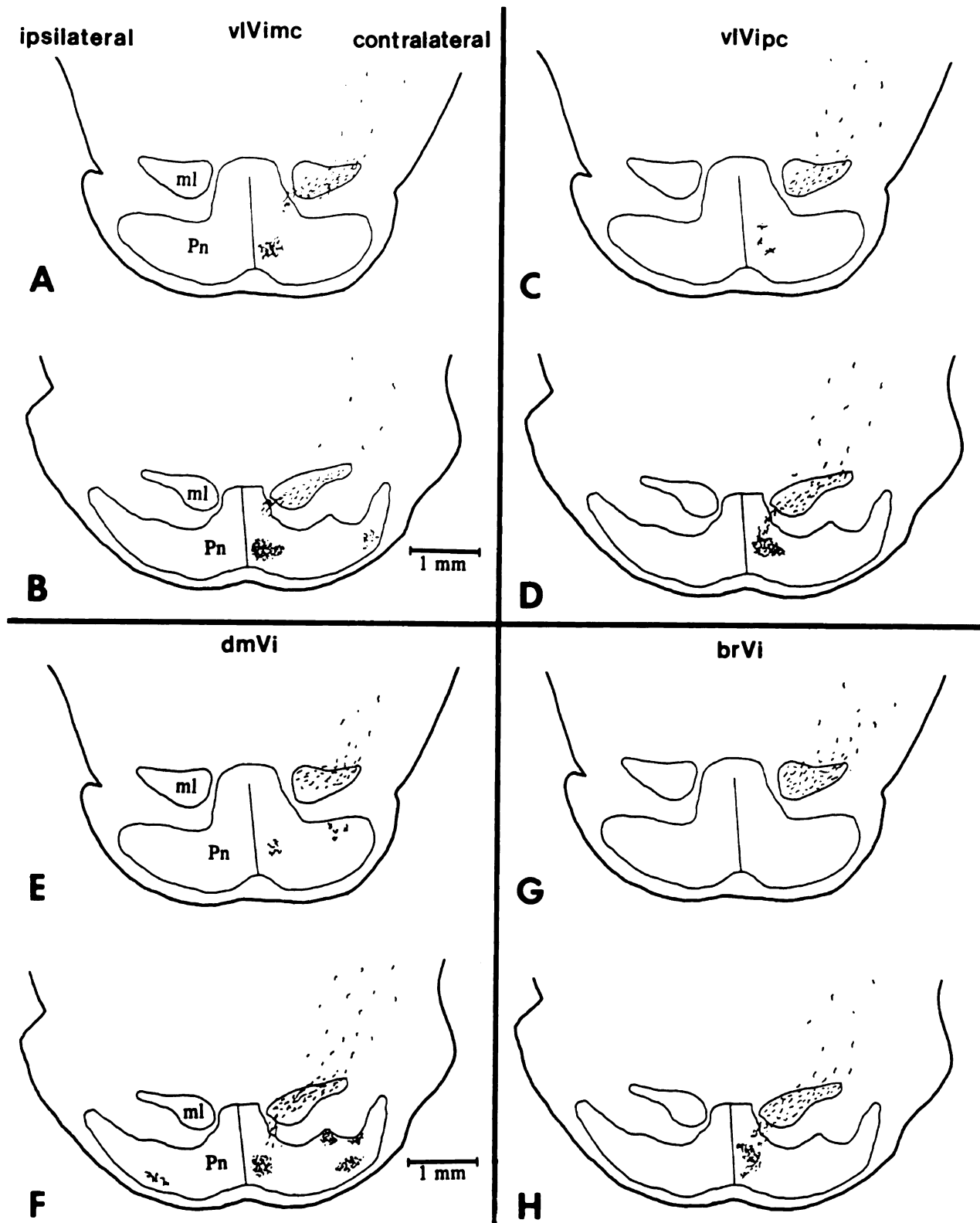


Figure 2

Figure 3: Pontomedullary Projections from vlVimc and vlVipc.

Schematic drawings of representative transverse sections through the pons and medulla from rostral to caudal, at the approximate interaural levels of -0.80 mm, -1.80 mm, -2.80 mm, -3.30 mm and -4.80 mm, respectively, showing the distribution of vlVimc (A-E) and vlVipc (F-J) efferent terminal axonal arborizations ipsilaterally in the ventrolateral portion of main sensory trigeminal nucleus (Vms), trigeminal nucleus oralis (Vo), medullary dorsal horn (MDH), contralaterally in Vi, as well as ipsilaterally in facial motor nucleus (VII) and bilaterally in inferior olive (IO) with contralateral predominance. Amb, ambiguous nucleus; icp, inferior cerebellar peduncle; IOD, inferior olive dorsal nucleus; IOPr, inferior olive principal nucleus; IS, injection site; LRt, lateral reticular nucleus; LSO, lateral superior olive; Mo5, motor trigeminal nucleus; PcRt, parvocellular reticular nucleus; Sol, solitary nucleus; svt, trigeminal tract; XII, hypoglossal nucleus.

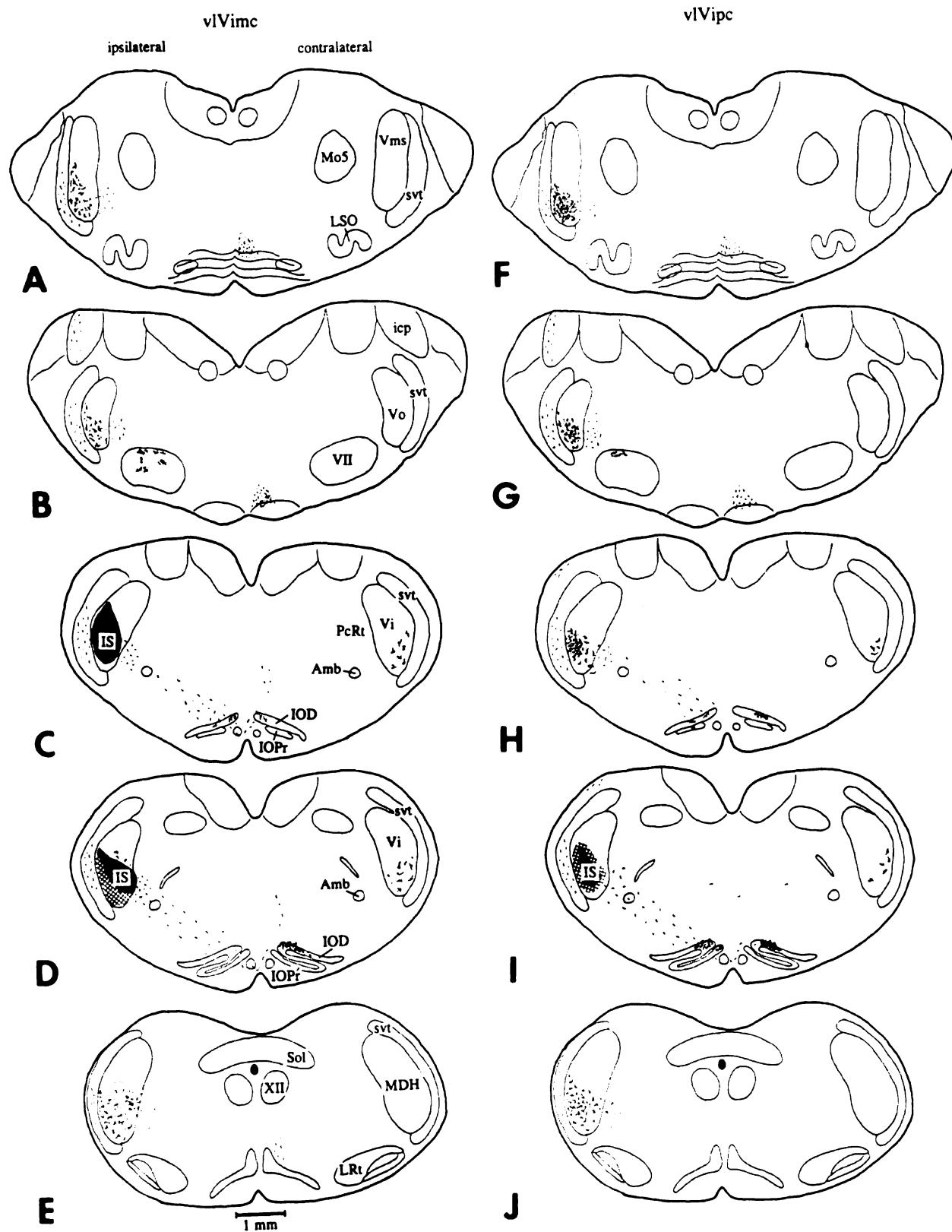


Figure 3

Figure 4: Pontomedullary Projections from dmVi and brVi.

A-E. Schematic drawings of representative transverse sections through the pons and medulla from rostral to caudal, respectively, showing the distribution of dmVi efferent terminal axonal arborizations ipsilaterally in dorsal Vms, Vo, MDH, contralaterally in Vi, as well as bilaterally in VII with ipsilateral predominance and bilaterally in IO with contralateral predominance. F-J. Shows distribution of brVi terminal arbors ipsilaterally in border zone of Vms, Vo, MDH, contralaterally in Vi, as well as ipsilaterally in VII and bilaterally in IO with contralateral predominance.

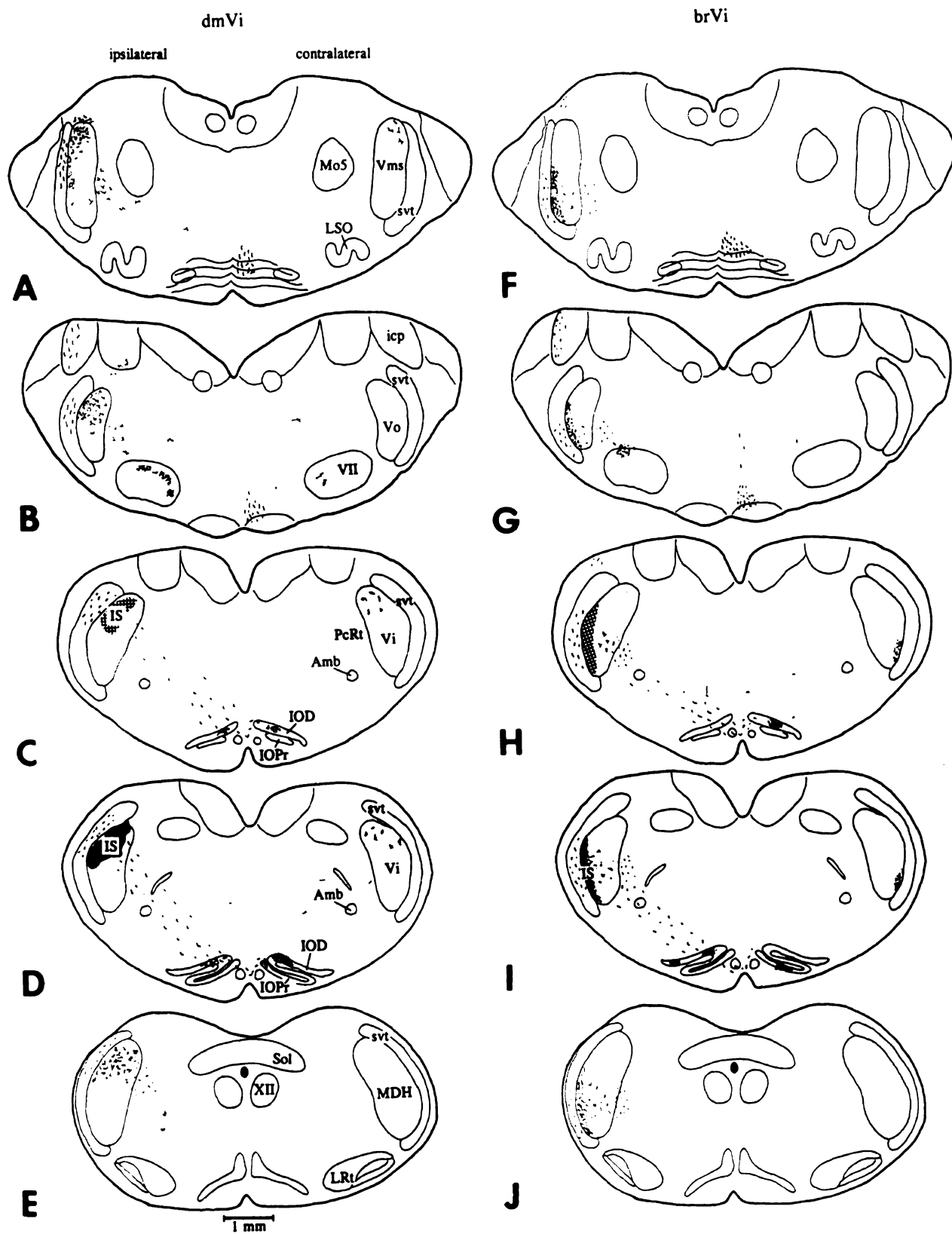


Figure 4

**Figure 5: Drawings of Terminal Axonal Arborizations in
Pn and VII.**

A. Representative drawings of Pn-type terminal axonal arborizations in Pn, characterized by branched terminal strands (ts) with multiple boutons (b). B. Representative drawings of VII-type terminal arbors in VII, characterized by branched terminal strands with multiple boutons. pf, parent fiber.

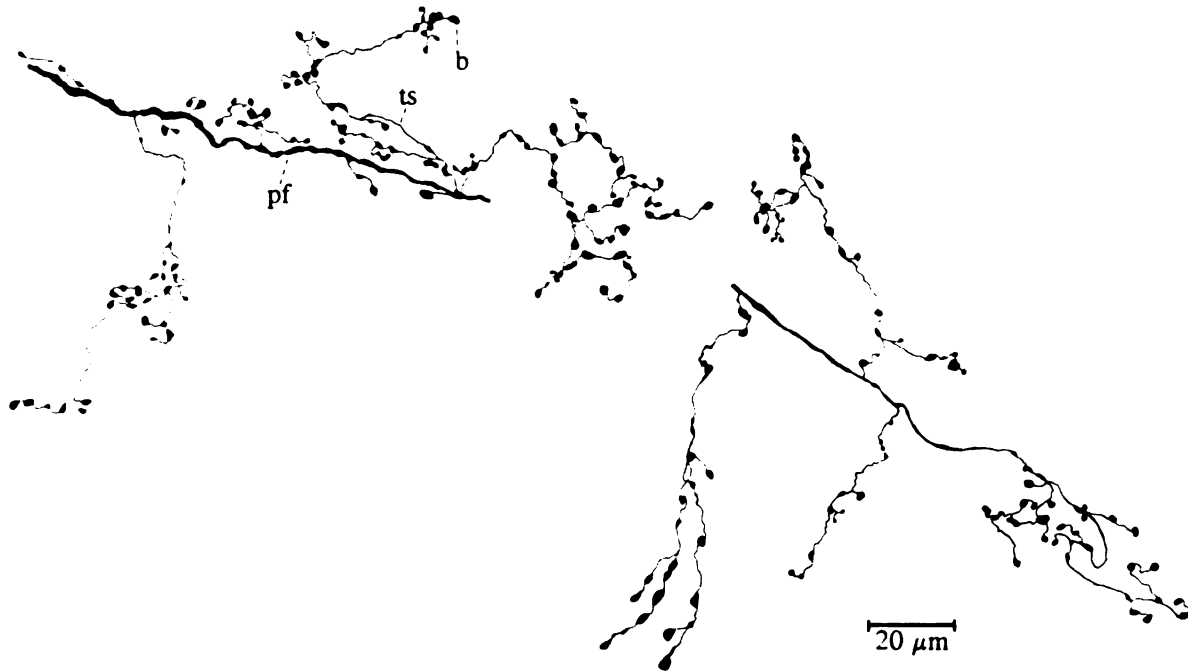
**A****B**

Figure 5

**Figure 6: Drawings of Terminal Axonal Arborizations in
IO and SVC.**

- A. Representative drawings of IO-type terminal axonal arborizations in IO, characterized by branched terminal strands with multiple closely spaced boutons.
- B. Representative drawings of SVC-type terminal arbors in the border zone (1,2) and dorsomedial and ventrolateral (3,4) portions of the nuclei of SVC, depicted by bouton-bearing branched terminal strands.

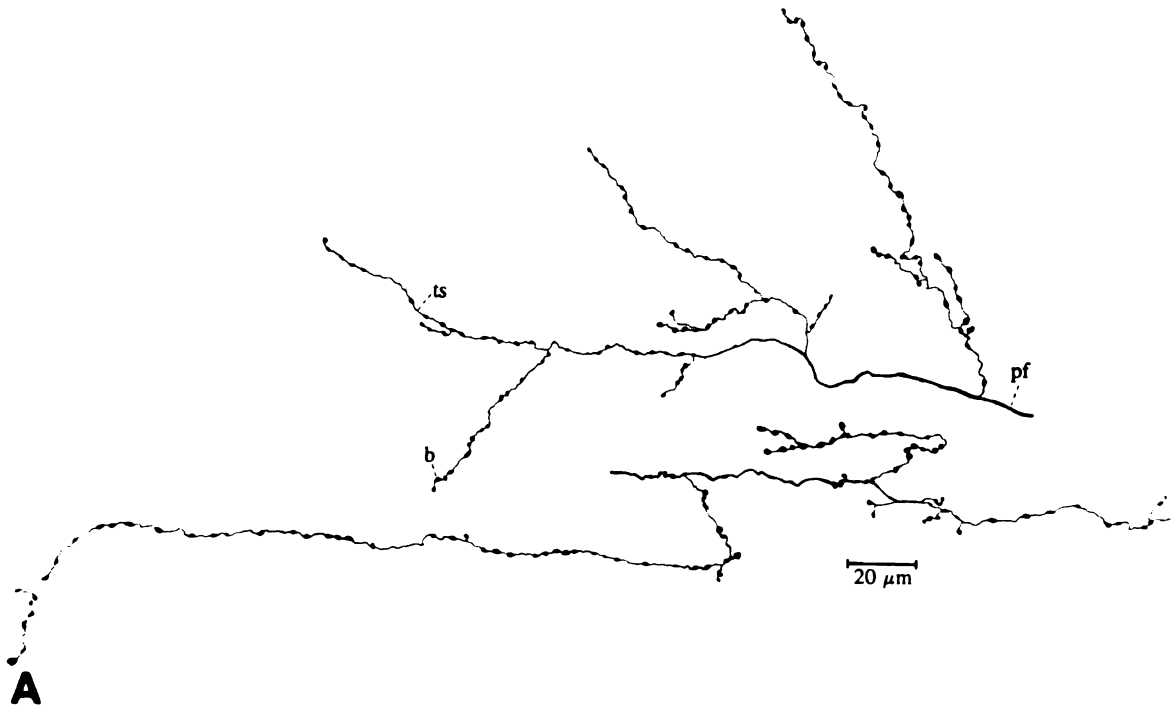


Figure 6

**Figure 7: Photomicrographs of Terminal Axonal Arborizations
in Pn, VII, IO and SVC.**

Photomicrographs that document the morphological characteristics of Pn-type (A), VII-type (B), IO-type (C) and SVC-type (D) efferent terminal axonal arborizations from neurons in Vi.

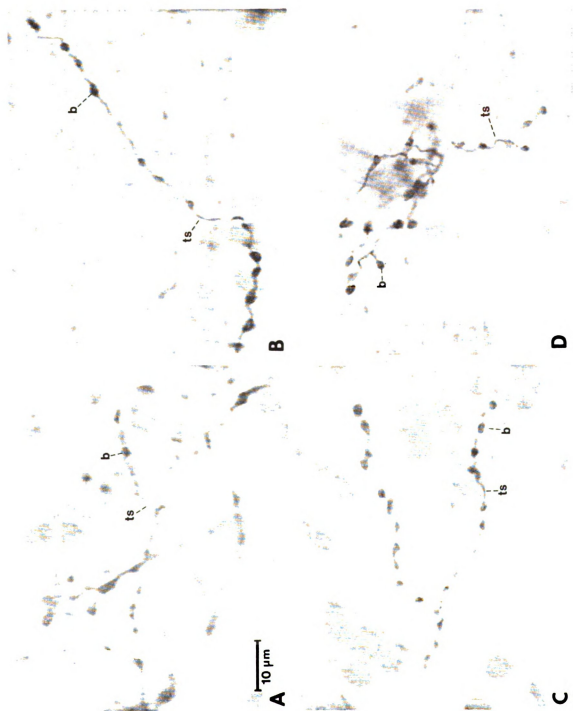


Figure 7

BIBLIOGRAPHY

1. Akaike, T. (1989) Electrophysiological analysis of the trigemino-olivo-cerebellar (crura I and II, lobulus simplex) projection in the rat. *Brain Res.* 482:402-406.
2. Anderson, W.A., and B.A. Flumerfelt. (1980) A light and electron microscope study of the effects of 3-acetylpyridine intoxication on the inferior olivary complex and cerebellar cortex. *J. Comp. Neurol.* 190:157-174.
3. Arvidsson, J. (1982) Somatotopic organization of vibrissae afferents in the trigeminal sensory nuclei of the rat studied by transganglionic transport of HRP. *J. Comp. Neurol.* 211:84-92.
4. Arvidsson, J. and S. Gobel (1980) An HRP study of the central projections of primary trigeminal neurons which innervate tooth pulps in the cat. *Brain Res.* 210:1-16.
5. Arvidsson, J. and F.L. Rice. (1991) Central projections of primary sensory neurons innervating different parts of the vibrissae follicles and intervibrissal skin on the mystacial pad of the rat. *J. Comp. Neurol.* 309:1-16.
6. Bates, C.A., and H.P. Killackey. (1985) The organization of the neonatal rat's brainstem trigeminal complex and its role in the formation of central trigeminal patterns. *J. Comp. Neurol.* 240:265-287.
7. Belford, G.R., and H.P. Killackey. (1979) Vibrissae representation in subcortical trigeminal centers of the neonatal rat. *J. Comp. Neurol.* 183:305-322.
8. Berkley, K.J., and P.J. Hand. (1978) Projections to the inferior olive of the cat - II Comparisons of input from the gracile, cuneate, and the spinal trigeminal nuclei. *J. Comp. Neurol.* 180:253-264.
9. Brodal, A., T. Szabo, and A. Torvik. (1956) Corticofugal fibers to sensory trigeminal nuclei and nucleus of the solitary tract. An experimental study in the cat. *J. Comp. Neurol.* 106:527-556.
10. Brown, J.T., V. Chan-Palay, and S.C. Palay. (1977) A study of afferent input to the inferior olivary complex in the rat by retrograde axonal transport of horseradish peroxidase. *J. Comp. Neurol.* 176:1-22.

11. Brown, P.A. (1980) The inferior olivary connections to the cerebellum in the rat studied by retrograde axonal transport of horseradish peroxidase. *Brain Res. Bull.* 5:267-275.
12. Burne, R.A., G.A. Mihailoff and D.J. Woodward. (1981) Visual corticopontine input to the paraflocculus: A combined autoradiographic and horseradish peroxidase study. *Brain Res.* 143:139-146.
13. Chiaia, N.L., P.R. Hess, M. Hosoi, and R.W. Rhoades. (1987) Morphological characteristics of low-threshold primary afferents in the trigeminal subnuclei interpolaris and caudalis (the medullary dorsal horn) of the golden hamster. *J. Comp. Neurol.* 264:527-546.
14. Cliffer, K.D., and G.J. Giesler Jr. (1988) PHA-L can be transported anterogradely through fibers of passage. *Brain Res.* 458:185-191.
15. Cook, J.R., and M. Wiesendanger. (1976) Input from trigeminal cutaneous afferents to neurones of the inferior olive in rats. *Exp. Brain Res.* 26:193-202.
16. Cook, M.S. and W.M. Falls. (1992a) Efferent projections of neurons in four subdivisional regions of rat trigeminal nucleus interpolaris to the diencephalon and midbrain: A PHA-L study. (In Preparation).
17. Cook, M.S. and W.M. Falls. (1992b) Efferent projections of neurons in four subdivisional regions of rat trigeminal nucleus interpolaris to the cerebellum and spinal cord: A PHA-L study. (In Preparation).
18. Courville, J., F. Faraco-Cantin, and L. Marcon. (1983) Projections from the reticular formation of the medulla, the spinal trigeminal and lateral reticular nuclei to the inferior olive. *Neurosci.* 9:129-139.
19. Desclin, J.C. (1974) Histological evidence supporting the inferior olive as a major source of cerebellar climbing fibers in the rat. *Brain Res.* 77:365-384.
20. Edwards, S.B. (1972) The ascending and descending projections of the red nucleus in the cat: An experimental study using an autoradiographic tracing method. *Brain Res.* 48:45-63.
21. Erzurumlu, R.S. and H.P. Killackey. (1979) Efferent connections of the brainstem trigeminal complex with the facial nucleus of the rat. *J. Comp. Neurol.* 188:75-86.

22. Erzurumlu, R.S., and H.P. Killackey. (1980) Diencephalic projections of the subnucleus interpolaris of the brainstem trigeminal complex in the rat. *Neurosci.* 5:1891-1901.
23. Falls, W.M. (1984a) The morphology of neurons in trigeminal nucleus oralis projecting to the medullary dorsal horn (trigeminal nucleus caudalis): A retrograde horseradish peroxidase and golgi study. *Neurosci.* Vol. 13. 4:1279-1298.
24. Falls, W.M. (1984b) Termination in trigeminal nucleus oralis of ascending intratrigeminal axons originating from neurons in the medullary dorsal horn: An HRP study in the rat employing light and electron microscopy. *Brain Res.* 290:136-140.
25. Flumerfelt, B.A. and D.G. Gwyn. (1974) The red nucleus of the rat: Its organization and interconnections. *J. Anat.* 118:374.
26. Fuxe, K. (1965) Evidence for the existence of monoamine neurons in the central nervous system. IV. Distribution of monoamine terminals in the central nervous system. *Acta Physiol. Scand.* 64 (Suppl. 247):37-85.
27. Gellman, R., J.C. Houk, and A.R. Gibson. (1983) Somatosensory properties of the inferior olive of the cat. *J. Comp. Neurol.* 215:228-243.
28. Gerfen, C.R. and P.E. Sawchenko. (1984) An anterograde neuroanatomical tracing method that shows the detailed morphology of neurons, their axons and terminals: Immunohistochemical localization of an axonally transported plant lectin, *Phaseolus vulgaris* leucoagglutinin (PHA-L). *Brain Res.* 290:219-238.
29. Gobel, S., and M.B. Purvis. (1972) Anatomical studies of the organization of the spinal V nucleus: The deep bundles and the spinal V tract. *Brain Res.* 48:27-44.
30. Hockfield, S., and S. Gobel. (1982) Anatomical demonstration of projections to the medullary dorsal horn (trigeminal nucleus caudalis) from rostral trigeminal nuclei and the contralateral caudal medulla. *Brain Res.* 252:203-211.
31. Huerta, M.F., A.J. Frankfurter, and J.K. Harting. (1983) Studies of the principal sensory and spinal trigeminal nuclei of the rat: Projections to the superior colliculus, inferior olive, and cerebellum. *J. Comp. Neurol.* 220:147-167.

32. Huerta, M.F., T. Hashikawa, M.J. Gayoso, and J.K. Harting. (1985) The trigemino-olivary projection in the cat: Contributions of individual subnuclei. *J. Comp. Neurol.* 241:180-190.
33. Ikeda, M., M. Matsushita and T. Tanami. (1982) Termination and cells of origin of the ascending intranuclear fibers in the spinal trigeminal nucleus of the cat. A study with the horseradish peroxidase technique. *Neurosci. Lett.* 31:215-220.
34. Ikeda, M., T. Tanami, and M. Matsushita. (1984) Ascending and descending internuclear connections of the trigeminal sensory nuclei in the cat. A study with the retrograde and anterograde horseradish peroxidase technique. *Neurosci.* 12:1243-1260.
35. Jacquin, M.F., N.L. Chiaia, J.H. Haring and R.W. Rhoades. (1990) Intersubnuclear connections within the rat trigeminal brainstem complex. *Somatosensory and Motor Res.* 7:399-420.
36. Jacquin, M.F., R.A. Stennett, W.E. Renehan and R.W. Rhoades. (1988) Structure-function relationships in the rat brainstem subnucleus interpolaris: II. Low and high threshold trigeminal primary afferents. *J. Comp. Neurol.* 267:107-130
37. Jacquin, M.F., D. Woerner, A.M. Szczepanik, V. Riecker, R.D. Mooney, and R.W. Rhoades. (1986) Structure-function relationships in rat brainstem subnucleus interpolaris. Vibrissa primary afferents. *J. Comp. Neurol.* 243:266-279.
38. Kawana, E. (1969) Projections of the anterior ectosylvian gyrus to the thalamus, the dorsal column nuclei, the trigeminal nuclei and the spinal cord in cats. *Brain Res.* 14:117-136.
39. Kerr, F.W.L. (1963) The divisional organization of afferent fibers of the trigeminal nerve. *Brain.* 86:721-732.
40. Kuypers, H.G.J.M. (1960) Central cortical projections to motor and somatosensory cell groups. *Brain* 83:161-184.

41. Martin, G.F., J. Culberson, C. Laxson, M. Linauts, M. Panneton, and I. Tschismadia. (1980) Afferent connections of the inferior olivary nucleus with preliminary notes on their development: Studies using the North American opossum. In J. Courville, C. Montigny, and Y. Lamarre (eds): The Inferior Olivary Nucleus: Anatomy and Physiology. New York: Raven Press, pp.35-72.
42. Martin, M.R. and D. Lodge. (1977) Morphology of the facial nucleus of the rat. Brain Res. 123:1-12.
43. Mihailoff, G.A., R.A. Burne, S.A. Azizi, G. Norell and D.J. Woodward. (1981) The pontocerebellar system in the rat: An HRP study. II. Hemispherical components. J. Comp. Neurol. 197:559-577.
44. Mihailoff, G.A., R.A. Burne and D.J. Woodward. (1978) Projections of the sensorimotor cortex to the basilar pontine nuclei in the rat: An autoradiographic study. Brain Res. 145:347-354.
45. Mihailoff, G.A., C.B. McArdle and C.E. Adams. (1981) The cytoarchitecture, cytology, and synaptic organization of the basilar pontine nuclei in the rat. I. Nissl and Golgi studies. J. Comp. Neurol. 195:181-201.
46. Miles, T.S., and M. Wiesindanger. (1975) Organization of climbing fiber projections to the cerebellar cortex from trigeminal cutaneous efferents and from SI face area of the cerebral cortex in the cat. J. Physiol. Lond. 245:409-424.
47. Miller, R.A., and N.L. Strominger. (1973) Efferent connections of the red nucleus in the brainstem and spinal cord of the rhesus monkey. J. Comp. Neurol. 152:327-346.
48. Moore, R.Y., and F.E. Bloom. (1979) Central catecholamine neuron systems: Anatomy and physiology of the norepinephrine and epinephrine systems. Annu. Rev. Neurosci. 2:113-168.
49. Nasution, I.D., and Y. Shigenaga. (1987) Ascending and descending internuclear projections within the trigeminal sensory nuclear complex. Brain Res. 425:234-247.
50. NIH Guide for the Care and Use of Laboratory Animals. NIH, 9000 Rockville Pike, Bethesda, MD 20892.

51. Palkovits, M., M. Brownstein, J.M. Saavedra, and J. Axelrod. (1974) Norepinephrine and dopamine content of hypothalamic nuclei of the rat. *Brain Res.* 77:137-149.
52. Panneton, W.M., and H. Burton. (1982) Origin of ascending intratrigeminal pathways in the cat. *Brain Res.* 236:463-470.
53. Paxinos, G. (1985) *The Rat Nervous System. Vol. 2. Hindbrain and Spinal Cord.* Academic Press Australia.
54. Paxinos, G., and C. Watson. (1986) *The Rat Brain in Stereotaxic Coordinates.* Academic Press, New York.
55. Phelan, K.D. and W.M. Falls. (1989) An analysis of the cyto- and myeloarchitectonic organization of trigeminal nucleus interpolaris in the rat. *Somatosensory Res.* Vol. 6, 4:333-366.
56. Phelan, K.D., and W.M. Falls. (1990) A comparison of the distribution and morphology of thalamic, cerebellar and spinal projection neurons in rat trigeminal nucleus interpolaris. *Neurosci.* 40:497-511.
57. Phelan, K.D., and W.M. Falls. (1991) The spinotrigeminal pathway and its spatial relationship to the origin of trigeminospinal projections in the rat. *Neuroscience* 40:477-496.
58. Potter, R.F., D.G. Ruegg and M. Wiesendanger. (1978) Responses of neurons of the pontine nuclei to stimulation of the sensorimotor, visual and auditory cortex of the rat. *Brain Res. Bull.* 3:15-19.
59. Provis, J. (1977) The organization of the facial nucleus of the brush-tailed possum (*Trichosurus vulpecula*). *J. Comp. Neurol.* 172: 177-188.
60. Rhoades, R.W., S.E. Fish, N.L. Chiaia, C. Bennett-Clarke, and R.D. Mooney. (1989) Organization of the projections from the trigeminal brainstem complex to the superior colliculus in the rat and hamster: Anterograde tracing with phaseolus vulgaris leukoagglutinin and intra-axonal injection. *J. Comp. Neurol.* 289:641-656.
61. Rossi, G.F., and A. Brodal. (1956) Spinal afferents to the trigeminal sensory nuclei and the nucleus of the solitary tract. *Confin, Neurol. (Basel)* 16:321-332.

62. Shohara, E. and A. Sakai (1983) Localization of motoneurons innervating deep and superficial facial muscles in the rat: A horseradish peroxidase and electrophysiologic study. *Exp. Neurol.* 81:14-33.
63. Smith, L.A. and W.M. Falls. (1992) Efferent projections to cranial nerve nuclei from rat trigeminal nucleus oralis. (In Press).
64. Steinbusch, H.W.M. (1981) Distribution of serotonin-immunoreactivity in the central nervous system of the rat cell bodies and terminals. *Neurosci.* 6:557-618.
65. Swenson, R.S., and A.J. Castro. (1983) The afferent connections of the inferior olivary complex in rats. An anterograde study using autoradiographic and axonal degeneration techniques. *Neurosci.* 8:259-275.
66. Szekely, G. and C. Matesz. (1982) The accessory motor nuclei of the trigeminal, facial, and abducens nerves in the rat. *J. Comp. Neurol.* 210:258-264.
67. Takemura, M., T. Sugimoto and A. Sakai. (1987) Topographic organization of central terminal region of different sensory branches of the rat mandibular nerve. *Exp. Neurol.* 96:540-557.
68. Torvik, A. (1956) Afferent connections to the sensory trigeminal nuclei, the nucleus of the solitary tract and adjacent structures. An experimental study in the rat. *J. Comp. Neurol.* 106:51-142.
69. Walberg, F. (1982) The trigemino-olivary projection in the cat as studied with retrograde transport of horseradish peroxidase. *Exp. Brain Res.* 45:101-107.
70. Watson, C.R.R., S. Sakai and W. Armstrong. (1982) Organization of the facial nucleus in the rat. *Brain Behav. Evol.* 20:19-28.
71. Wiesendanger, R. and M. Wiesendanger. (1982a) The corticopontine system in the rat. I. Mapping of corticopontine neurons. *J. Comp. Neurol.* 208: 215-226.
72. Wiesendanger, R. and M. Wiesendanger. (1982b) The corticopontine system in the rat. II. The projection pattern. *J. Comp. Neurol.* 208:227-238.
73. Wise, S.P., E.A. Murray, and J.D. Coulter. (1979) Somatotopic organization of corticospinal and corticotrigeminal neurons in the rat. *Neurosci.* 4:65-78.

CHAPTER III

Efferent Projections of Neurons in Four Subdivisional Regions of Rat Trigeminal Nucleus Interpolaris to the Cerebellum and Spinal Cord: A PHA-L Study

INTRODUCTION

Trigeminal nucleus interpolaris (Vi) receives sensory information from primary trigeminal neurons innervating orofacial receptive fields. Within Vi this orofacial sensory information undergoes processing and modification before being relayed by projection neurons to several target nuclei along the neuraxis, including the cerebellum and spinal cord. Anatomical and electrophysiological techniques have shown that neurons in rat Vi emit axons which terminate in the cerebellum (69,96,97) and spinal cord (48,69,78).

Efferent Vi projections to cerebellum and spinal cord have been described without much consideration for their subdivisional origin within the nucleus. This is to be expected, since only recently have six separate and distinct subdivisions of rat Vi been delineated based on differences in their overall cyto- and myeloarchitecture, as well as connectional criteria (68). The six Vi subdivisions include ventrolateral magnocellular (vlVimc), ventrolateral

parvocellular (vlVipc), border region (brVi), dorsolateral (dlVi), dorsal cap (dcVi) and intermediate region (irVi). In addition, previous studies have provided relatively little information regarding the morphological characteristics of the terminal axonal arborizations of Vi projection neurons. The present study was conducted to determine the distribution of efferent axons from neurons in four distinct Vi subdivisional regions, to the cerebellum and spinal cord as well as to describe the morphological characteristics of the mossy fibers and terminal axonal arborizations of these neurons. The four subdivisional regions of Vi from which these projections are described include vlVimc, vlVipc, brVi and dorsomedial Vi (dmVi), which includes dlVi, dcVi and irVi. Iontophoretic injections of the anterograde tracer, Phaseolus vulgaris leucoagglutinin (PHA-L), permit one to make injections into Vi subdivisional regions, and visualize the distribution and morphological characteristics of the axons and terminal ramifications of Vi neurons in the various targets. The morphological details of Vi axons and their terminal ramifications are necessary if one is to begin to understand the effects of Vi inputs on the activity of neurons in the cerebellum and spinal cord. Research has been conducted, regarding the distribution and morphology of efferent axons and terminal arborizations from these four Vi subdivisional areas to target nuclei in the diencephalon and midbrain (22) as well as to the pons and medulla (23).

MATERIALS AND METHODS

The descriptions of experimental procedures and methods of data collection outlined in Chapter I of this thesis should be referred to for this study as well. The injection sites and identification of cerebellar and spinal cord targets were also based on descriptions by Paxinos and Watson (54) and the previous studies of Phelan and Falls (55,56). However, in this study the cerebellum and spinal cord were sectioned at 30-50 μm on an Oxford Vibratome in either the transverse, horizontal or sagittal plane. The distinction of the types of mossy fibers described were based on previous descriptions by Palay and Chan-Palay ('74) and the cytoarchitectonic organization of the cervical spinal cord was based on studies by Molander et. al. ('89).

RESULTS

The data provided for this study were based on successful injections of PHA-L in a total of eight animals, two injections for each of the four Vi subdivisional regions. Although two separate injections were made into each subdivisional region, only one representative injection site for each will be used for illustrative purposes (Fig. 1). For descriptions of the individual PHA-L injection sites, see the Results section of Chapter I.

Projections to the Cerebellum

It is well known that the cerebellar cortex receives afferent input from five principal groups including vestibular nuclei, spinal cord, pontine nuclei (mainly from cerebral cortex), olivary and reticular nuclei (24,80). This study shows that Vi also provides substantial input to widespread areas of the cerebellar cortex. Injections of PHA-L into any of the four Vi subdivisional regions, vlVimc, vlVipc, dmVi and brVi, labeled projection neurons whose axons traversed the inferior cerebellar peduncle and entered the ipsilateral cerebellar hemisphere. The labeled axons entered the cerebellum (CB) at the at the level of the lateral cerebellar nucleus. Most axons coursed dorsal to the lateral and intermediate cerebellar nuclei as they entered CB,

however, a few passed through the nuclei. Axons which terminated in the lateral portions of the granule cell layer (GCL) of ipsilateral CB coursed from the white matter to the various lobules, while those terminating in more medial portions, or contralaterally, traveled medially in the white matter before entering the various regions of CB. Axons from neurons in vlVimc, vlVipc and brVi were distributed in ipsilateral CB, while axons from dmVi neurons projected bilaterally, with ipsilateral predominance.

General Distribution of Mossy Fibers in Cerebellar Cortex

The greatest density of labeled mossy fibers (MFs) and terminal axonal arborizations in CB resulted from injections into dmVi. This Vi subdivisional region was also the only one to project bilaterally to the GCL and deep cerebellar nuclei (DCN), however, contralateral projections were less dense. The regions of ipsilateral CB which receive the majority of MFs included lobule 9 (uvula), paramedian lobule (PML), Crus II, simple lobule (SIM) and Crus I (Fig. 2). Fewer MFs were located in lobules 4, 5 and 6. Contralaterally, MFs were found in widespread areas of GCL, including lobules 4-7, lobule 9, Crus I, Crus II, PML and SIM (Fig. 3). In addition, terminal axonal arborizations were located bilaterally in all of the DCN.

Following vlVimc injections, labeled axons coursed to various regions of ipsilateral CB and gave rise to MFs of

greatest density in lobule 9, SIM and Crus II (Fig. 4). Areas receiving fewer numbers of vlVimc MFs included PML, Crus I and lobules 5 and 7. Axons from vlVimc neurons did not give rise to substantial numbers of terminal arborizations in the DCN. Injections into vlVipc resulted in labeled MFs distributed with greatest density in lobule 9 and Crura I and II (Fig. 5). Fewer MFs were located in SIM, and sparse numbers were found in lobules 5, 6 and 7. Axons from neurons in vlVipc gave rise to a substantial number of terminal arborizations in the DCN.

The overall number of labeled MFs and their terminal axonal arborizations following brVi injections was less than those observed following injections into the other Vi subdivisional regions. Labeled axons from brVi neurons gave rise to MFs primarily in lobule 9 and Crus I, and only a sparse number in Crus II and SIM (Fig. 6). No substantial labeling of terminal axonal arborizations were found in the DCN.

Projections to the Vermis

Projections to the vermis were most dense from dmVi, and included ipsilateral as well as contralateral input. Ipsilaterally, dmVi MFs were found in the distal portion (crown) of lobule 9a, lobules 3-5, 6A, 7, and copula pyramis (Fig. 2A-C). Contralaterally, MFs from dmVi neurons were distributed similarly in the same lobules, but less dense

(Fig. 3A-C). Labeled axons from vlVimc and vlVipc injections were distributed similarly in the ipsilateral vermis (Figs. 4A-C; 5A-C). The majority of axons from these subdivisions gave rise to MFs in the crown of lobule 9a. A few entered the wall and crown of the GCL of lobule 6a, adjacent to the primary fissure (PrF), as well as in the wall of lobule 5. Injections in brVi produced labeled MFs only in lobule 9a of the ipsilateral vermis (Fig. 6A-C).

Projections to the Simple Lobule

Projections to SIM differed from each of the four Vi subdivisional regions. Labeled axons of dmVi neurons gave rise to MFs bilaterally in SIM, with the greatest density ipsilaterally. Ipsilaterally, labeled MFs entered the GCL of all portions of SIM along the mediolateral extent (Fig. 2D-F). However, they were most dense at the level of the lateral cerebellar nucleus (LAT) (Fig. 2E). Contralaterally, MFs were much more sparse and were distributed to posterior SIM (Fig. 3D-F). Labeled MFs from vlVimc were located in anterior and posterior portions of ipsilateral SIM, at the level of LAT (Fig. 4E). Lateral and medial to this area of termination, MFs were sparse (Fig. 4D,F). A similar projection of resulted from vlVipc injections, however, they were slightly less dense (Fig. 5 D-F). Injections of PHA-L into brVi did not label any MFs in SIM.

Projections to Crus I

Projections to ipsilateral Crus I were most dense following dmVi and vlVipc injections, and least dense following vlVimc and brVi injections. Neurons in dmVi gave rise to MFs bilaterally in Crus I, with the greatest density ipsilaterally. Those found ipsilaterally were distributed to the walls and distal portions of Crus Ia and c, and were most numerous at the level of LAT (Fig. 2D-F). Contralaterally, dmVi MFs terminated primarily in Crus Ia and b (Fig. 3D-F). The MFs of vlVipc neurons entered the GCL of the wall and distal portion of Crus Ia and c, at the level of LAT (Fig. 5E). Lateral and medial to LAT, MFs were sparse and located in the deep portion of Crus I (Fig. 5D,F). Labeled fibers in Crus I following vlVimc and brVi injections were sparse, and entered the walls of Crus Ia (Fig. 4D-F) and Ic (Fig. 6D-F), respectively.

Projections to Crus II

Labeled MFs in Crus II were most dense following dmVi injections, less dense following vlVimc and vlVipc injections, and completely absent following brVi injections. Projections to Crus II from dmVi were bilateral, with ipsilateral predominance. Ipsilaterally, MFs were found in all portions of the GCL of Crus II (Fig. 2D-F), but were most numerous at the level of LAT (Fig. 2E). Contralaterally, the projections were similar, however, the MFs avoided Crus IIb

(Fig. 3D-F). The distribution of endings in Crus II from vlVimc and vlVipc were similar (Figs. 4D-F; 5D-F). The MFs from these subdivisions entered the walls and distal portions of Crus IIa and b, at the level of LAT, while medial and lateral to LAT, they were more sparse and located in the wall of Crus II, adjacent to the intercrural fissure.

Projections to the Paramedian Lobule

The projections to PML were most dense from dmVi, less dense from vlVimc and vlVipc, and absent from brVi. Labeled axons from dmVi neurons gave rise to MFs throughout PML ipsilaterally (Figs. 2D-F) and contralaterally (Fig. 3D-F), but were more dense ipsilaterally. Following vlVimc and vlVipc injections, labeled MFs were found mainly at the level of LAT (Figs. 4E; 5E).

Projections to the Deep Cerebellar Nuclei

The axons from dmVi neurons provided the greatest density of terminal arborizations to the DCN. Ipsilaterally, dmVi terminal axonal arborizations were distributed in widespread portions of all of the DCN, including LAT, medial (MED), and intermediate (INT) cerebellar nuclei (Fig. 2B-E). Labeled terminal axonal arborizations were also located in these nuclei contralaterally following dmVi injections, although less dense (Fig. 3B-E). Labeled axons from vlVipc neurons gave rise to sparse numbers of terminal arborizations

in ipsilateral MED, INT and LAT (Fig. 5B-E). Injections in vlVimc produced only a few labeled terminal axonal arborizations in INT (Fig. 4D), while brVi injections did not result in any labeled terminal arborizations in the DCN.

Morphology of Mossy Fibers and Terminal Axonal Arborizations in CB

The axonal endings, located in the GCL of the cerebellar cortex were morphologically distinct from those endings in the DCN. Those in the GCL were typical endings of MFs (Fig. 7), while those in the DCN resembled terminal axonal arborizations (Fig. 8) similar to those located in other target nuclei along the neuraxis (22,23).

Two types of MFs were observed branching in the white matter and in the GCL of the various cortical receptive regions (Figs. 7, 12). One type was a simple MF ending, characterized by an axon (approximately 1.0 to 2.0 μm in diameter) that gave rise to irregular enlargements (ranging in size from approximately 5.0 x 7.0 to 7.0 x 7.0 μm) that were fairly simple and fusiform in shape, with smooth globular contours and a few short, finger-like projections. The enlargements either occurred along the course of the fiber (en passant swellings), at branching points (bifurcating swellings), or at the end of the fibers (terminal swellings). The second type was a complex MF, characterized by an axon (approximately 1.0 to 2.0 μm in

diameter) with irregular swellings (ranging in size from approximately 5.0×5.0 to $7.0 \times 14 \mu\text{m}$) that were more complicated in shape than the simple MFs, with a massive convoluted central expansion out of which projected several tapering or filiform appendages, with terminal strand diameters of approximately $0.5 \mu\text{m}$ in diameter and terminal swellings approximately 1.0 to $2.0 \mu\text{m}$ in diameter. The irregular swellings of the complex-MFs, like those of the simple-MFs, occurred either along the course of the axon, at a bifurcation point, or at the end of the fiber. Although most of the PHA-L labeled MFs branched and ended in the GCL, some were observed to extend to, and closely appose, Purkinje Cell bodies (Figs. 7,12D).

The axons which terminated in the DCN were collaterals from MFs in the main bundle which arched dorsally over the nuclei on their way to the cortex. The collaterals which coursed throughout the DCN (approximately 1.0 to $1.5 \mu\text{m}$ in diameter) gave rise to a single type of terminal arborization (Fig. 8), which consisted of several thin, branched terminal strands (approximately $0.5 \mu\text{m}$ in diameter) with numerous widely spaced boutons en passant and end boutons (approximately 1.0 to $2.0 \mu\text{m}$ in diameter). Terminal arbors in DCN were mainly oriented dorsoventrally.

Projections to the Cervical Spinal Cord

PHA-L labeled axons gave rise to terminal arborizations in the cervical spinal cord (CSC). The greatest density of terminal arbors was in the rostral cervical cord (RCC) with the cervical enlargement (CE) receiving considerably fewer terminal arbors. Projections to the CE did not extend caudally past the level of C7. Labeled axons from neurons in all four Vi subdivisional regions descended directly through MDH, in the deep axonal bundles, to the ipsilateral dorsal horn, where they gave rise to terminal arborizations predominantly in laminae III and IV of the RCC and CE (Figs. 9,10). The density of labeled terminal axonal arborizations decreased from RCC to CE, and the overall density was less following brVi injections than they were from injections into the other subdivisional regions. An occasional labeled terminal arbor was seen in laminae V and VI of the ipsilateral dorsal horn following the various injections, and no labeled axon extended into the ipsilateral ventral horn. While vlVimc and dmVi injections produced labeling in the contralateral CSC (Figs. 9C,D; 10C,D), vlVipc and brVi injections did not (Figs. 9A,B; 10A,B). PHA-L injections into vlVimc and dmVi labeled axons which coursed medially from the respective injection sites, decussated and descended in the contralateral ventral funiculus. From the RCC ventral funiculus, labeled axons coursed dorsally through the ventral horn, where they gave rise to terminal arbors in lamina IX,

and several continued dorsally through the intermediate gray to the dorsal horn where sparse numbers of axons ended in laminae III and IV. Although a substantial number of axons from vlVimc neurons extended to the CE in the contralateral ventral funiculus, where they gave rise to substantial terminal arbors in laminae IX and laminae III and IV (Fig. 9D), axons from dmVi did not.

The terminal arborizations located in the ipsilateral dorsal horn originated from axons (approximately 1.0 to 1.5 μm in diameter) which descended within the deep axonal bundles and were of one type (Fig.11). They were characterized by thin, branched terminal strands (approximately 0.5 μm in diameter) with multiple en passant and end boutons (approximately 1.0 to 2.0 μm in diameter). The terminal arbors were generally oriented rostrocaudally, often with ascending and descending limbs spanning considerable distances (up to 580 μm). The labeled terminal arborizations located in the contralateral CSC were from axons that were thicker (approximately 2.0 μm in diameter) than those that projected to the ipsilateral dorsal horn, however they were similarly branched and had multiple en passant and end boutons (Figs. 13C,D).



DISCUSSION

This study examined the projections from Vi to the cerebellum and spinal cord based on recently delineated Vi subdivisions (68), using the anterograde PHA-L method (30). This study also provided detailed descriptions of the morphological characteristics of PHA-L labeled MFs in the GCL, as well as the characteristics of the terminal axonal arborizations in the DCN and CSC.

For a discussion of differences between the various Vi subdivisions and the benefits of utilizing the anterograde PHA-L method in this study, see the Discussion section of Chapter I. However, it is important to mention here that although it has been shown that PHA-L can be transported retrogradely (74) and anterogradely by fibers of passage (21), these modes of transportation did not appear to affect the results of this study. Only a few retrogradely labeled neuronal somata were located in rostral MDH. Regarding the labeling of fibers of passage, one of the main routes for trigeminospinal axons is through the more caudal trigeminal sensory nuclei (31,40,41,61). So although the potential exists for labeling the fibers of more rostral trigeminal sensory nuclei, which travel through Vi to the spinal cord, this did not appear to be the case in the present study. The projections from Vi to the CSC described in this study, are

different from those described from Vo using the same technique (85). If PHA-L injections into Vi did not label fibers of passage from neurons in Vo, there is no reason to believe that fibers of passage from neurons in Vms would also be labeled.

Projections to the GCL of the Cerebellar Cortex

Projections from Vi to CB have been extensively studied anatomically and electrophysiologically in the rat (39,46,51,65,84,93,96,97) and cat (33,86) as well as in other mammalian species (64,80). Vi has been shown to be the main nuclear contributor to the trigeminocerebellar projection (93). Up to 70% of its neurons have been shown to project directly to CB, mainly ipsilaterally (86), with a smaller constituent of cells projecting contralaterally (26,64,65).

Many previous studies which investigated trigemino-cerebellar projections described their distribution in areas of the cerebellar cortex known to receive orofacial tactile input. These orofacial tactile areas, lobule 9a of the vermis (46,86), PML, Crura I and II (83,86), and SIM (82,86), contain representations of orofacial regions that are disproportionately large compared to other body parts. The present study adds support to these findings by showing that these orofacial tactile areas are the main CB targets of Vi neurons. The major projection to the vermis from all Vi subdivisional regions was to lobule 9a. Lobule 9a has been

shown to contain projection areas from cutaneous receptive fields (RFs) mostly from mystacial vibrissae and the upper lip (83). The primary Vi projections to the hemisphere was to Crura I and II, PML and SIM. These regions also receive tactile information from orofacial regions (82,83). Crus I receives patch-like inputs from the head and upper face (including the crown, ear, eyelids, nose, upper and lower lips, and mystacial vibrissae), however lacks input from perioral regions. Crus II receives input from perioral structures, as well as from incisors and intraoral skin of the furry buccal pad. PML receives tactile input from the entire body, but primarily from perioral structures. Finally, SIM has been shown to receive input only from regions within and around the face and mouth (including the gingiva, incisors, lips and vibrissae). The neurons in the dorsal portion of Vi (dmVi), presumably receiving mandibular primary afferent input, are shown by the present study, and supported by other studies (39,65), to be the main contributor of axons to these regions.

The MFs from Vi neurons described in the present study, branched within the white matter and GCL, while giving rise to large, irregular swellings only in the GCL. During their course through the white matter, MFs divide several times, giving off as many as 30 collaterals to the GCL as they course towards the distal portion (crown) of the folia (62). Some fibers branch deep in the white matter to serve

different folia, as well as within a particular folium to serve its different parts. This branching of MFs may be, in part, responsible for the fractured pattern of distribution of orofacial RFs in CB (46,82,83), where multiple representations of body parts exist in a particular folium, or in several folia, forming patches sometimes referred to as a "mosaic". For example, vibrissae and/or dorsal head regions are represented on five different folia (Crus Ia,b and c, Crus IIa, and PML), and the perioral tissues on three folia (Crus IIa and b, and PML). Also, within a particular folium, a specific body structure may project to more than one patch, often separated from each other by patch projections from other body regions. One previous study in the rat (96) provides additional evidence that trigeminocerebellar MF branching is related to this somatotopical organization of the GCL. Although this pattern of MF distribution may not appear indicative of a well-organized system, microelectrode mapping of these tactile areas have revealed that they are highly organized, but multiple, representations (83). Recordings from orofacial regions to the respective patches in CB, have shown latencies of 3-5 msec. A similar study recorded latencies of 2-4 msec., in lobule 9a of the uvula and crura I and II, when the snout was stimulated (6). These latency times are short enough to allow only a single relay in the medulla, most likely in part, in Vi.

The RFs for a particular patch can be recorded in a

vertical column in the GCL. This may be due to the morphology of the MFs, as described in the present study as well as in other examinations (62,81), which illustrate that the large irregular swellings of a particular MF, or groups of MFs, are distributed throughout the deep, middle and superficial portions of the GCL. Although three morphologically distinct types of MFs have been described (62), only two have been identified in the present study, a simple and complex type.

The present study shows that dmVi provides the most robust input from Vi to all of the CB receptive areas. Although previous studies have shown that this appears to be true for projections to PML (65) and Crura I and II (39) in the rat, this is not supported for projections to PML in the tree shrew (64). A more extensive study of subdivisional origin of Vi-CB neurons in the rat revealed that they were distributed throughout the rostrocaudal extent of Vi (69).

Vi has also been shown to provide substantial input to major pre-cerebellar nuclei which are known to project to the cerebellum, including the pontine nuclei (Pn) (23,56) and inferior olive (IO) (23,58). Another Vi target which has been shown to provide input to the cerebellum is the superior colliculus (22). The neurons in Pn provide a major source of MFs to most regions of CB cortex and DCN, and it is generally accepted that all cells in Pn project predominantly to CB contralaterally. The areas of Pn which receive which Vi

input have been shown to project to orofacial portions of CB including SIM, PML, and Crura I and II (57). The neurons in IO are thought to be the sole source of climbing fibers to the CB cortex in the rat (4,24), and it is generally accepted that all neurons in IO send their axons to CB. The trigemino- receptive regions of IO have also been shown to provide climbing fiber input to some of the same areas that receive direct Vi MF input, including Crura I and II, PML and SIM. The superior colliculus (SC), although not generally considered a major pre-cerebellar nucleus (66), is another region which receives direct Vi input (22) and also provides input to tactile areas of the CB hemispheres in rat (47). Using micromapping techniques, stimulation of the tactile-responsive intermediate layers of SC evoke responses in tactile regions of contralateral GCL of CB. Responses to SC stimulation were found in Crura I and II, SIM and PML, but not in the uvula (47). The peripheral receptive fields of interconnected SC and GCL loci consisted exclusively of facial structures, especially from the vibrissae, crown, bridge of nose and eyelids.

This pathway, along with an additional pathway from SC to IO and subsequently to the CB (3,38), appears to provide a significant alternative pathway for information from Vi to reach CB. Thus, Vi not only has the ability to influence CB activity by means of direct projections, but also through indirect routes through Pn, IO and SC. This indicates that

a major role of Vi is to convey orofacial tactile information to the cerebellum by direct and indirect paths, and has the ability to significantly effect the activity in CB through various MF and climbing fiber endings. This is important because the control of movement and posture by CB is achieved by adjusting the degree of contraction of skeletal muscles, which requires that CB be provided with a continuous flow of information about the events in the periphery during the course of movement. It appears that direct Vi input to CB, as well as indirect projections through Pn, IO and SC, provides this kind of continuous flow of information.

Projections to the Deep Cerebellar Nuclei

In addition to describing MF distribution in the cerebellar cortex, this study also shows the distribution of terminal axonal arborizations from the Vi subdivisional regions to the DCN, including the MED (fastigial), INT (interpositus) and LAT (dentate) nuclei. As was the case for projections from Vi to the GCL of the cerebellar cortex, the most robust projection to the DCN was from dmVi. Labeled axons of dmVi neurons gave rise to terminal arborizations bilaterally in the DCN, with ipsilateral predominance. The terminal arborizations were located bilaterally in widespread portions of MED, INT and LAT. Injections in vlVipic labeled a relatively small number of terminal arborizations in each of the DCN ipsilaterally, while axons of vlVimc neurons gave

rise to only a few in ipsilateral INT. No labeled terminal axonal arborizations were found in the DCN following brVi injections. It appeared that most of the labeled axons which entered the DCN were collaterals of those destined for the cerebellar cortex. This is in agreement with previous studies (18,62). Although the axons which coursed to the DCN were apparently collaterals of those bound for the cerebellar cortex, not all axons which traveled to the cortex provided collaterals to the DCN. This was demonstrated in the present study where brVi injections labeled MFs in the cortex, but did not label terminal axonal arborizations in the DCN.

It is well known that the DCN receive input from pontine nuclei (Pn), inferior olive (IO), red nucleus (RN) as well as several other areas (25). However, information regarding trigeminal projections to the DCN is limited. Stimulation of cutaneous trigeminal branches, including supraorbital, infraorbital and mental nerves, have been shown to activate neurons in the ipsilateral INT (76). The retrograde HRP technique has revealed input to LAT from the ipsilateral spinal trigeminal nucleus (76). This technique further demonstrated that Vi is the main contributor of trigeminocerebellar axons to the DCN (86).

Previous investigations have provided substantial information regarding cerebellar outflow from the DCN. Efferent projections from MED have been shown to terminate in several target nuclei, including the ventrolateral thalamic

nuclei, superior colliculus, Pn, vestibular nuclei, IO and spinal cord (5,12,13,94). The termination of axons from INT have been shown to occur in the ventrolateral and intralaminar thalamic nuclei, RN, central gray (CG), nucleus of Darkschewitsch (DK), IO and spinal cord (28,35,53,89). Efferent connections of LAT also involve several of the same target nuclei including the thalamus, parvocellular RN, oculomotor nucleus, Edinger-Westphal nucleus, DK, Pn, CG and IO (12,15,19,28,35). It is interesting that the DCN project to the ventrolateral thalamus, Pn, RN, superior colliculus, and spinal cord, because these are areas shown to receive direct Vi input (22,23). Until it can be confirmed that Vi terminal axonal arborizations synapse with cells that project to these same targets, the meaning of this alternative pathway cannot be determined.

The morphological characteristics of the terminal axonal arborizations in the DCN from extra-cerebellar sources are not well documented. The utilization of the anterograde PHA-L method has allowed the structural features of the terminal axonal arborizations from Vi to be described in the present study. Only one type of terminal arbor was found in DCN following injections in dmVi, vlVimc and vlVipc, which was characterized by thin, branched terminal strands bearing modest numbers of en passant and terminal boutons. The importance of this is two-fold. First, it shows that axons from neurons in Vi give rise to collaterals to the DCN which

have terminal arborizations that are morphologically different than the MF endings of their continuations. Secondly, the fact that the terminal arbors found in DCN have a number of swellings, or boutons along their length, is suggestive of synaptic activity in these nuclei.

This study provides evidence that Vi provides input to the GCL of the cerebellar cortex and the DCN. In the GCL, MFs activate granule cells, among others, which send processes to the molecular layer to contact Purkinje Cell dendrites (62,63). The Purkinje Cells, in turn, provide the efferents from the cerebellar cortex, with the majority terminating in the central nuclei. This projection is organized into orderly longitudinal (rostrocaudal) zones, with a medial vermal zone projecting to MED, an intermediate (paravermal) zone projecting to INT and a lateral (hemispherical) zone connecting to LAT (19,32). It has also been shown as a result of several previous studies that the afferent projections of the cerebellar cortex and DCN, as well as cortico-nuclear projections in CB, are also based on a sagittal zonal organization (17,19,34,81,91). In the present study, projections from Vi to CB were examined in sagittal and horizontal sections and there was no obvious zonal distribution of labeled axons and their terminal ramifications in the cortex or DCN. The lack of obvious zonal banding of Vi MFs may have been due to the fact that relatively small PHA-L injections were made in the various Vi

subdivisional regions, labeling fewer axons and MFs at one time than would result from large injections in Vi. This is an aspect of the trigeminocerebellar projections that deserves further attention in future studies.

Projections to the Spinal Cord

In addition to describing trigeminocerebellar projections from Vi, this study also shows that PHA-L injections into four subdivisional regions of Vi resulted in labeled axons and terminal arborizations in the CSC. These findings are in good agreement with previous studies in rat (48,69,78) and cat (54,55). Trigemino-spinal axons originating from Vi neurons have been shown to terminate predominantly at upper levels (C1-2) of the CSC (69), with progressively fewer axons terminating at mid-to-lower cervical and thoracic levels (27). One previous study, which used the retrograde HRP method, described projections from the spinal trigeminal nucleus, including Vi, to all levels of the spinal cord as far as the lumbosacral cord (78). The retrogradely labeled cell bodies in Vi were described as being located ventrally at the transition zone between Vi and MDH. It is possible, due to the description and illustration of the location of the labeled cell bodies, that they were actually located in MDH, since no cytological distinction between Vi and MDH was mentioned. Most of the previous studies which addressed trigemino-spinal projections did not

provide very much information on the specific Vi subdivisions which projected to the spinal cord. The lack of information regarding the Vi subdivisions which contribute to spinal cord projections was probably due to the fact that the delineation of subdivisional differences in Vi had not been revealed until recently (68). However, one study reported that retrogradely labeled neurons occurred mostly in the rostroventral part of Vi following HRP injections into the spinal cord (48). A more recent study, which utilized the same method, described a more widespread distribution of these neurons in Vi (69). In this study, injections of HRP into mid-to-lower levels of the CSC labeled neurons in dlVi and vlVimc, while RCC injections resulted in a greater density of retrogradely labeled cells in brVi, dlVi, vlVipc and vlVimc. The labeled trigeminospinal neurons in Vi following CSC injections exhibited a wide range in cell sizes, including small, medium and large somata. In the present study, the most substantial input to the CSC was from neurons in vlVimc and dmVi (which includes dlVi). Together with a previous study by Phelan and Falls ('91), it appears that dlVi and vlVimc are primary contributors of Vi-CSC projections.

Another important aspect of the Vi-CSC projection is the identification of the specific spinal cord laminae which receive Vi input. Previous studies, which utilized retrograde tracing methods, were unable to localize the

precise laminae of termination of Vi-CSC projections because of the nature of the injection sites. They were usually too extensive, spreading throughout a large area of spinal gray matter. However, the utilization of PHA-L in this study revealed the specific laminae of termination of Vi axons. Labeled axons from neurons in all four Vi subdivisional regions examined, including vlVimc, vlVipc, dmVi and brVi, coursed caudally through MDH and the spinal V tract to the ipsilateral CSC dorsal horn. There they gave rise to terminal arborizations in laminae III and IV, with sparse labeling in lamina V. Some axons from dmVi and vlVimc neurons also decussated in the midline at the level of the injection site and descended in the ventral funiculus. These axons then coursed dorsally through the ventral horn, where they gave rise to terminal arbors in laminae IX, and with some then continuing dorsally to the dorsal horn where they issued terminal arbors to laminae III and IV. Generally, the ipsilateral projections to the dorsal horn were more substantial than those to the contralateral dorsal and ventral horns.

It is well known that laminae III and IV receive tactile information, by means of a large variety of A β cutaneous mechanoreceptive fibers and mechanosensitive fine myelinated A δ fibers from the skin and hair follicles for discriminative touch (14,71). In addition, these laminae also receive afferent fibers from the somatosensory cortex (14,71).

Projections from the somatosensory cortex have been shown to be somatotopically organized with those projecting to cervical segments originating mainly from neurons in neck and posterior head representation areas of the SI cortex (95). It has also been demonstrated that the collaterals of Pacinian corpuscles in glabrous skin have terminal arborizations that occupy the medial one-third of the dorsal horn, similar to where the majority of spinal cord projecting Vi axons terminate (29). In this region, axon collaterals pass ventrally through laminae I and II, or enter lamina III directly from its medial border and form profuse terminal arbors in laminae III and IV, with smaller secondary terminal arbors in laminae V and VI. In addition to the Pacinian corpuscles, another type of rapidly adapting mechanoreceptor occurs in glabrous skin, the Meissner corpuscle. These are innervated by large diameter myelinated fibers which enter the dorsal or dorsomedial part of the dorsal horn and give rise to terminal arborizations in medial lamina III (29). Sensitive slowly adapting cutaneous mechanoreceptors have also been found to arborize profusely in laminae III, IV and V.

Another input to the CSC is from primary trigeminal fibers which innervate orofacial regions. Trigeminal primary input from face, intra- and perioral structures have been shown to activate neurons in the dorsal horn (1,2) as well as neck motor neurons (1,2,50,88). Primary trigeminal input has

repeatedly been shown to terminate in laminae III-IV. In one study, large myelinated cutaneous afferent fibers innervating the face were stained intra-axonally with HRP (36). The terminal arborizations of collaterals given off from a single parent axon entered not only the spinal trigeminal nuclei, but also laminae III and IV of the cervical dorsal horn. In addition, HRP injections into the trigeminal ganglion labeled primary afferents which terminated most heavily in laminae III-V of the contralateral dorsal horn at C1 and C2 levels (42). It is evident that the vibrissae are, in part, responsible for the activation of dorsal horn cells in the cervical cord. Retrograde and transganglionic transport of HRP revealed that the deep vibrissae nerve, which innervates vibrissae follicles, projects to the C1 dorsal horn and is entirely restricted to laminae III-V (9). Thus, if spinal and trigeminal primary input convey tactile information from cutaneous receptors to laminae III-V, it is suggested that the same kind of information is relayed by Vi to these same laminae, especially III and IV. The purpose of this projection may be involved with the modulation of convergent sensory input bilaterally to the ipsilateral cervical dorsal horn, with greater ipsilateral influence.

The functional significance of the projections from vlVimc and dmVi to laminae IX of the contralateral ventral horn is probably for the purpose of activating motor neurons which innervate neck musculature during orienting behavior.

Although this hypothesis cannot be confirmed without further electrophysiological and electron microscopic studies, previous studies support a trigeminospinal projection which effects the activity of neck motorneuronal output (1,2,50,88,92). Several studies have indicated a close functional relationship between the trigeminal system and upper cervical cord motor neurons. Stimulation of several trigeminal primary afferents have been shown to excite cells in the ventral horn of the upper cervical cord. Abrahams et. al. ('79) reported that neck motor neurons are most powerfully excited by stimulation of the infraorbital (IO) nerves. Sumino and Nozaki ('77) have demonstrated that the neck motor neurons also receive input from the inferior alveolar, lingual and masseter nerves, suggesting that the trigeminospinal reflex is induced not only by cutaneous input from the face region, but also by input from intraoral structures. It has also been observed that the IO and supraorbital (SO) nerves, which innervate the nose and forehead regions, respectively, elicit different response patterns from the cervical motor neurons and muscles (77). The response of neck muscle motorneurons to IO nerve stimulation is consistent with a movement which involves raising the animal's head in an avoidance posture to a stimulus applied to the nose. On the other hand, SO nerve stimulation results in a complex movement involving twisting of the head away from the stimulus and raising of the head

towards the stimulus. Such a movement is similar to, and thought to be directly involved with, suckling and orientation reflexes. Although the projections from Vi have been shown to primarily terminate in the rostral cervical cord, with fewer projections to the cervical enlargement, it has also been previously suggested that the presence of secondary trigeminal fibers at caudal cervical and thoracic levels might also be related to reflex swallowing mechanisms, i.e., that sensory stimulation of the oral cavity might reflexly inhibit phrenic and intercostal activity (16).

This study described the morphological characteristics of terminal arborizations of axons from Vi neurons in the CSC. These terminal arbors were derived from two major groups of axons. One group, which were located in the ipsilateral dorsal horn, originated from thin parent fibers which coursed from Vi caudally through MDH mainly to laminae III and IV. The second group of terminal arbors were derived from thicker parent axons which crossed the midline from the injection site, and descended in the ventral funiculus. From the ventral funiculus, this second group of axons coursed dorsally through the ventral horn to the dorsal horn. These two paths to the CSC are also utilized by axons of Vo trigeminospinal projection neurons (85), and the morphological characteristics of their terminal arborizations are similar to those from Vi axons. The terminal axonal arborizations that were labeled in the cervical cord

following Vi injections were rostrocaudally oriented in the spinal gray matter. The predominantly rostrocaudal orientation of Vi terminal arborizations matches those of primary spinal afferent terminal arborizations in laminae III and IV (71,73), and parallels the longitudinally oriented dendrites of cells in these laminae (72,73).

Finally, it appears that SC may play a role in contributing to an alternative, indirect pathway for information from Vi to the spinal cord. It has been shown in the cat and rat (60), as well as in the hamster (75), that neurons mainly located in the intermediate laminae of the lateral SC project primarily to the cervical cord. Tectospinal neurons projecting to the rostral segments of the cervical spinal cord are found over a larger extent of the contralateral SC than those terminating in the cervical enlargement. The tectospinal projection to the cervical enlargement in both rats and cats arise almost exclusively from the caudolateral quadrant of the contralateral SC, whereas the tectal projection to the rostral (upper) cervical spinal cord originates, in cats, from almost the entire extent of the colliculus and, in rats, from its greater part. Most of the tectospinal neurons were located in the intermediate laminae. No evidence for tectospinal projections to the thoracic or lumbar levels of the spinal cord was found in the cat or rat. Because the retrograde HRP technique was used to determine the location of tectospinal

neurons in these experiments, the specific cervical cord laminae in which the tectospinal axons terminated was not determined. Intracellular recording and horseradish peroxidase injection techniques were used to delineate the structural and functional characteristics of the SC cells in the hamster, which could be antidromically activated from the first cervical segment of the spinal cord (75). Most of the tectospinal cells were exclusively somatosensory and gave rapidly adapting responses to deflection of vibrissae and/or guard hairs, and greater than 50% of the cells were located in the lateral portion of the intermediate laminae. These cells were located in the same general region that receive Vi input (22). These findings indicate that in addition to direct input to the CSC, Vi may utilize an alternative pathway through the neurons in SC to convey somatosensory information from orofacial regions to the cervical cord to contribute to the regulation of head and neck movements which orient the animal toward stimuli in its environment.

Collateral Projections

Previous studies have indicated that axons of some Vi projection neurons send collaterals to more than one target nucleus along the neuraxis. Double retrograde fluorescent labeling techniques in the rat have shown a significant number of neurons in Vi which project to both the thalamic ventrobasal complex and CB (65,84). This has been disputed

by antidromic collision techniques, combined electrophysiological recording and antidromic stimulation techniques, and double retrograde transport of Fast Blue and HRP, which have revealed that very few, if any, Vi neurons project to both the ventrobasal thalamus and the CB (43,51,97). Thus, collateralization of trigeminothalamic axons to the CB is debatable. A more recent study revealed that at least some of the axons of Vi cells are collateralized (69). When HRP was injected into the thalamus, 80% of the large multipolar neurons were labeled, 50% of these neurons were labeled after cerebellar injections, and 60% were labeled following spinal cord injections. These data indicate that there must be collateralization of at least 30% of the large multipolar neurons in Vi. It has been suggested by Phelan and Falls ('90) that since the collateralization of trigeminothalamic and trigeminospinal cells has not previously been reported, the collateralization must exist between trigeminothalamic and trigeminocerebellar neurons.

Similarities and Differences in Vi Subdivisional Projections to the Cerebellum and Spinal Cord

The present study demonstrates that there are similarities and differences between the projections from four Vi subdivisional regions to the cerebellum and spinal cord. Regarding projections to CB, the four Vi subdivisional

regions were similar in that they all projected to ipsilateral lobule 9a of the vermis and Crus I, and all but brVi projected to ipsilateral SIM, Crus II and PML. Thus, the major CB cortical projections were similar for all regions. In addition, axons from neurons in all regions gave rise to complex MFs in the GCL, however, most simple MFs resulted from vlVimc injections. Neurons in dmVi differed from neurons in all other Vi subdivisional regions in that they also projected to contralateral lobule 9a, Crura I and II, PML and SIM.

The projections from the four Vi subdivisional regions to the DCN were all different. Injections of PHA-L into dmVi produced labeled terminal axonal arborizations in all nuclei bilaterally, including MED, INT and LAT. Injections in vlVipic produced labeled terminal arbors in all of the nuclei ipsilaterally, and only a few labeled terminal arbors were found in ipsilateral INT following injections into vlVimc. No labeled terminal arbors were found in the DCN following brVi injections.

The four Vi subdivisional regions were also similar in that they all projected to the CSC, with decreasing density from RCC to CE. In all cases, the major projection was ipsilateral to laminae III and IV with similar types of rostrocaudally oriented terminal arborizations. However, vlVimc and dmVi differed from vlVipic and brVi in that they also projected to contralateral CSC, specifically to laminae

III, IV and IX. Furthermore, the axons that coursed to contralateral CSC were thicker than those that projected ipsilaterally.

Although some significant differences were found in the CB and spinal cord projections from vlVimc, vlVipc dmVi and brVi, it is possible that injections into dmVi may have masked more subtle differences between the three subdivisions which comprise it, including dlVi, dcVi and irVi. These three dorsal subdivisions have been shown to be morphologically distinct based on cyto- and myeloarchitectural studies (68), as well as being different based on afferent input from primary trigeminal neurons innervating orofacial regions (44,90). Attempts to make precise, well-contained injections into these dorsal subdivisions were unsuccessful due to their relatively small size. Thus, differences in the projections from the six Vi subdivisions are possibly greater than those revealed by the present study. Further efforts to make micro-injections into these regions and define their specific projections will be reserved for future studies.

Figure 1. PHA-L Injection Sites.

Schematic drawings (E-H) of representative transverse sections (A-D) through PHA-L injection sites (IS) in four subdivisional regions of rat trigeminal nucleus interpolaris (Vi). These regions are: ventrolateral magnocellular (vlVimc;A,E), ventrolateral parvocellular (vlVipc;B,F), dorsomedial (dmVi;C,G) and border region (brVi;D,H). The injection sites were, for the most part, confined to the respective subdivisional area of rat Vi. Amb, ambiguous nucleus; IO, inferior olive; svt, spinal trigeminal tract.

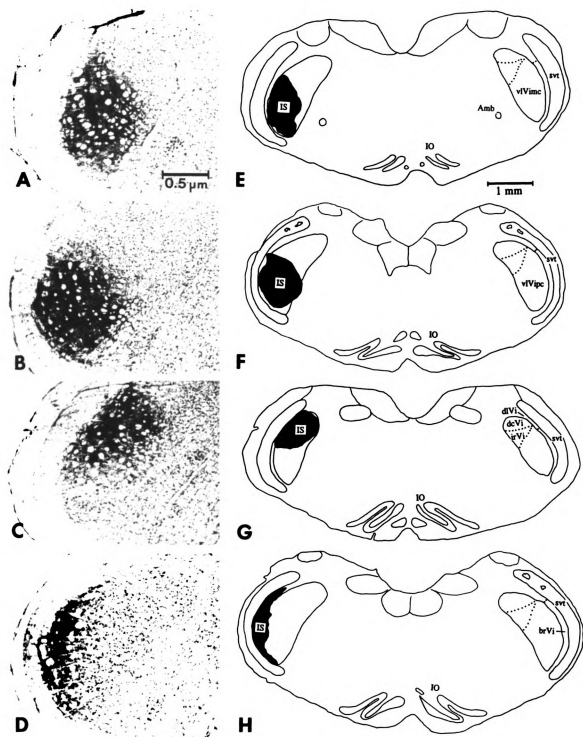


Figure 1

Figure 2: Cerebellar Projections from dmVi.

A-F. Schematic drawings of representative sagittal sections through the mediolateral extent of the ipsilateral cerebellum (CB), showing the distribution of labeled axons and terminal arbors, in the granule cell layer (GCL) and deep cerebellar nuclei (DCN), following the injection of PHA-L into dmVi. In the GCL, labeled mossy fibers (MFs) were found predominantly in lobule 9a, Crura I and II, paramedian lobule (PML) and simple lobule (Sim). In the DCN, labeled terminal arborizations were located in the medial (Med), intermediate (Int) and lateral nuclei (Lat). Numerals 1-10 indicate lobules. Cop, copula pyramis; ICF, intercrural fissure; PCF, preculminate fissure; PrF, primary fissure; PSF, posterior superior fissure; SF, secondary fissure.

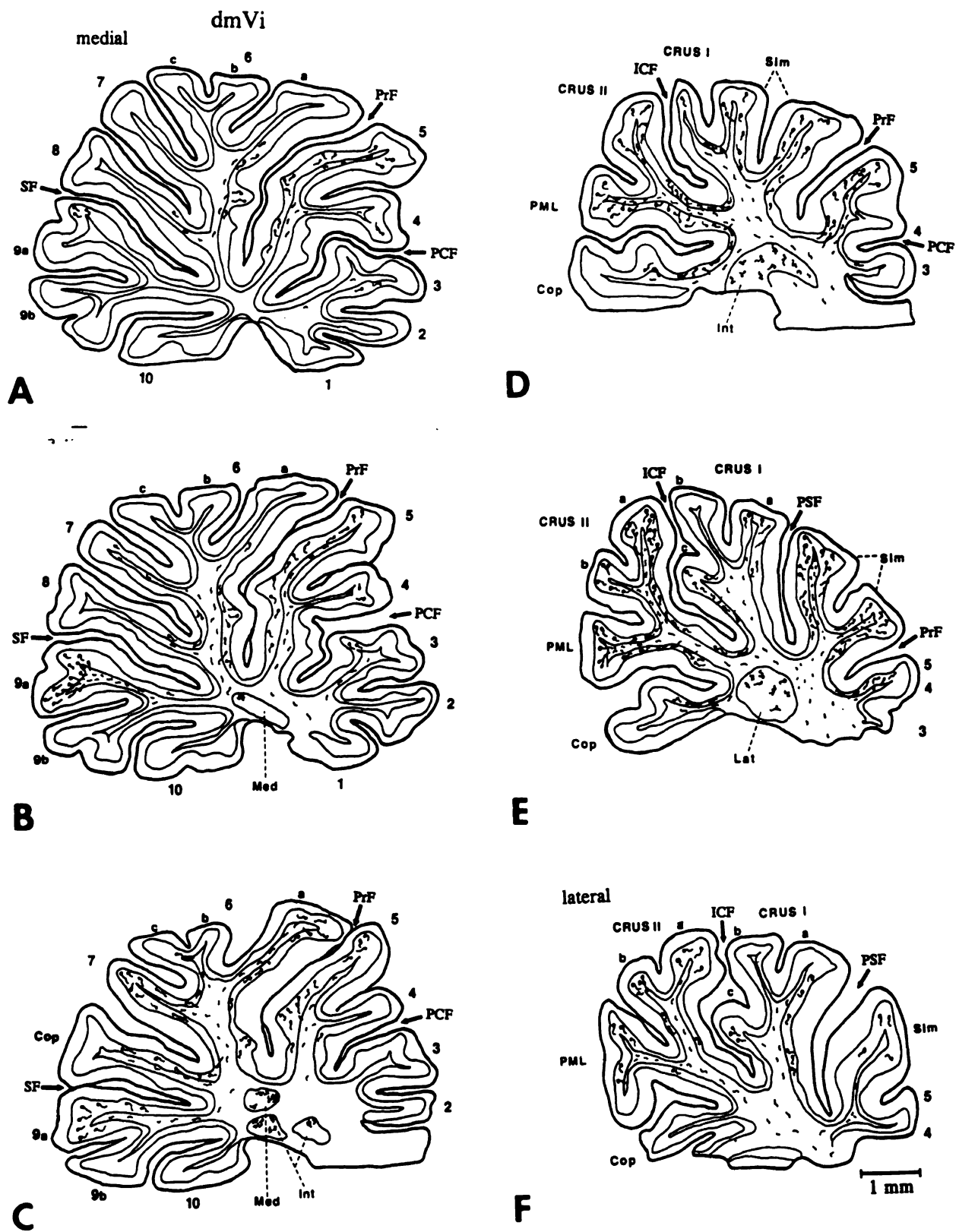


Figure 2

Figure 3: Cerebellar Projections from dmVi.

A-F. Schematic drawings of representative sagittal sections through the mediolateral extent of the contralateral CB, showing the distribution of labeled axons and terminal arbors, in the GCL and DCN, following the injection of PHA-L into dmVi. In the GCL, labeled MFs were found predominantly in lobules 6a, 9a, Crura I and II, and PML. In the DCN, labeled terminal arborizations were located in Med, Int and Lat. There were fewer labeled MFs and terminal axonal arborizations in contralateral CB than there were in ipsilateral CB following dmVi injections.

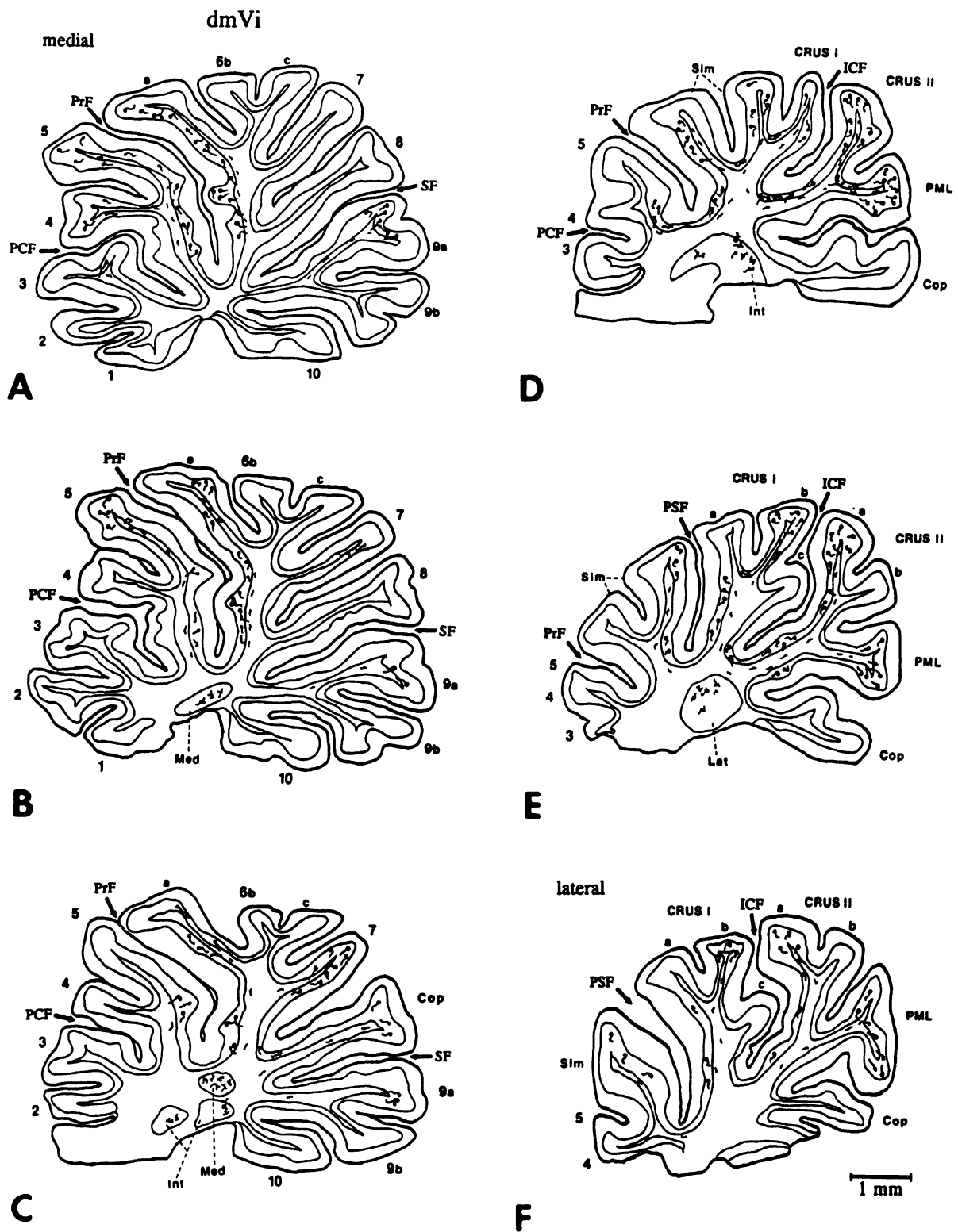


Figure 3

Figure 4: Cerebellar Projections from vlVimc.

A-F. Schematic drawings of representative sagittal sections through the mediolateral extent of the ipsilateral CB, showing the distribution of labeled axons and terminal arbors, in the GCL and DCN, following the injection of PHA-L into vlVimc. In the GCL, labeled MFs were found predominantly in lobule 9a, Crus II and Sim. In the DCN, labeled terminal arborizations were located in Int.

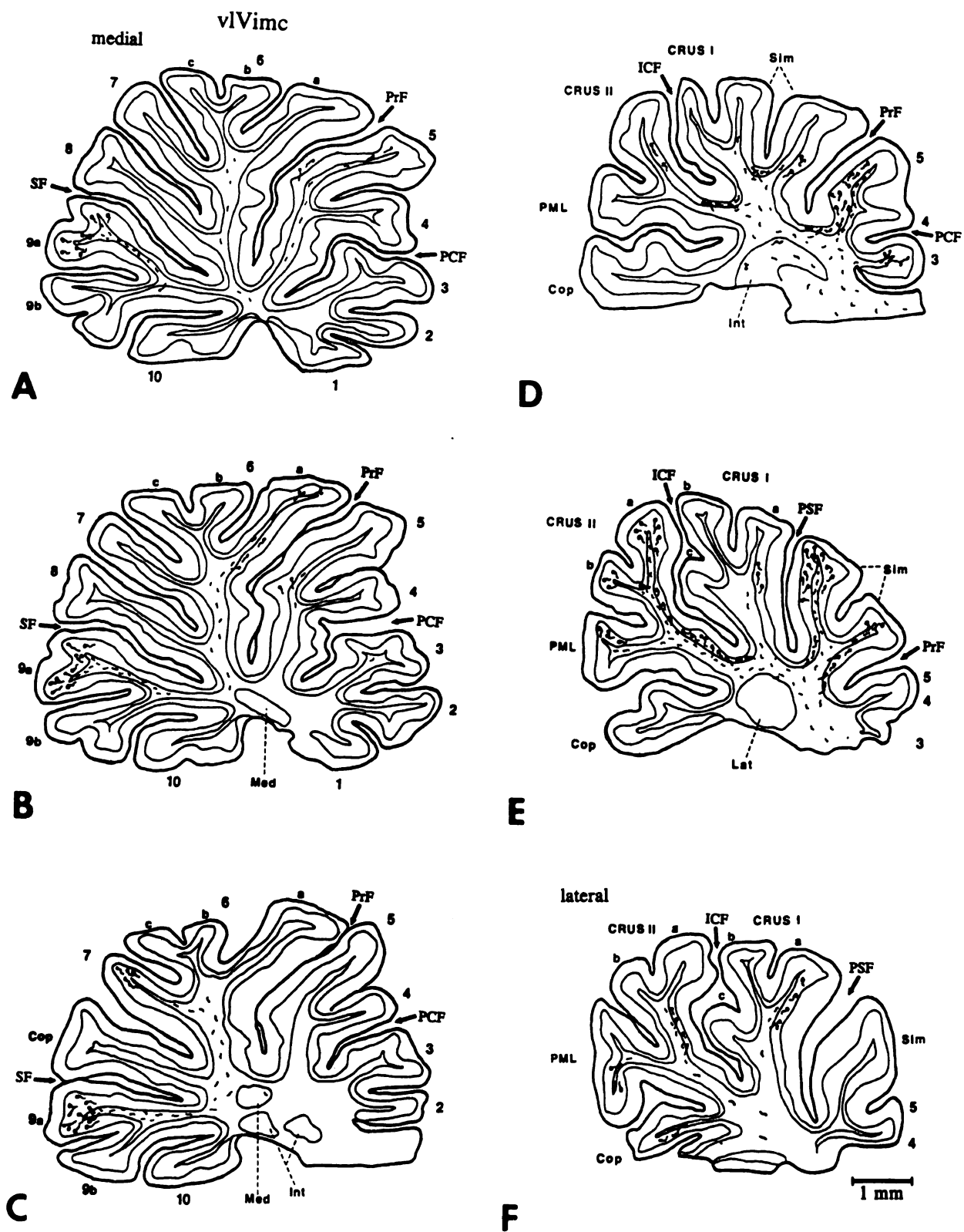


Figure 4

Figure 5: Cerebellar Projections from vlVipc.

A-F. Schematic drawings of representative sagittal sections through the mediolateral extent of the ipsilateral CB, showing the distribution of labeled axons and terminal arbors, in the GCL and DCN, following the injection of PHA-L into vlVipc. In the GCL, labeled MFs were found predominantly in lobule 9a and Crura I and II. In the DCN, a few labeled terminal arborizations were located in Med, Int, and Lat.

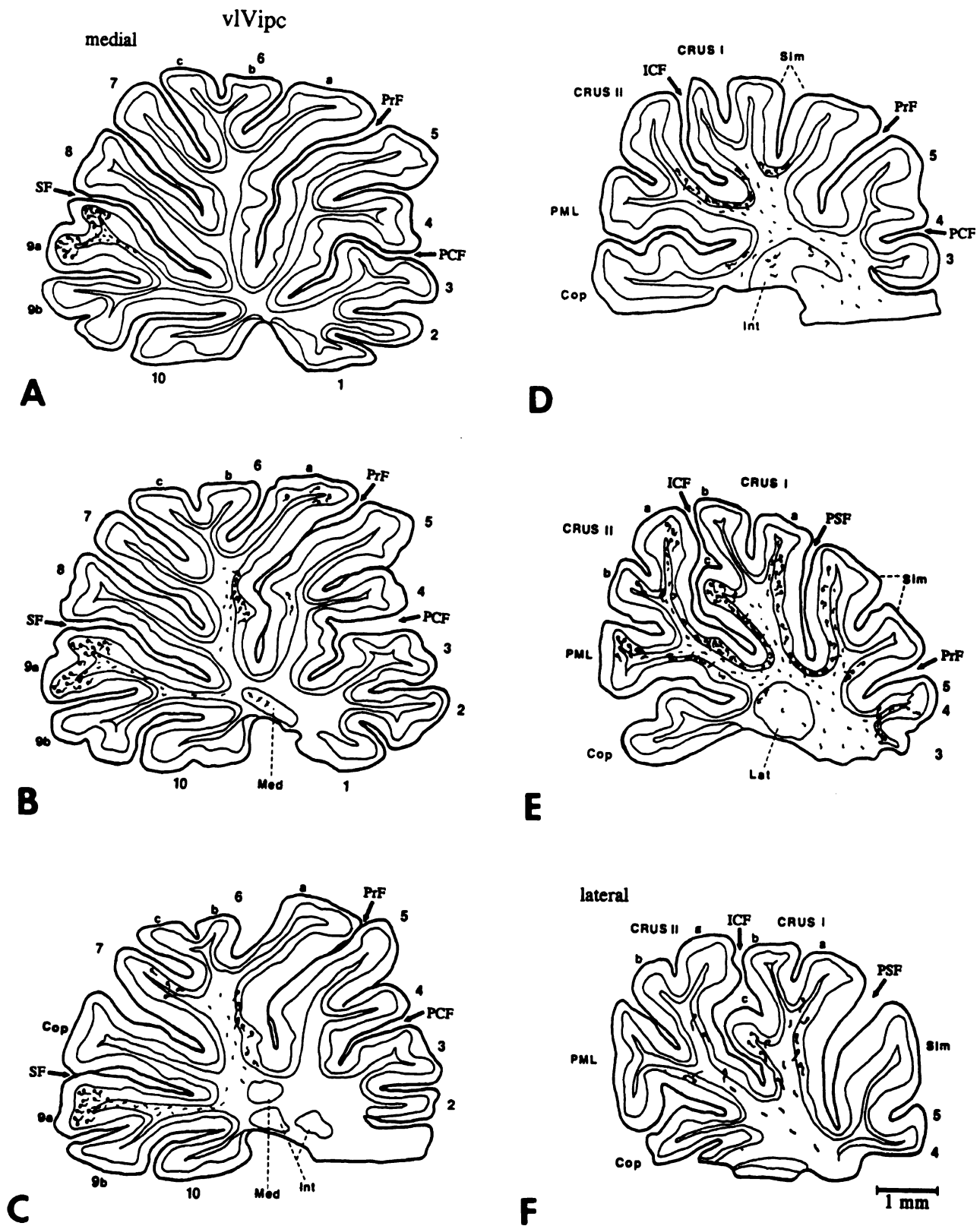


Figure 5

Figure 6: Cerebellar Projections from brVi.

A-F. Schematic drawings of representative sagittal sections through the mediolateral extent of the ipsilateral CB, showing the distribution of labeled MFs in the GCL following the injection of PHA-L into brVI. Labeled MFs were found predominantly in lobule 9a and Crus I. No labeled terminal axonal arborizations were found in the DCN.

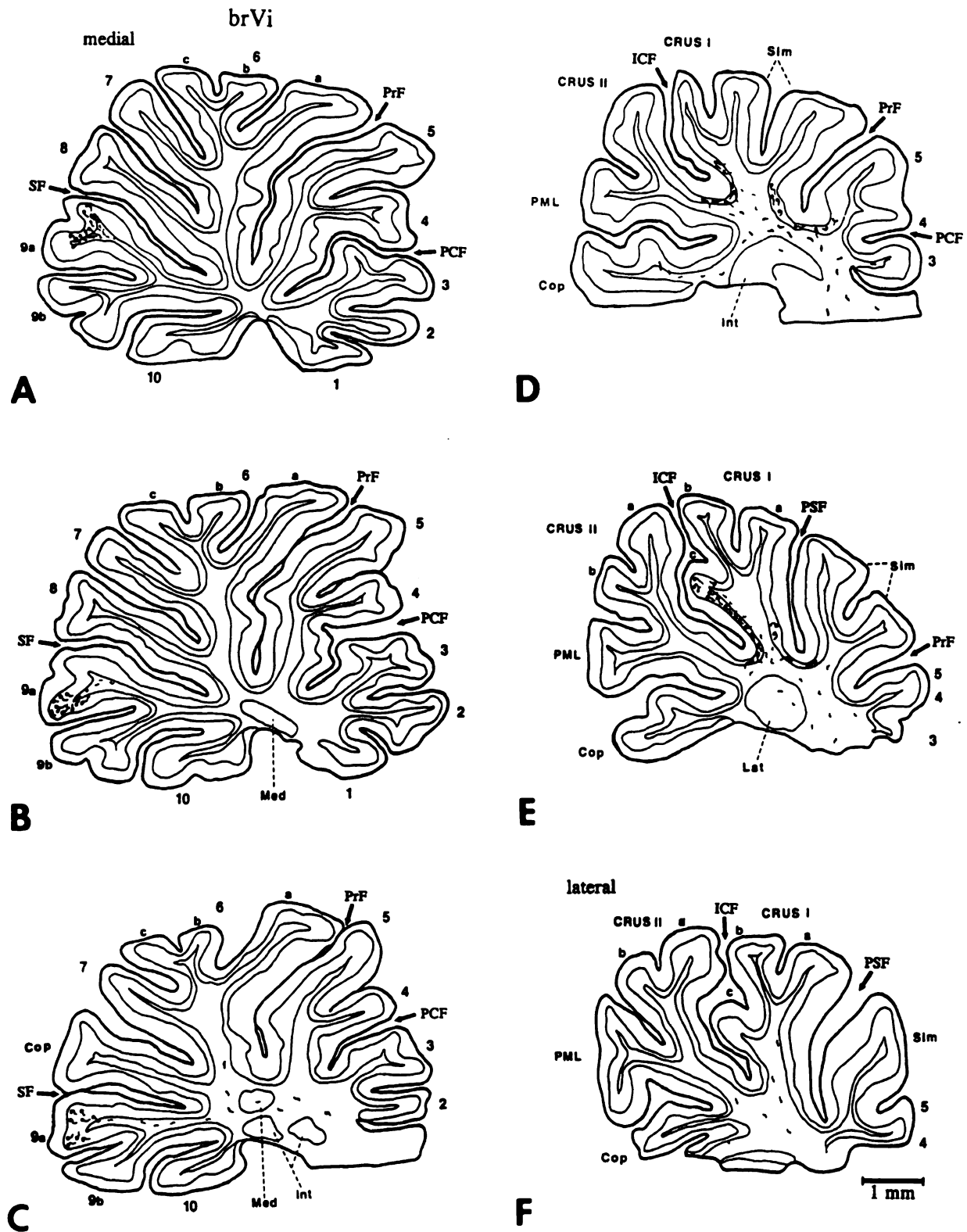


Figure 6

Figure 7: Drawings of Mossy Fibers in CB Granule Cell Layer.

Representative drawings of the two types of MFs located in the GCL. Some were simple MFs (asterisks), characterized by an axon that gave rise to irregular enlargements that were simple and fusiform, with smooth globular contours and a few short, finger-like projections. The majority were complex MFs, characterized by an axon with irregular swellings that were more complicated in shape than the simple MFs, displaying large convoluted expansions out of which projected several tapering or filiform appendages (arrows).

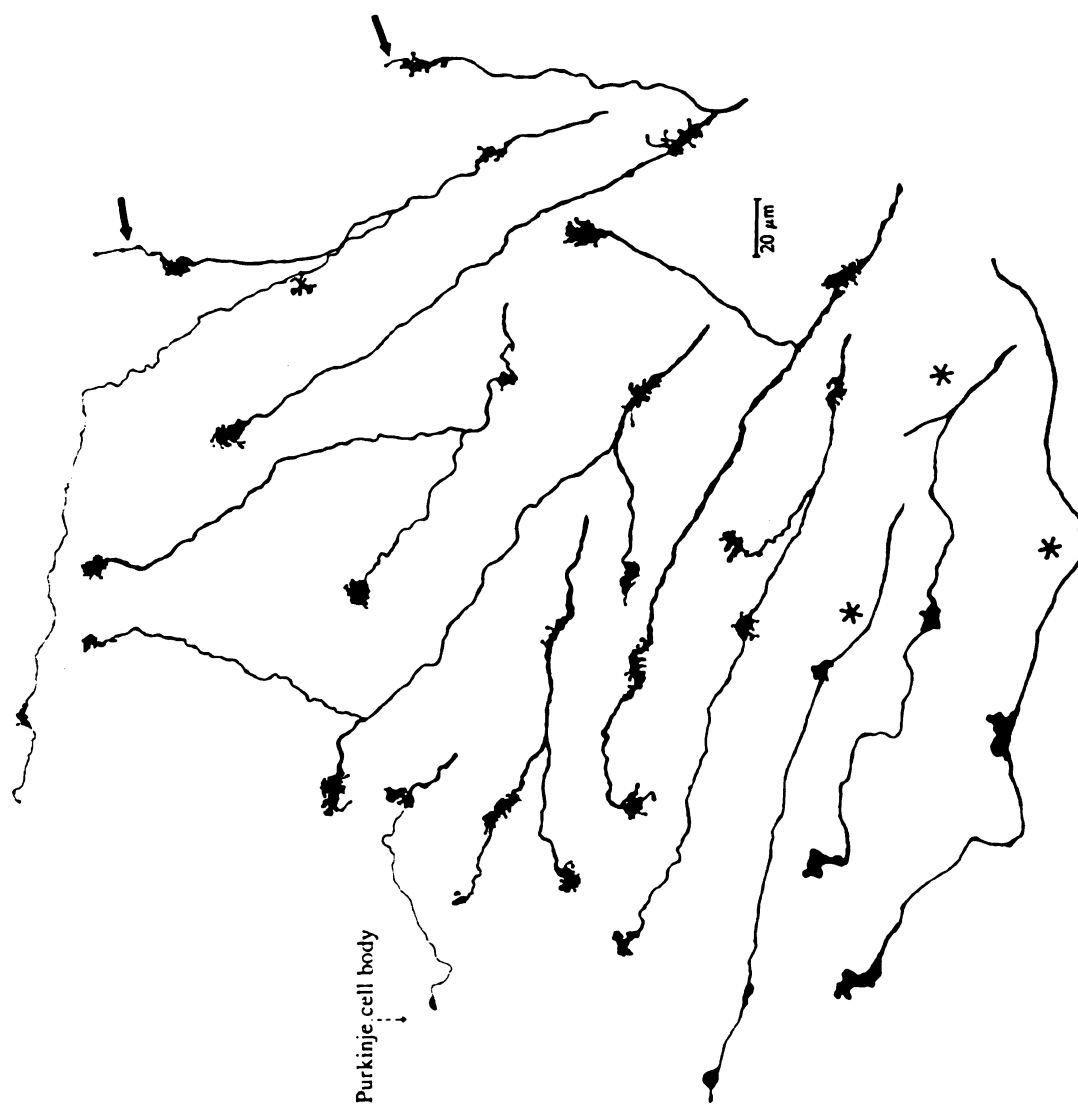


Figure 7

Figure 8: Drawings of Terminal Axonal Arborizations in DCN.

Representative drawings of the type of terminal axonal arborizations found in the DCN. They consisted of thin, branched terminal strands with numerous widely spaced boutons. b, bouton; pf, parent fiber; ts, terminal strand.

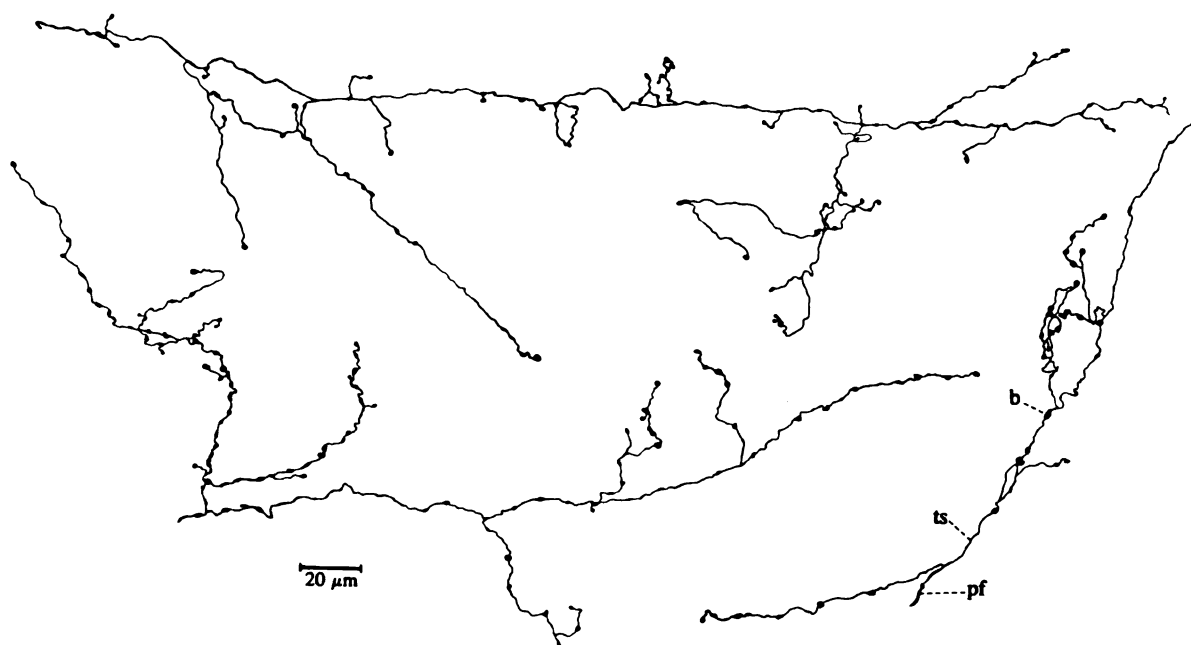


Figure 8

Figure 9: Spinal Cord Projections from vlVipc and vlVimc.

A,B. Schematic drawings of transverse sections through C2 and C5 of the cervical spinal cord (CSC) showing the distribution of labeled axons and terminal arborizations following the injection of PHA-L into vlVipc. The projection from vlVipc to the CSC was ipsilateral and predominantly terminated in laminae III and IV of the ipsilateral dorsal horn. Some terminal branches extended ventrally to lamina V. No labeled axons gave rise to terminal arborizations in the ventral horns or contralateral dorsal horn. C,D. Shows the distribution of labeled axons and terminal arborizations in C2 and C5 following the injection of PHA-L into vlVimc. The projection to the CSC was bilateral. Ipsilaterally, terminal arborizations were dense in laminae III and IV, with a few in lamina V. Contralaterally, labeled terminal arbors branched in lamina IX of the ventral horn, and laminae III and IV of the dorsal horn. i, ipsilateral.

Figure 10: Spinal Cord Projections from brVi and dmVi.

A,B. Schematic drawings of representative transverse sections through C2 and C5 of the cervical spinal cord (CSC) showing the distribution of labeled axons and terminal arborizations following the injection of PHA-L into brVi. The projection from brVi to the CSC was weak, and confined to laminae III and IV of the ipsilateral dorsal horn. C,D. Shows the distribution of labeled axons and terminal arborizations in C2 and C5 following the injection of PHA-L into dmVi. The projection to the CSC from dmVi was bilateral. Ipsilaterally, terminal arborizations were relatively dense in laminae III and IV, with a few in lamina V. Contralaterally, labeled terminal arbors branched in lamina IX of the ventral horn, of the rostral cervical cord, and laminae III and IV of the dorsal horn. i, ipsilateral.

Figure 11: Drawings of Terminal Axonal Arborizations in CSC.

Representative drawings of the type of terminal axonal arborizations found in the CSC. They consisted of thin, branched terminal strands with multiple en passant and end boutons. The terminal arbors spanned considerable distances (up to 580 μm) rostrocaudally.

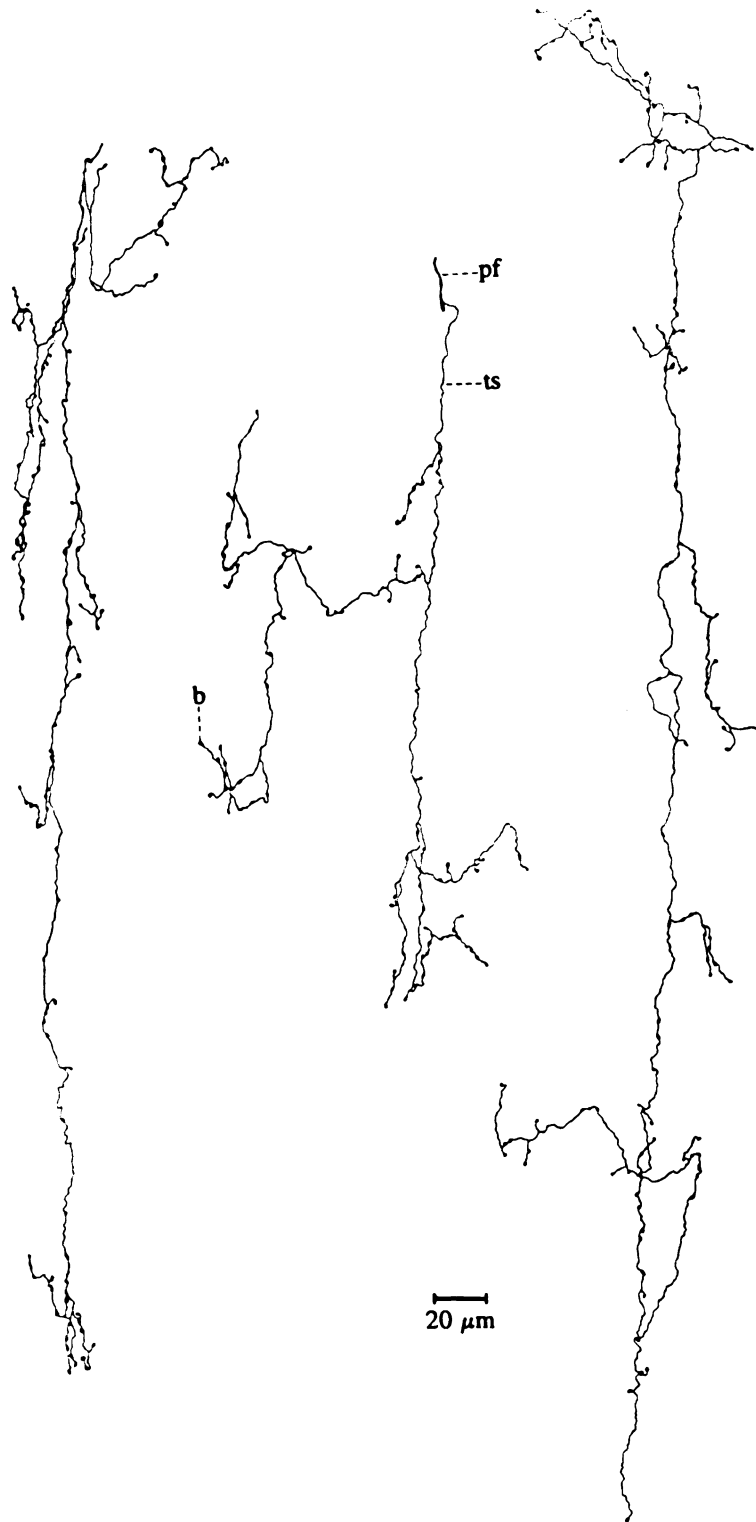


Figure 11

Figure 12: Photomicrographs of Mossy Fibers in CB.

Photomicrographs that show portions of the PHA-L labeled MFs located in the GCL of the CB. A,B. Photomicrographs of complex types of MFs showing the massive convoluted central expansions (large arrows) out of which several tapering or filiform appendages projected (small arrows). C. End of a simple type of MF with an axon bearing an irregular, fusiform enlargement, with smooth globular contours. D. A MF with a central expansion from which a thin filamentous strand coursed to the Purkinje Cell layer and terminated in a bouton in close approximation to a Purkinje Cell body (PCb).

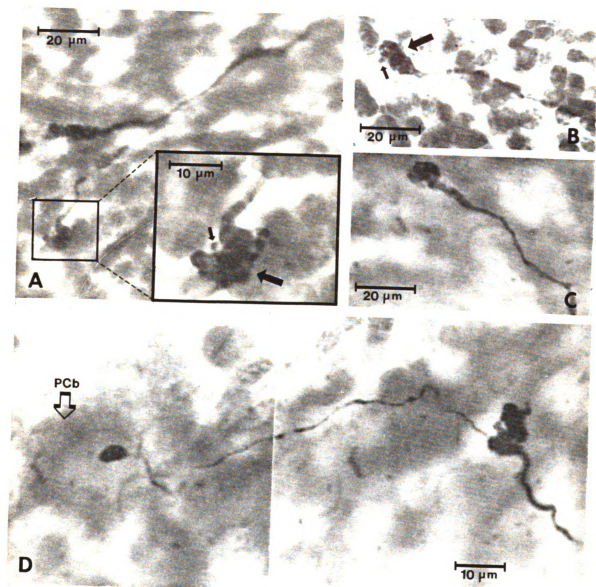


Figure 12

**Figure 13: Photomicrographs of Terminal Axonal Arborizations
in DCN and CSC.**

A,B. Photomicrographs that show portions of PHA-L labeled terminal axonal arborizations located in the DCN. C,D. Photomicrographs that show portions of the type of PHA-L labeled terminal axonal arborizations located in the CSC, specifically from ipsilateral lamina IV (c) and contralateral laminae IX (d).

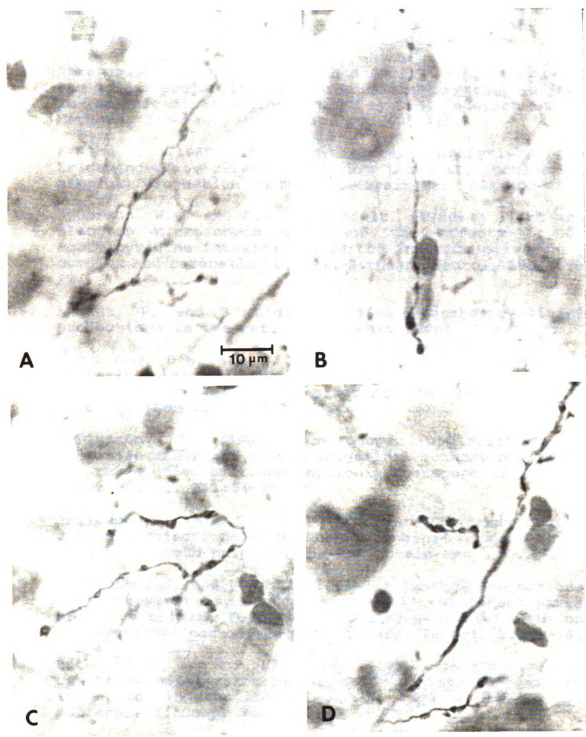


Figure 13

BIBLIOGRAPHY

1. Abrahams, V.C., G. Anstee, F.J.R. Richmond and P.K. Rose. (1979) Neck muscle and trigeminal input to the upper cervical cord and lower medulla of the cat. *Can. J. Physiol. Pharmacol.* Vol. 57, pp. 642-651.
2. Abrahams, V.C. and F.J.R. Richmond. (1977) Motor role of the spinal projections of the trigeminal system. In *Pain In The Trigeminal Region*. Edited by D.S. Anderson and B. Mathews. Elsevier, Amsterdam. pp. 405-413.
3. Akaike, T. (1989) Electrophysiological analysis of the trigemino-olivo-cerebellar (crura I and II, lobulus simplex) projection in the rat. *Brain Res.* 482:402-406.
4. Anderson, W.A. and B.A. Flumerfelt. (1980) A light and electron microscopic study of the effects of 3-acetylpyridine intoxication on the inferior olivary complex and cerebellar cortex. *J. Comp. Neurol.* 190:157-174.
5. Angaut, P. and F. Cicirta. (1982) Cerebello-olivary projections in the rat. *Brain Behav. Evol.* 21:24-33.
6. Armstrong, D.M. and T. Drew. (1980) Responses in the posterior lobe of the rat cerebellum to electrical stimulation of cutaneous afferents to the snout. *J. Physiol. (Lond.)* 309:357-374.
7. Arvidsson, J. (1982) Somatotopic organization of vibrissae afferents in the trigeminal sensory nuclei of the rat studied by transganglionic transport of HRP. *J. Comp. Neurol.* 211:84-92.
8. Arvidsson, J. and S. Gobel (1980) An HRP study of the central projections of primary trigeminal neurons which innervate tooth pulps in the cat. *Brain Res.* 210:1-16.
9. Arvidsson, J. and F.L. Rice. (1991) Central projections of primary sensory neurons innervating different parts of the vibrissae follicles and intervibrissal skin on the mystacial pad of the rat. *J. Comp. Neurol.* 309:1-16.
10. Bates, C.A., and H.P. Killackey. (1985) The organization of the neonatal rat's brainstem trigeminal complex and its role in the formation of central trigeminal patterns. *J. Comp. Neurol.* 240:265-287.

11. Belford, G.R., and H.P. Killackey. (1979) Vibrissae representation in subcortical trigeminal centers of the neonatal rat. *J. Comp. Neurol.* 183:305-322.
12. Bentivoglio, M. and H.G.J.M. Kuypers (1982) Divergent axon collaterals from rat cerebellar nuclei to diencephalon, mesencephalon, medulla oblongata and cervical cord: A fluorescent double-labeling study. *Exp. Brain Res.* 46:339-356.
13. Brodal, A. and O. Pompeiano. (1957) The vestibular nuclei in the cat. *J. Anat.* 91:438-454.
14. Brown, A.G. (1982) The dorsal horn of the spinal cord. *J. Exp. Physiol.* 67:193-212.
15. Brown, J.T., V. Chan-Palay, and S.C. Palay. (1977) A study of afferent input to the inferior olivary complex in the rat by retrograde axonal transport of horseradish peroxidase. *J. Comp. Neurol.* 176:1-22.
16. Burton, H. and A.D. Loewy (1977) Projections to the spinal cord from medullary somatosensory relay nuclei. *J. Comp. Neurol.* 173:773-792.
17. Campbell, N.C. and D.M. Armstrong. (1983) Topographical localization in the olivocerebellar projection in the rat: An autoradiographic study. *Brain Res.* 275:235-249.
18. Chan-Palay, V. (1977) *Cerebellar Dentate Nucleus: Organization, Cytology and Transmitters.* Springer-Verlag, Berlin.
19. Chan-Palay, V., S.L. Palay, J.T. Brown and C. Van Itallie. (1977) Sagittal organization of olivocerebellar and reticulocerebellar projections: Autoradiographic studies with ³⁵S-Methionine. *Exp. Brain Res.* 30:561-576.
20. Chiaia, N.L., P.R. Hess, M. Hosoi, and R.W. Rhoades. (1987) Morphological characteristics of low-threshold primary afferents in the trigeminal subnuclei interpolaris and caudalis (the medullary dorsal horn) of the golden hamster. *J. Comp. Neurol.* 264:527-546.
21. Cliffer, K.D., and G.J. Giesler Jr. (1988) PHA-L can be transported anterogradely through fibers of passage. *Brain Res.* 458:185-191.
22. Cook, M.S. and W.M. Falls (1992) Efferent projections of neurons in four subdivisional regions of rat trigeminal nucleus interpolaris to the diencephalon and midbrain: A PHA-L study. (In Preparation).

23. Cook, M.S. and W.M. Falls (1992) Efferent projections of neurons in four subdivisional regions of rat trigeminal nucleus interpolaris to pontomedullary regions: A PHA-L study. (In Preparation).
24. Desclin, J.C. (1974) Histological evidence supporting the inferior olive as a major source of cerebellar climbing fibers in the rat. *Brain Res.* 77:365-384.
25. Eller, T.W. and V. Chan-Palay. (1976) Afferents to the cerebellar lateral nucleus. Evidence from retrograde transport of horseradish peroxidase after pressure injections through micropipettes. *J. Comp. Neurol.* 166:285-301.
26. Falls, W.M. and D.L. Race. (1986) Morphological features of identified neurons in rat trigeminal nucleus interpolaris projecting to orofacial tactile areas of the cerebellar hemisphere. *Exp. Brain Res. Anat. Rec.* 214:104A.
27. Falls, W.M., L.A. Smith and J. Stuk. (1990) Origins and terminations of trigeminal projections to rat spinal cord. *Soc. Neurosci. Abstr.* 16:223.
28. Flumerfelt, B.A., S. Otabe, and J. Courville. (1973) Distinct projections to the red nucleus from the dentate and interposed nuclei in the monkey. *Brain Res.* 50:408-414.
29. Fyffe, R.E.W. Organization of the olivocerebellar projection in the rat. *Brain Behav. Evol.* 27:132-152.
30. Gerfen, C.R., and P.E. Sawchenko. (1984) An anterograde neuroanatomical tracing method that shows the detailed morphology of neurons, their axons and terminals: Immunohistochemical localization of an axonally transported plant lectin, *Phaseolus vulgaris* leucoagglutinin (PHA-L). *Brain Res.* 290:219-238.
31. Gobel, S., and M.B. Purvis. (1972) Anatomical studies of the organization of the spinal V nucleus: The deep bundles and the spinal V tract. *Brain Res.* 48:27-44.
32. Goodman, D.C., R.E. Hallett and R.B. Welch. (1963) Patterns of localization in the cerebellar corticonuclear projections of the albino rat. *J. Comp. Neurol.* 121:51-67.
33. Gould, B. (1980) Organization of afferents from the brain stem nuclei to the cerebellar cortex in the cat. *Adv. Anat. Embryol. Cell Biol.* 62:1-79.

34. Haines, D.E. and S.L. Koletar. (1979) Topography of cerebellar corticonuclear fibers of the albino rat. *Brain Behav. Evol.* 16:271-292.
35. Haroian, A.J., L.C. Massopust and P.A. Young (1981) Cerebellothalamic projections in the rat: An autoradiographic and degeneration study. *J. Comp. Neurol.* 197:217-236.
36. Hayashi, H. (1982) Differential terminal distribution of single, large cutaneous afferent fibers in the spinal trigeminal nucleus and in the cervical spinal dorsal horn. *Brain Res.* 244:173-177.
37. Hayashi, H., R. Sumino and B.J. Sessle. (1984) Functional organization of trigeminal subnucleus interpolaris: Nociceptive and innocuous afferent inputs, projections to thalamus, cerebellum, and spinal cord and descending modulation from periaqueductal gray. *J. Neurophysiol.* 51:890-905.
38. Hess, D.T. (1982) The tecto-olivo-cerebellar pathway. *Brain Res.* 250:143-148.
39. Huerta, M.F., A.J. Frankfurter, and J.K. Harting. (1983) Studies of the principal sensory and spinal trigeminal nuclei of the rat: Projections to the superior colliculus, inferior olive, and cerebellum. *J. Comp. Neurol.* 220:147-167.
40. Ikeda, M., T. Tanami, and M. Matsushita. (1984) Ascending and descending internuclear connections of the trigeminal sensory nuclei in the cat. A study with the retrograde and anterograde horseradish peroxidase technique. *Neurosci.* 12:1243-1260.
41. Jacquin, M.F., N.L. Chiaia, J.H. Haring and R.W. Rhoades. (1990) Intersubnuclear connections within the rat trigeminal brainstem complex. *Somatosensory and Motor Res.* 7:399-420.
42. Jacquin, M.F., N.L. Chiaia and R.W. Rhoades. (1990) Trigeminal projections to contralateral dorsal horn: Central extent, peripheral origins, and plasticity. *Somatosens. and Motor Res.* 7:153-183.
43. Jacquin, M.F., R.D. Mooney, and R.W. Rhoades. (1986) Morphology, response properties, and collateral projections of trigeminothalamic neurons in the brainstem subnucleus interpolaris of rat. *Exp. Brain Res.* 61:457-468.

44. Jacquin, M.F., K. Semba, M.D. Egger and R.W. Rhoades. (1983) Organization of HRP-labeled trigeminal mandibular primary afferent neurons in the rat. *J. Comp. Neurol.* 215:397-420.
45. Jacquin, M.F., D. Woerner, A.M. Szczepanik, V. Riecker, R.D. Mooney, and R.W. Rhoades. (1986) Structure-function relationships in rat brainstem subnucleus interpolaris. I. Vibrissa primary afferents. *J. Comp. Neurol.* 243:266-279.
46. Joseph, J.W., G.M. Shambes, J.M. Gibson and W. Welker. (1978) Tactile projections to granule cells in caudal vermis of the rat's cerebellum. *Brain Behav. Evol.* 15:141-149.
47. Kassel, J. (1980) Superior colliculus projections to tactile areas of rat cerebellar hemispheres. *Brain Res.* 202:291-305.
48. Leong, S.K., J.Y. Shieh and W.C. Wong. (1984) Localizing spinal-cord-projecting neurons in adult albino rats. *J. Comp. Neurol.* 228:1-17.
49. Ma, P.M. and T.A. Woolsey. (1984) Cytoarchitectonic correlates of the vibrissae in the medullary trigeminal complex of the mouse. *Brain Res.* 306:374-379.
50. Manni, E., G. Palmieri, R. Marini and V.E. Pettorossi. (1975) Trigeminal influences on extensory muscles of the neck. *Exp. Neurol.* 47:330-342.
51. Mantle-St.John, L.A., and D.J. Tracey. (1987) Somatosensory nuclei in the brainstem of the rat: Independent projections to the thalamus and cerebellum. *J. Comp. Neurol.* 255:259-271.
52. Marfurt, C.F. (1981) The central projections of trigeminal primary afferent neurons in the cat as determined by the transganglionic transport of horseradish peroxidase. *J. Comp. Neurol.* 203:785-798.
53. Matsushita, M. and Y. Hosoya. (1978) The location of spinal projection neurons in the cerebellar nuclei (cerebello-spinal tract neurons) of the cat: A study with the HRP technique. *Brain Res.* 142:237-248.
54. Matsushita, M., M. Ikeda, and N. Okado. (1982) The cells of origin of the trigeminothalamic, trigeminospinal and trigeminocerebellar projections in the cat. *Neurosci.* 7:1439-1454.

55. Matsushita, M., O. Nobuo, M. Ikeda and Y. Hosoya. (1981) Descending projections from the spinal and mesencephalic nuclei of the trigeminal nerve to the spinal cord in the cat. A study with the horseradish peroxidase technique. J. Comp. Neurol. 196:173-187.
56. Mihailoff, G.A., R.A. Burne, S.A. Azizi, G. Norell and D.J. Woodward. (1981) The pontocerebellar system in the rat: An HRP study. II. Hemispherical components. J. Comp. Neurol. 197:559-577.
57. Mihailoff, G.A., R.A. Burne and D.J. Woodward. (1978) Projections of the sensorimotor cortex to the basilar pontine nuclei in the rat: An autoradiographic study. Brain Res. 145:347-354.
58. Miles, T.S. and M. Wiesindanger. (1975) Organization of climbing fiber projections to the cerebellar cortex from trigeminal cutaneous efferents and from SI face area of the cerebral cortex in the cat. J. Physiol. Lond. 245:409-424.
59. Molander, C., Q. Xu, C. Rivero-Melian and G. Grant. (1989) Cytoarchitectonic organization of the spinal cord in the rat: II. The cervical and upper thoracic cord. J. Comp. Neurol. 289:375-385.
60. Murray, E.A., and J.D. Coulter. (1981) Organization of tectospinal neurons in the cat and rat superior colliculus. Brain Res. 243:201-214.
61. Nasution, I.D., and Y. Shigenaga. (1987) Ascending and descending internuclear projections within the trigeminal sensory nuclear complex. Brain Res. 425:234-247.
62. Palay, S.L. and Chan-Palay, V. (1974) Cerebellar Cortex: Cytology and Organization. Springer, Berlin.
63. Palkovits, M., P. Magyar, and J. Szentagothai. (1972) Quantitative histological analysis of the cerebellar cortex in the cat IV. Mossy fiber - Purkinje cell numerical transfer. Brain Res. 45:15-29.
64. Patrick, G.W. and D.E. Haines. (1982) Cerebellar afferents to paramedian lobule from the trigeminal complex in Tupaia glis: A horseradish peroxidase (HRP) study. J. Morph. 172:209-222.

65. Patrick, G.W., and M.A. Robinson. (1987) Collateral projections from trigeminal sensory nuclei to ventrobasal thalamus and cerebellar cortex in rats. *J. Morphol.* 192:229-236.
66. Paxinos, G. (1985) The Rat Nervous System. Vol. 2.: Hindbrain and Spinal Cord. Academic Press Australia.
67. Paxinos, G., and C. Watson. (1986) The Rat Brain in Stereotaxic Coordinates. Academic Press, New York.
68. Phelan, K.D. and W.M. Falls. (1989) An analysis of the cyto- and myeloarchitectonic organization of trigeminal nucleus interpolaris in the rat. *Somatosensory Res.* Vol. 6, 4:333-366.
69. Phelan, K.D., and W.M. Falls. (1990) A comparison of the distribution and morphology of thalamic, cerebellar and spinal projection neurons in rat trigeminal nucleus interpolaris. *Neurosci.* 40:497-511.
70. Phelan, K.D., and W.M. Falls. (1991) The spinotrigeminal pathway and its spatial relationship to the origin of trigeminospinal projections in the rat. *Neurosci.* 40:477-496.
71. Rethelyi, M. Synaptic Connectivity in the Spinal Dorsal Horn.
72. Rethelyi, M. (1981) Geometry of the dorsal horn. In *Spinal Cord Sensation*, A.G. Brown and M. Rethelyi (Eds.), Scottish Academic Press, Edinburgh, pp. 1-11.
73. Rethelyi, M. and J. Szentagothai. (1973) Distribution and connections of afferent fibers in the spinal cord. In *Handbook of Sensory Physiology, Vol. II, Somatosensory System*, A. Iggo (Ed.), Springer, New York, pp. 207-252.
74. Rhoades, R.W., S.E. Fish, N.L. Chiaia, C. Bennett-Clarke, and R.D. Mooney. (1989) Organization of the projections from the trigeminal brainstem complex to the superior colliculus in the rat and hamster: Anterograde tracing with phaseolus vulgaris leucoagglutinin and intra-axonal injection. *J. Comp. Neurol.* 289:641-656.
75. Rhoades, R.W., R.D. Mooney, B.G. Klein, M.F. Jacquin, A.M. Szczepanik, and N.L. Chiaia. (1987) The structural and functional characteristics of tectospinal neurons in the golden hamster. *J. Comp. Neurol.* 255:451-465.

76. Richardson, H.C., F.W.J. Cody, V.E. Paul and A.G. Thomas. (1978) Convergence of trigeminal and limb inputs onto cerebellar interpositus nuclear neurones in the cat. *Brain Res.* 156:355-359.
77. Rose, P.K. and N. Sprott. (1978) Proprioceptive and somatosensory influences on neck muscle motoneurons. In *Reflex Control of Posture and Movement*, vol. 50, Progress in Brain Res., R. Granit, O. Pompeiano (Eds.), Elsevier/North-Holland Biomedical Press, New York, pp. 255-262.
78. Ruggiero, D.A., C.A. Ross and D.J. Reis. (1981) Projections from the spinal trigeminal nucleus to the entire length of the spinal cord in the rat. *Brain Res.* 225:225-233.
79. Sahibzada, N., P. Dean, and P. Redgrave. (1986) Movements resembling orientation or avoidance elicited by electrical stimulation of the superior colliculus in rats. *J. Neurosci.* 6:723-733.
80. Saigal, R.P., A.N. Karamanlidis, J. Voogd, O. Mangana and H. Michaloudi. (1980) Secondary trigeminocerebellar projections in sheep studied with the horseradish peroxidase tracing method. *J. Comp. Neurol.* 189:537-553.
81. Scheibel, A.B. (1977) Sagittal organization of mossy fiber terminal systems in the cerebellum of the rat: A Golgi study. *Exp. Neurol.* 57:1067-1070.
82. Shambes, G.M., D.H. Berman and W. Welker. (1978a) Multiple tactile areas in cerebellar cortex: another patchy cutaneous projection to granule cell columns in rats. *Brain Res.* 157:123-128.
83. Shambes, G.M., J.M. Gibson and W. Welker. (1978b) Fractured somatotopy in granule cell tactile area of rat cerebellar hemispheres revealed by micromapping. *Brain Behav. Evol.* 15:94-140.
84. Silverman, J.D., and L. Kruger. (1985) Projections of the rat trigeminal sensory nuclear complex demonstrated by multiple fluorescent dye retrograde transport. *Brain Res. Short Comm.* 383-388.
85. Smith, L.A. and W.M. Falls (1992) Descending projections to rat dorsal column nuclei and spinal cord from identified subdivisional areas within trigeminal nucleus oralis utilizing the method of PHA-L. (In Press).

86. Somana, R., N. Kotchabhakdi and F. Walberg. (1980) Cerebellar afferents from the trigeminal sensory nuclei in the cat. *Exp. Brain Res.* 38:57-64.
87. Steindler, D.A. (1985) Trigemino-cerebellar, trigeminotectal, and trigeminothalamic projections: A double retrograde axonal tracing study in the mouse. *J. Comp. Neurol.* 237:155-175.
88. Sumino, R. and Y. Nakamura. (1977) Synaptic potentials of hypoglossal motoneurons and a common inhibitory interneuron in the trigemino-hypoglossal reflex. *Brain Res.* 73:439-454.
89. Swenson, R.S., and A.J. Castro. (1983) The afferent connections of the inferior olivary complex in rat: A study using the retrograde transport of horseradish peroxidase. *Am. J. Anat.* 166:329-341.
90. Takemura, M., T. Sugimoto and A. Sakai. (1987) Topographic organization of central terminal region of different sensory branches of the rat mandibular nerve. *Exp. Neurol.* 96:540-557.
91. Umetani, T., T. Tabuchi and R. Ichimura (1986) Cerebellar corticonuclear and corticovestibular fibers from the posterior lobe of the albino rat, with comments on zones. *Brain Behav. Evol.* 29:54-67.
92. Wall, P.D. and A. Taub (1962) Four aspects of trigeminal nucleus and a paradox. *J. Neurophysiol.* 25:110-126.
93. Watson, C.R.R. and R.C. Switzer III. (1978) Trigeminal projections to cerebellar tactile areas in the rat—origin mainly from N. interpolaris and N. principalis. *Neurosci. Lett.* 10:77-82.
94. Watt, C.B. and G.A. Mihailoff. (1983) The cerebellopontine system in the rat. I. Autoradiographic studies. *J. Comp. Neurol.* 215:312-330.
95. Wise, S.P., E.A. Murray, and J.D. Coulter. (1979) Somatotopic organization of corticospinal and corticotrigeminal neurons in the rat. *Neurosci.* 4:65-78.
96. Woolston, D.C., J. Kassel and J.M. Gibson (1981) Trigemino-cerebellar mossy fiber branching to granule cell layer patches in the rat cerebellum. *Brain Res.* 209:255-269.